

Extracellular vesicle release of α -Synuclein is mediated by SUMOylation

Dissertation

for the award of the degree

“Doctor rerum naturalium”

of the Georg-August-Universität Göttingen

within the Program *Molecular Physiology of the Brain*

of the Georg-August University School of Science (GAUSS)

submitted by

Marcel Kunadt

from Eisenhüttenstadt

Göttingen, 2015

Members of Thesis Committee

Prof. Dr. Mikael Simons

Dept. of Cellular Neuroscience, MPI for Experimental Medicine

Prof. Dr. André Fischer

Dept. of Psychiatry and Psychotherapy, University Medical Center Göttingen, DZNE Göttingen

Prof. Dr. Silvio Rizzoli

Dept. of Neuro-and Sensory Physiology, University Medical Center Göttingen

Members of the Examination Board

Prof. Dr. Dr. Hannelore Ehrenreich

Dept. of Clinical Neuroscience, MPI for Experimental Medicine

Prof. Dr. Tiago Fleming Outeiro

Dept. of Neurodegeneration and Restorative Research, University Medical Center Göttingen

Prof. Dr. Alexander Flügel

Institute for Multiple Sclerosis Research, University Medical Center Göttingen, Dept. of Neuroimmunology

Date of oral examination: 11.06.2015

Affirmation

I hereby declare that this thesis was written independently and with no other sources and aids than quoted.

Göttingen, 08.05.2015

Marcel Kunadt

Acknowledgements – Danksagung

Mein besonderer Dank gilt in erster Linie meiner Doktormutter Frau Prof. Dr. Anja Schneider, für das mir entgegengebrachte Vertrauen, für ihre exzellente Betreuung dieser Doktorarbeit, für die aktuelle und interessante Themenstellung, ihre wissenschaftlichen Ratschläge und Anregungen, sowie ihr aufrichtiges Interesse am Fortgang dieser Arbeit. Ein weiterer Dank geht an Thomas M. Jovin für seine großes Engagement bei der Analyse der SUMO-Lipidbindungsstudien und seine stets fruchtbaren Ratschläge bei der Verbesserung dieser neuen Messmethode.

Weiterhin gebührt mein Dank den Mitgliedern meines „Thesis Committees“, Prof. Dr. Mikael Simons, Prof. Dr. André Fischer und Prof. Dr. Silvio Rizzoli, für die Unterstützung und die stets fruchtbaren Diskussionen und Kommentare, die zum Abschluss dieser Arbeit beigetragen haben. Ein weiterer Dank gilt den Mitgliedern meines erweiterten Prüfungsausschusses, Prof. Dr. Dr. Hannelore Ehrenreich, Prof. Dr. Tiago Fleming Outeiro, sowie Prof. Dr. Alexander Flügel.

Einen speziellen Dank möchte ich an die vielen Kollaborationspartner richten, die maßgeblich zum Erfolg dieser Arbeit beigetragen haben. Für die finanzielle Unterstützung danke ich der DFG (Deutsche Forschungsgemeinschaft), sowie dem DFG Research Center Nanoscale Microscopy and Molecular Physiology of the Brain (CNMPB).

Danke sagen möchte ich auch an alle derzeitigen und ehemaligen Mitglieder der AG Schneider. Ich danke euch allen für das wundervolle Arbeitsklima, die Mittagspausen in der Sonne, oder einfach mal für das „Käffchen“ nebenbei. Weiterhin danke ich euch für die große Unterstützung in der letzten Zügen dieser Arbeit. Danke, dass ihr immer bemüht wart mich aufzumuntern und immer ein offenes Ohr für mich hattet. Ein spezieller Dank gilt vor allem Anne, Belisa und Beate für die Korrekturen dieser Arbeit. Petra Wilken gebührt ein weiterer Dank für die vielen lustigen Stunden auch außerhalb des Labors. Aus der AG Simons danke ich Tina Kling, für die tollen Gespräche und für deinen Benni, der mich immer ein wenig aufgebaut und im höchsten Maße zum Lachen gebracht hat.

Anne dir gilt mein besonderer Dank. Zuerst möchte ich dir danken, dass es dich überhaupt gibt und dass du trotz diverser Macken immer zu mir gehalten hast und mich so akzeptierst wie ich bin. Ich weiß die letzte Zeit war nicht einfach für uns beide. Du hast mich in der ganzen Zeit immer wieder aufgebaut und warst auch in schwierigen Situationen immer für mich da und hast an mich geglaubt.

Ich danke dir von ganzem Herzen für deine scheinbar unerschöpfliche Kraft, sowie deine seelische und moralische Unterstützung beim Anfertigen dieser Arbeit. Danke Anne für alles.

Meine „Schergen“ haben ebenfalls einen besonderen Dank verdient. Ich danke euch für die gemeinsame Zeit und all den Spaß den wir zusammen erlebt haben. Ingo dir gebührt ein besonderer Dank. Du bist der beste Mitbewohner und Freund den Man(n) sich wünschen kann. Ich danke dir dafür, dass du immer da warst, mich immer wieder aufgerichtet hast und immer ein offenes Ohr für mich hattest. An all die anderen Verrückten, danke für eure Freundschaft. Danke an Boscabana und seine anderen Kollegen.

Zum Schluss geht ein ganz besonderer Dank an meine ganze Familie. Insbesondere möchte ich meinen Eltern Viola und Andreas danken, sowie dir Oma Inge. Ich danke euch, dass ihr mir das Studium ermöglicht habt, dass ihr immer für mich da wart wenn ich euch gebraucht habe und immer ein offenes Ohr für mich hattet und versucht habt, auch wenn es nicht immer leicht war, mich zum weiter machen zu motivieren. Auch dir Linda möchte ich danken, danke, dass ich dich als Schwester habe und auch wenn wir uns selten sehen, es immer schön ist wenn wir uns mal treffen und ein wenig Zeit zusammen haben.

Zum Schluss noch ein Dank an dich Opa. Leider hast du es nicht mehr geschafft so lange zu kämpfen, um den Abschluss meiner Doktorarbeit zu erleben. Ich weiß, dass du voller Stolz von oben herab schaust und mitbekommen wirst, dass ich es geschafft habe. Danke Opa für alles was du mir beigebracht hast, dir sei diese Arbeit gewidmet.

I. Table of Contents

1. Introduction.....	2
1.1. Synuclein.....	2
1.1.1. Structure of α -Synuclein	3
1.1.2. Posttranslational modifications of α -Syn	4
1.1.3. Function of α -Synuclein	5
1.2. Synucleinopathies	6
1.2.1. Parkinson's disease.....	6
1.2.1.1. Familial Parkinson's disease	6
1.2.2. Dementia with Lewy bodies (DLB).....	7
1.2.3. Multiple system atrophy (MSA)	7
1.3. Spreading of disease pathology	8
1.3.1. Permissive templating	8
1.3.2. Transmission of α -Synuclein in a prion-like manner.....	9
1.4. Extracellular vesicles.....	11
1.4.1. Morphology and composition of extracellular vesicles	11
1.4.2. Biogenesis of extracellular vesicles	14
1.4.3. Secretion of extracellular vesicles.....	16
1.4.4. Function of extracellular vesicles	17
1.5. SUMOylation.....	18
1.5.1. The family of small ubiquitin like modifiers SUMO	18
1.5.2. The SUMOylation pathway	19
1.5.2.1. Enzymes involved in the SUMOylation process	20
1.5.2.2. Non covalent SUMO binding mediated by SIM	21
1.5.3. SUMOylation in neurodegenerative diseases	21
1.5.3.1. SUMOylation in Alzheimer's disease.....	21
1.5.3.2. SUMOylation in Huntington's disease	22
1.5.3.3. SUMOylation in Parkinson's disease.....	22
2. Materials and Methods	24
2.1. Materials	24
2.1.1. Chemicals and Consumables	24
2.1.2. Cell lines and primary cells	24
2.1.2.1. Cell lines	24
2.1.2.2. Primary cells	24
2.1.3. Antibodies	25
2.1.4. Nucleotide constructs	25
2.1.4.1. Previously published plasmids	25
2.1.4.2. Self constructed plasmids	26
2.1.4.3. siRNA constructs	26

2.1.5.	Phospholipids	27
2.1.6.	Buffer and Solutions	28
2.1.6.1.	Phosphate buffered saline (PBS)	28
2.1.6.2.	Tris buffered saline (TBS)	28
2.1.6.3.	HEPES/sucrose stock solution.....	28
2.1.6.4.	Homogenisation-buffer (HB)	29
2.1.6.5.	CHAPS lysis buffer	29
2.1.6.6.	Protein loading buffer	29
2.1.6.7.	Resolving gel buffer	30
2.1.6.8.	Stacking gel buffer	30
2.1.6.9.	10x Running buffer.....	30
2.1.6.10.	10x Transfer buffer	30
2.1.6.11.	10x Transfer buffer	30
2.1.7.	Media and sera.....	31
2.1.7.1.	Commercial media	31
2.1.7.2.	General growth medium.....	31
2.1.7.3.	SATO-medium	32
2.1.7.4.	MEM-B27	32
2.1.8.	Commercial kits.....	33
2.1.9.	Software	33
2.2.	Methods	34
2.2.1.	Molecular biology methods	34
2.2.1.1.	Site-directed mutagenesis.....	34
2.2.1.2.	Transformation of <i>Escherichia coli</i> (<i>E. coli</i>)	34
2.2.1.3.	Plasmid DNA isolation from <i>E. coli</i>	34
2.2.1.4.	Determination of DNA concentration	34
2.2.1.5.	Expression and purification of sumoylated α -Synuclein.....	35
2.2.1.6.	Expression of recombinant SUMO-2 for NMR	35
2.2.2.	Cell culture	36
2.2.2.1.	Growth and maintenance of cells	36
2.2.2.2.	Cryoconservation of cells	37
2.2.2.3.	Transfection of plasmids	37
2.2.2.4.	RNA interference	38
2.2.2.5.	Collection of extracellular vesicles	38
2.2.2.6.	Luciferase activity assay	38
2.2.2.7.	Membrane preparation.....	38
2.2.3.	Extracellular vesicle purification and analysis	39
2.2.3.1.	Ultracentrifugation.....	39
2.2.3.2.	Sucrose gradient ultracentrifugation.....	39
2.2.3.3.	Nanoparticle tracking analysis (NTA)	40

2.2.4. Protein biochemistry	41
2.2.4.1. SDS-PAGE	41
2.2.4.2. Western blotting	42
2.2.4.3. FCS/SIFT measurements	42
2.2.4.4. Electrochemiluminescence assay for quantification of α -Synuclein	43
2.2.4.5. Labelling of SUMO-2 with the ESPIT dye MFM.....	43
2.2.5. Lipid biochemistry	44
2.2.5.1. Preparation of Small Unilamellar Vesicles (SUVs)	44
2.2.5.2. Membrane binding assay of SUMO-2	44
2.2.6. NMR spectroscopy	45
2.2.7. Immunocytochemistry	45
2.2.7.1. Immunofluorescence staining.....	45
2.2.8. Microscopy	47
2.2.8.1. Confocal microscopy.....	47
2.2.8.2. Electron microscopy.....	47
2.2.9. Image processing and statistical analysis	47
2.2.9.1. Quantification of extracellular vesicle secretion.....	47
2.2.9.2. Statistical analysis.....	48
3. Results	49
3.1. α-Synuclein is released in extracellular vesicles	49
3.1.1. α -Synuclein is released in extracellular vesicles derived from N2a cells	49
3.1.2. α -Synuclein is localized in extracellular vesicles <i>in vivo</i>	51
3.1.3. α -Synuclein is predominantly localized in the lumen of EVs.....	53
3.2. The extracellular release of α-Synuclein is regulated by membrane binding	56
3.3. SUMOylation regulates membrane binding and extracellular vesicle release of α-Synuclein	58
3.3.1. SUMOylation modulates membrane binding of α -Synuclein	58
3.3.2. Extracellular vesicle release of α -Synuclein is regulated by SUMOylation	62
3.3.2.1. Silencing of Ubc9 decreases the release of α -Synuclein within extracellular vesicles	64
3.3.2.2. α -Synuclein fusion with SUMO-2 increases the release of α -Synuclein within extracellular vesicles.....	67
3.3.2.3. Co-expression of SUMO-2 increases the release of α -Synuclein within extracellular vesicles.....	68
3.3.2.4. Isopeptidase activity in extracellular vesicles results in a rapid de-conjugation of SUMO.....	71
3.4. SUMOylation can act as sorting signal for the release within extracellular vesicles	74
3.4.1. SUMO-2 targets the cytosolic protein GFP to extracellular vesicle release.....	76
3.4.2. SUMO-1 also modulates extracellular vesicle sorting of the cytosolic protein GFP.....	78
3.4.3. SUMOylation increases the extracellular vesicle release of the transmembrane protein amyloid precursor protein (APP)	79

3.5. Extracellular vesicle release of SUMO-2 is ESCRT-dependent.....	81
3.5.1. RNA Interference with the ESCRT components Alix and Tsg101 decrease extracellular vesicle release of a SUMO-2-GFP fusion protein	81
3.5.2. Co-expression of the dominant negative mutant of VPS4 decreases the extracellular vesicles release of a GFP-SUMO-2 fusion protein.....	85
3.5.3. Extracellular vesicle release of SUMO-2 does not depend on the canonical SUMO protein interaction motif Q30 F31 I33	87
3.6. SUMO-lipid interaction	88
3.6.1. SUMO-2 interacts with phosphoinositols	88
3.7. Identification of the membrane interaction motif of SUMO-2.....	90
3.7.1. The membrane interaction motif of SUMO-2 is localised to the hydrophobic cleft and nearby loops	90
3.7.1.1. Mutations in the hydrophobic cleft and N-terminally loop domains of SUMO-2 decreases the membrane binding propensity of SUMO-2.....	92
3.7.1.2. Mutations in the hydrophobic cleft and N-terminally loop domains of SUMO-2 decreases sorting into extracellular vesicles.....	94
3.8. Co-expression of the dominant negative mutant of VPS4 decreases extracellular vesicle release of α-Synuclein.....	95
3.9. Inhibition of endosome maturation by overexpression of dominant negative Rab5 does not trap α-Syn or SUMO-2 in enlarged intraluminal vesicles	96
4. Discussion	98
4.1. α-Synuclein is localised in EVs <i>in vitro</i>.....	98
4.2. Microvesicles or exosomes?	99
4.3. SUMO-2 interacts with phosphoinositols.....	100
4.3.1. SUMO binding to plasma membranes is mediated by PI(3,4,5)P ₃	100
4.4. α-Synuclein is localised in EVs <i>in vivo</i>.....	101
4.5. Extracellular vesicles as carrier for pathogenic proteins	101
4.5.1. Interneuronal spreading of α -Syn pathology	102
4.6. SUMO modification in neurodegenerative diseases	103
5. Summary	104
6. References	105
7. Appendix	123
Curriculum Vitae.....	124
Publications.....	125

II. List of Figures

Fig. 1: Schematic representation of the α -Syn amino acid sequence	3
Fig. 2: Possible mechanisms for the intercellular transmission of α -Synuclein	10
Fig. 3: Schematic view of the protein and lipid composition of exosomes.....	13
Fig. 4: Biogenesis of extracellular vesicles.....	14
Fig. 5: Schematic representation of the SUMO cycle	19
Fig. 6: α -Synuclein is released in extracellular vesicles derived from N2a cells.....	50
Fig. 7: Characterization of extracellular vesicles in cerebrospinal fluid	52
Fig. 8: α -Syn is localised in the intraluminal compartment of extracellular vesicles	54
Fig. 9: Membrane binding regulates release of α -Synuclein within extracellular vesicles	57
Fig. 10: Membrane binding of SUMO-deficient α -Syn mutants 2 KR and 2 AA	59
Fig. 11: Membrane binding of a myc- α -Syn-SUMO fusion construct	60
Fig. 12: SIFT assay for vesicle binding properties of sumoylated and non-sumoylated α -Syn.....	61
Fig. 13: Extracellular vesicle release of SUMOylation deficient α -Syn.....	63
Fig. 14: Primary cortical neurons were infected with AAV to either express α -Syn-wt or the SUMOylation-deficient mutant α Syn-2 KR	64
Fig. 15: Down-regulation of Ubc9 protein levels with siRNA.....	66
Fig. 16: SUMO-2 fusion increases extracellular vesicle release of α -Syn.....	67
Fig. 17: Co-expression of SUMO-2 increases release of α -Syn with extracellular vesicles...68	
Fig. 18: Co-expression of SUMO-2 does not increase the production and release of extracellular vesicles itself	69
Fig. 19: Summary of α -Syn membrane binding and release with extracellular vesicles	70
Fig. 20: Extracellular vesicles contain desumoylase activity.....	71
Fig. 21: Sumoylated α -Syn is enriched in extracellular vesicles	73
Fig. 22: SUMO-2 is released within extracellular vesicles	75
Fig. 23: SUMO-2 fusion leads to extracellular vesicle sorting of GFP.....	77
Fig. 24: Comparison of SUMO-1 and SUMO-2 release within extracellular vesicles	78
Fig. 25: SUMO-2 increases extracellular vesicle release of the transmembrane protein APP.....	80
Fig. 26: Down-regulation of Tsg 101 and Alix with siRNA	82
Fig. 27: Alix and TSG101 are required for the extracellular vesicle release of SUMO-2	83
Fig. 28: Release of SUMO-2 with extracellular vesicles is dependent on ESCRT	84
Fig. 29: Interference with VPS4 function inhibits release of SUMO-2 within extracellular vesicles.....	86

Fig. 30: Mutation of the SIM motif in SUMO-2 increases extracellular vesicle release of SUMO-2	87
Fig. 31: Microplate titration assay of SUMO-2-MFM.....	89
Fig. 32: Membrane binding of SUMO-2 analysed by NMR spectroscopy	91
Fig. 33: Mutation of amino acids H16A, Q30A, F31A, K32A, I33A, H36, L42A, Y46A and D62 in the cleft and loop domains of SUMO-2 decreases membrane binding.....	93
Fig. 34: Mutated amino acids H16A, Q30A, F31A, K32A, I33A, H36, L42A, Y46A and D62 in the cleft and loop domains of SUMO-2 decreases extracellular vesicle sorting ...	94
Fig. 35: Release of α -Syn-SUMO-2 fusion protein with extracellular vesicles is dependent on the ESCRT	95
Fig. 36: Subcellular distribution of SUMO-2 and α -Synuclein	97

III. List of Tables

Table 1: Cell lines	24
Table 2: Primary Antibodies	25
Table 3: Previously published plasmids	25
Table 4: siRNA constructs	26
Table 5: Phospholipids.....	27
Table 6: Commercial media and solutions	31
Table 7: Commercial Kits	33
Table 8: Software.....	33
Table 9: Transfection protocols	37
Table 10: Sucrose density gradient.....	40
Table 11: Stacking gel (4%)	41
Table 12: Resolving gel (12%)	41
Table 13: Summary of NTA measurements	123

IV. List of Abbreviations

aa	amino acid
AD	Alzheimer's disease
APC	antigen presenting cell
APS	ammonium persulfate
APP	amyloid precursor protein
α -Syn	α -Synuclein
AAV	adeno-associated virus
A β	amyloid beta protein
CHAPS	3-[3-(Cholamidopropyl)dimethylammonio]-1-proanesulfonate
CNS	central nervous system
CSF	cerebral spinal fluid
CSP α	cysteine-string protein alpha
DABCO	1,4-Diazabicyclo[2.2.2]octan
DLB	dementia with Lewy Bodies
DNA	desoxyribonuclein acid
DTT	dithiothreitol
<i>E. coli</i>	<i>Escherichia coli</i>
EDTA	ethylenediaminetetraacetic acid
ELISA	enzyme-linked immunosorbent assay
ER	endoplasmic Reticulum
ESCRT	endosomal complex required for transport
ESPIT	excited state intramolecular proton transfer
EVs	extracellular vesicles
FCS	fetal calf serum
FCS	fluorescence correlation spectroscopy
g	gramm
GFP	green fluorescent proteine
h	hour
HB	homogenisation Buffer
HBSS	Hanks' balanced salt solution
HEPES	hydroxyethylpiperazine-N-2-ethanesulfonic acid
HIV	human immunodeficiency virus
HRP	horse radish peroxidise
ILV	intraluminal vesicle
kDa	kilo Dalton

L	liter
LB	Lewy Body
min	minute
MSA	multiple system atrophy
MVE	multivesicular endosome
NEM	N-ethylmaleimide
NAC	non-amyloid beta component
NTA	nanoparticle tracking analysis
PAGE	polyacrylamide gel electrophoresis
PBS	phosphate buffered saline
PD	parkinson's disease
PFA	paraformaldehyde
PIAS	protein inhibitors of activated STAT
PI(3)P	1,2-dioleoyl-sn-glycero-3-phospho-(1'-myo-inositol-3'-phosphate)
PI(3,4,5)P3	1,2-dioleoyl-sn-glycero-3-phospho-(1'-myo-inositol-3',4',5'-trisphosphate)
PI(3,5)P2	1,2-dioleoyl-sn-glycero-3-phospho-(1'-myo-inositol-3',5'-bisphosphate)
PI(4,5)P2	1,2-dioleoyl-sn-glycero-3-phospho-(1'-myo-inositol-4',5'-bisphosphate)
PI(5)P	1,2-dioleoyl-sn-glycero-3-phospho-(1'-myo-inositol-5'-phosphate)
PIPs	Posphatidylinositol-Phosphates
PLL	poly-L-lysine
PLP	proteolipid protein
POPC	1-palmitoyl-2-oleoyl-sn-glycero-3-phosphocholine
POPS	1-palmitoyl-2-oleoyl-sn-glycero-3-phospho-L-serine
PTM	post translational modification
Rab	Ras like protein in brain
RanBP2	Ran binding protein 2
rpm	revolutions per minute
SDS	Sodium dodecyl sulphate
SEM	standard error of the mean
SOD1	Cu/Zn superoxide dismutase
SUMO	small ubiquitin-like modifier
SIFT	scanning for intensely fluorescent targets

SIM	SUMO interacting motif
SNARE	soluble <i>N</i> -ethylmaleimide-sensitive-factor attachment receptor
SNc	substantia nigra pars compacta
SUV	Small Unilamellar Vesicle
TBS	Tris buffered saline
TDP43	TAR-DNA binding protein 43
TEMED	N'N'N'-tetramethylethylene diamine
Tnt	tunneling nanotube
Tris	Tris(hydroxymethyl)aminomethane
Tsg101	tumor susceptibility gene 101
wt	wild-type
WB	Western blot
YFP	yellow fluorescent protein

Abstract

Extracellular α -Synuclein has been implicated in interneuronal propagation of disease pathology in Parkinson's disease. How α -Synuclein is released into the extracellular space is still unclear. Here, we show that α -Synuclein is present in extracellular vesicles in the central nervous system (CNS). We find that sorting of α -Synuclein in extracellular vesicles is regulated by sumoylation and that sumoylation acts as a sorting factor for targeting of both, cytosolic and transmembrane proteins, to extracellular vesicles. We provide evidence that the SUMO-dependent sorting utilizes the endosomal sorting complex required for transport (ESCRT) by interaction with phosphoinositols. Ubiquitination of cargo proteins is so far the only known determinant for ESCRT-dependent sorting into the extracellular vesicle pathway. Our study reveals a function of SUMO protein modification as an ubiquitin-independent ESCRT sorting signal, regulating the extracellular vesicle release of α -Synuclein. We deciphered in detail the molecular mechanism which directs α -Synuclein into extracellular vesicles which is of highest relevance for the understanding of Parkinson's disease pathogenesis and progression at the molecular level. We furthermore propose that SUMO-dependent sorting constitutes a mechanism with more general implications for cell biology.

1. Introduction

1.1. Synuclein

α -Synuclein (α -Syn) is part of a protein family called the synuclein family. α -Syn was first discovered during the purification of cholinergic vesicles from the electric organ of a *Torpedo californica* fish (Maroteaux *et al.* 1988), which was the first hint for a presynaptic role of α -Synuclein. Maroteaux and colleagues were also able to detect this protein at the nuclear envelope of neurons and therefore the researchers called the unknown protein “synuclein”. Other researchers found that α -Syn is localised in the nucleus (McLean *et al.* 2000, Mori *et al.* 2002, Goncalves *et al.* 2013). Later, Maroteaux *et al.* were able to identify another protein in rat brains which was highly homologous to α -Syn (Maroteaux *et al.* 1991). In amyloid plaques from Alzheimer’s disease patients a peptide was identified, called non-amyloid beta component (NAC). Interestingly, the precursor protein of NAC, the NACP, was homologous to rat synuclein protein (Ueda *et al.* 1993). Further investigations on these synuclein proteins led to the discovery of two additional synuclein-related proteins with a length of 134 and 140 amino acids (aa) in human brain samples (Jakes *et al.* 1994). The protein with a length of 140 aa was found to be homologous to the precursor protein of NAC peptide (NACP). Furthermore, this human protein also shared a high conformity with the protein found in rat brains and in *Torpedo californica*. Thus, this protein was finally called α -Syn. Subsequently it was possible to identify two isoforms of α -Syn with a length of 112 aa and 126 aa which were identified as products of an alternative splicing pathway of the gene encoding for α -Syn (Xia *et al.* 2001, Uversky 2007). Besides α -Syn, the synuclein family also includes two other proteins, β -Synuclein (β -Syn) and γ -Synuclein (γ -Syn). β -Syn was firstly identified in extracts of human brains (Jakes *et al.* 1994). In 1984 γ -Syn was identified as the third member of the Synuclein family with a 75.3 % homology to the *Torpedo californica* Synuclein (Lavedan 1998, Lavedan *et al.* 1998).

The expression of α -Syn and β -Syn has been primarily shown in the CNS, especially in presynaptic nerve terminals in the neocortex, hippocampus, striatum, thalamus, cerebellum, cerebellar cortex, substantia nigra and brain stem (Jakes *et al.* 1994, Iwai *et al.* 1995, Irizarry *et al.* 1996) and located in the cytosol. Nakajo and co-workers have shown that both proteins are located at presynaptic terminals (Nakajo *et al.* 1994). In contrast to α -Syn and β -Syn, the third protein γ -Syn is mainly expressed in the peripheral nervous system (Buchman *et al.* 1998). Furthermore, it is known that γ -Syn is also moderately expressed in heart, skeletal muscles, and to a lesser extent in the kidney, liver and pancreas (Lavedan *et al.* 1998) and in many types of cancers, such as breast tumours (Jia *et al.* 1999).

1.1.1. Structure of α -Synuclein

α -Syn is a small 140 aa protein. It is natively unfolded and is present in neuronal cytosol and enriched in synapses. It is known that α -Syn is unstructured in aqueous solutions and that it is mainly localised to presynaptic areas, where it has also been found associated with synaptic vesicles (Cookson 2005, Lee *et al.* 2006). The sequence of α -Syn can be divided into three main regions, as indicated in Fig. 1. The amino terminal region consists of 60 aa characterised by four imperfect repeats of 11 aa, with the highly conserved KTKEGV motif, which is known to bind phospholipids (Perrin *et al.* 2000). The binding of α -Syn to lipids and thereby to membranes is a two-step process. The first step involves the binding of amino acids 3-25 and the second step includes a conformational shift of aa 26-100 into a helical structure. This conformational change further leads to the binding of α -Syn to membranes in a cooperative manner (Bartels *et al.* 2010, Bodner *et al.* 2010). A lack of aa 2-19 of α -Syn results in a decreased membrane binding of α -Syn (Karube *et al.* 2008, Bartels *et al.* 2010), indicating that this portion of the protein mediates lipid interaction.

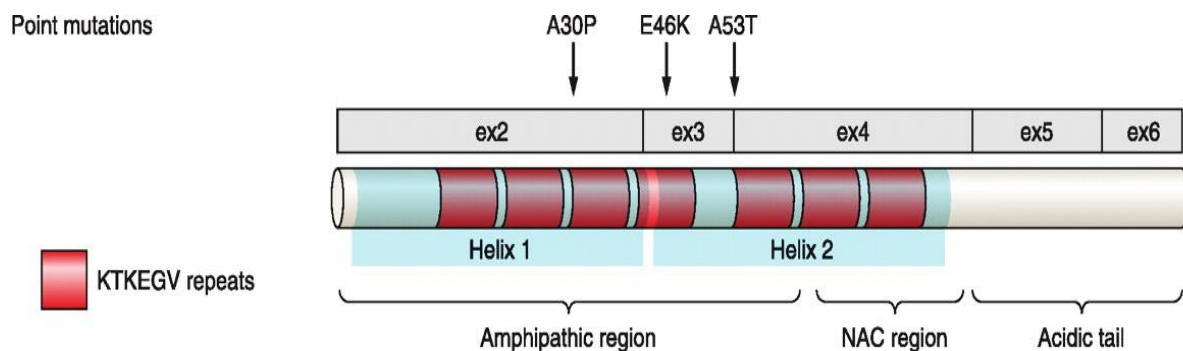


Fig. 1: Schematic representation of the α -Syn amino acid sequence

α -Syn consist three main domains. The N-terminally located amphipathic region, the hydrophobic NAC domain in the centre and an acidic C-terminal domain. Autosomal dominant mutations found in familial cases of PD are indicated with arrows. Adapted and modified from (Corti *et al.* 2011).

A hydrophobic centre domain corresponding to the NAC domain is located between aa 61-95. The NAC region contains two additional imperfect repeats and is believed to form β -rich fibrils of α -Syn. The aa 71-82 within the NAC are mainly responsible for fibril formation of α -Syn (Bodles *et al.* 2001, Giasson *et al.* 2001, Uversky *et al.* 2002) and deletion of aa 71-82 in human α -Syn prevents the protein's aggregation (Giasson *et al.* 2001). Furthermore, the NAC domain shares sequence homology with the aa sequence which is responsible for the aggregation of other amyloidogenic peptides, such as A β and prion protein (El-Agnaf *et al.* 1998). Aa 96-140 represents a highly negatively charged region at the C-terminal end of α -Syn which mainly consists of acidic residues.

It has been shown that a C-terminally truncated version of α -Syn is able to aggregate more rapidly compared to the full length protein, indicating that the C-terminus might play a role in the regulation of α -Syn aggregation (Murray *et al.* 2003).

1.1.2. Posttranslational modifications of α -Syn

The C-terminus of α -Syn is a potential target for post-translational modifications (PTM) of α -Syn. It has been shown that phosphorylation is the most common posttranslational modification of α -Syn, which predominantly occurs at aa S129 and to a lesser extent at S87 and additionally at the aa residues Y125, Y133 and Y135 (Okochi *et al.* 2000, Nakamura *et al.* 2001). Furthermore, insoluble α -Syn is extensively phosphorylated at Ser 129 in DLB brain tissue (Fujiwara *et al.* 2002). It has been shown that under physiological conditions only 4% of the soluble monomeric form of α -Syn appears phosphorylated *in vivo*. In contrast to this, 90% of α -Syn in its aggregated form is phosphorylated in Lewy bodies (LB) (Fujiwara *et al.* 2002, Anderson *et al.* 2006). This fact lead to the assumption that the phosphorylation of α -Syn at aa S129 directly correlates with the aggregation level of α -Syn (Tenreiro *et al.* 2014).

Another post-translational modification of α -Syn is the nitration of aa residues Y39, Y125, Y133 and Y136, these residues are also predominantly located in the C-terminal region of α -Syn (Giasson *et al.* 2000). Interestingly, high concentrations of nitrated α -synuclein have been found in LB (Giasson *et al.* 2000). During increased oxidative stress conditions it has been shown that α -Syn is nitrated to a higher level, suggesting an important role of oxidative stress in LB diseases (Kim *et al.* 2014). Furthermore, *in vitro* studies on the nitration of α -Syn have shown that nitration is able to induce the oligomerisation of α -Syn, which is leading to mitochondrial defects and results in apoptosis and cell death (Liu *et al.* 2011), as well as the overproduction of nitric oxide, which mediates the increase of neurotoxic α -Syn species (Danielson *et al.* 2009). Another PTM of α -Syn is SUMOylation. Dorval and Co-workers postulate that α -Syn is preferentially sumoylated by SUMO-1 (Dorval *et al.* 2006).

In contrast to this, Krumova and colleagues have shown that α -Syn can be modified by SUMO-1 and SUMO-2 in different cell lines (Krumova *et al.* 2011). In addition they demonstrate that α -Syn is sumoylated in rat brains *in vivo* and additionally that covalent attached SUMO is able to regulate aggregation induced toxicity of α -Syn (Krumova *et al.* 2011).

1.1.3. Function of α -Synuclein

α -Syn plays a major role in a variety of neurodegenerative diseases, so called Synucleinopathies. The exact physiological role of α -Syn remains poorly understood. As indicated above, α -Syn is able to bind to membranes (lipids); together with the findings of Maroteaux *et al.* in 1988 that showed synaptic localisation of Synuclein protein, this led to the assumption of a synaptic function of α -Syn. Interestingly, it has been shown by Abeliovich *et al.* that α -Syn deficient mice display a reduction in the levels of striatal dopamine including released dopamine (Abeliovich *et al.* 2000).

Overexpression of α -Syn in yeast resulted in the appearance of cytosolic lipid inclusions and the accumulation of vesicles, indicating impaired ER-Golgi trafficking induced by α -Syn (Outeiro *et al.* 2003). This notion was supported by the finding that overexpression of the small GTPase Rab1 could partially restore α -Syn toxicity and the α -Syn induced block of ER-Golgi trafficking (Outeiro *et al.* 2003, Cooper *et al.* 2006, Gitler *et al.* 2008).

Similar results have been also reported in non-neuronal cell lines (Thayanidhi *et al.* 2010), in the nematode *Caenorhabditis elegans* (Cooper *et al.* 2006, Gitler *et al.* 2008, Kuwahara *et al.* 2008, van Ham *et al.* 2008) and as well in *Drosophila melanogaster* (Cooper *et al.* 2006). These data lead to the assumption that α -Syn might play a role in the blocking of vesicle trafficking pathways. The majority of α -Syn is physiologically located at distal pre-synapses. Scott and Co-workers suggested that impairment of vesicle trafficking first occurs at synapses and might be mediated by neuronal α -Syn (Scott *et al.* 2012). They found that an excess of α -Syn is involved in the impaired mobility of recycling pool vesicles and also inhibits inter-synaptic trafficking (Scott *et al.* 2012). Furthermore, an additional study has shown that the over-expression of α -Syn significantly inhibits the release of neurotransmitters, mediated through a significant reduction in the amount of the vesicle recycling pool (Nemani *et al.* 2010). Additionally, Nemani and co-workers ruled out by ultrastructural analysis that an over-expression of α -Syn also resulted in a reduction of the density of synaptic vesicles in the active zone, combined with an impairment of vesicle re-clustering after endocytosis (Nemani *et al.* 2010). These findings are consistent with the previous findings of Scott *et al.* In conclusion it can be assumed that α -Syn plays a role in synaptic vesicle trafficking although α -Syn knockout mice display no obvious phenotype (Abeliovich *et al.* 2000). However, subtle memory deficits were recently described in these animals, supporting a potential function of α -Syn in synapse function (Kokhan *et al.* 2012). Further research will be needed to uncover to complete physiological role of α -Syn.

1.2. Synucleinopathies

Neurodegenerative diseases which are characterised by the pathological aggregation of α -Syn are termed synucleinopathies. Filamentous intracytoplasmic α -Syn inclusions are called Lewy bodies and Lewy neuritis, which are the pathological hallmarks in Parkinson's disease (PD) and dementia with Lewy bodies (DLB) (Spillantini *et al.* 1997, Spillantini *et al.* 1998b). Multiple system atrophy (MSA), a disease which is characterised by oligodendroglial inclusions of α -Syn, so called Papp-Lantos bodies (Spillantini *et al.* 1998a, Tu *et al.* 1998, Wakabayashi *et al.* 1998), also belongs to the group of synucleinopathies.

1.2.1. Parkinson's disease

Parkinson's disease (PD) is one of the most common neurodegenerative disorders affecting 1-2 % of the global population at the age of 65 years (de Lau *et al.* 2006) and about 5% of the individuals older than 85 years of age. PD is a progressive disease characterised by a specific loss of neurons, most notably dopaminergic neurons in the substantia nigra pars compacta (SNc) of basal ganglia in the midbrain. The primary symptoms in PD, which occur due to the neuronal loss, are severe motor deficits including bradykinesia, postural instability, rigidity and resting tremor, usually accompanied with a shuffling gait. The first evidence of an involvement of α -Syn pathology in PD came up in 1997, due to the identification of the missense mutation A53T in the α -Syn gene locus (*SNCA*) of familial PD patients (Polymeropoulos *et al.* 1997). Moreover, Spillantini and colleagues could demonstrate that α -Syn is the major component of Lewy bodies (Spillantini *et al.* 1997). In further investigations two additional mutations in the *SNCA* were discovered. In 1998 Krüger *et al.* discovered the familial A30P mutation and six years later the E46K mutation in *SNCA* was identified (Zarranz *et al.* 2004). In addition it has been shown that triplication of the α -Syn wt form is also responsible for autosomal dominant forms of PD (Krüger *et al.* 1998, Zarranz *et al.* 2004).

1.2.1.1. Familial Parkinson's disease

Genetically induced cases of PD are relatively rare, compared to sporadic PD cases. Several gene mutations have been described in patients with a familial form of PD. Three of the most prominent mutations are already mentioned in section 1.2.1 (A53T, A30P and E46K). In addition to mutations of the *SNCA* genes, mutations in the *Parkin* (*PARK2*) gene have been identified, as a potential source for an early onset Parkinsonism (Klein *et al.* 2007).

Interestingly, a mutation in the *PARK2* gene causes similar symptoms compared to idiopathic PD patients. Another mutation which causes familial PD has been identified in a German family in the *UCH-L1* (*PARK5*) gene, which is encoding for the ubiquitin C-terminal hydrolase-1 (Leroy *et al.* 1998). Additional mutations have been found in *PINK1* (*PARK6*) (Valente *et al.* 2002a, Valente *et al.* 2002b), the *DJ-1* gene (*PARK7*) (Bonifati *et al.* 2003) and the *LRRK2* gene (*PARK8*) (Mata *et al.* 2006).

1.2.2. Dementia with Lewy bodies (DLB)

DLB was described as a neurodegenerative dementia with Lewy body pathology (McKeith *et al.* 2005). Clinically, DLB is characterized by early cognitive impairment, visual hallucinations, Parkinson syndrome, REM sleep behavior disorder and fluctuating cognition and alertness and neuroleptic sensitivity (McKeith *et al.* 2006). The distribution of Lewy body pathology differs from that observed in PD and includes cortex and brainstem (McKeith *et al.* 2005). Some patients with PD will progress towards PD dementia (PDD) which is paralleled by an emerging cortical distribution of Lewy body pathology. This led to the assumption that PDD and DLB may represent a disease continuum rather than 2 distinct disease entities (Donaghy *et al.* 2014).

1.2.3. Multiple system atrophy (MSA)

MSA is a progressive neurodegenerative disorder characterised by a Parkinson syndrome,, cerebellar symptoms, autonomic failure. Neuronal loss was observed in the substantia nigra, the cerebellum, the pons and in the spinal cord (Bendor *et al.* 2013). In contrast to DLB and PD, α -Syn deposits predominantly occur in oligodendroglia rather than in neurons (Kim *et al.* 2014). This is followed by demyelination and subsequent neurodegeneration (Baker *et al.* 2006, Song *et al.* 2007, Huang *et al.* 2008). In contrast to PD, no familial mutations are known in the case of MSA (Ozawa *et al.* 1999, Morris *et al.* 2000, Jin *et al.* 2008).

1.3. Spreading of disease pathology

In many neurodegenerative disorders, misfolded proteins play an important role in the pathogenesis. The misfolding of these proteins promotes the fibrillar aggregation of these proteins which are neuropathological hallmarks of the respective diseases.

1.3.1. Permissive templating

The concept of permissive templating of protein misfolding and aggregation in neurodegenerative diseases is widely discussed. Permissive templating describes the induction of a disease-causing conformation by exposure of a protein to a misfolded seed, occurring in a susceptible environment. This is followed by abnormal aggregation. Induced aggregates can initiate misfolding of further proteins. Therefore, the process can proceed independently of the initial pathogenic protein, because the pathogenesis, if once initiated, becomes self-propagating (Hardy 2005). The process is characterised by a propagation phase in which the native protein will be changed to pathogenic seed, which is mediated by efficient templating of the native protein (Hardy 2005).

In the case of α -Syn it has been assumed that misfolded, monomeric α -Syn can act as a template for other monomeric α -Syn species, to convert the non-pathogenic α -helix form into the pathogenic β -sheet rich structure of α -Syn (Brundin *et al.* 2008). This is consistent with the assumption that α -Syn fibrils or rather their breakdown products are able to act as seeds. These seeds can further interact with monomeric α -Syn and are capable to induce the fibrillization of monomeric α -Syn species (Wood *et al.* 1999). According to these findings, it has been shown that seeds derived from the A30P mutant version of α -Syn are able to convert wt α -Syn into A30P fibrils (Yonetani *et al.* 2009). The process described above is comparable to the templated conversion of the non-infectious prion protein PrP^c to the infectious scrapie form PrP^{Sc} (Angot *et al.* 2010).

1.3.2. Transmission of α -Synuclein in a prion-like manner

Braak and Co-workers have shown that the progression of α -Syn pathology seems to follow a stereotypical anatomical path throughout the brain. According to Braak et al, α -Syn pathology starts in the nucleus vagus from where it spreads to the substantia nigra, followed by spreading to higher basal ganglia and neocortical regions of the brain (Braak et al. 2003). The notion of intracerebral propagation of α -Syn pathology gained much attention following *in vivo* evidence of interneuronal diseases propagation in human brains. In these studies the researchers transplanted successfully foetal dopaminergic neurons in patients with PD pathology, to compensate for the loss of dopaminergic neurons in the substantia nigra (Bjorklund et al. 2003, Olanow et al. 2003, Kordower et al. 2008a, Kordower et al. 2008b, Li et al. 2008, Mendez et al. 2008). The grafted neurons showed a robust survival and no loss in dopaminergic activity when the tissue was analysed 18 months after the surgery when one of the patients died (Kordower et al. 1995). In contrast, in post mortem brain tissues of several patients who died 14 years after the transplantation, the grafted neurons revealed Lewy body pathology (Kordower et al. 2008a, Kordower et al. 2008b, Li et al. 2008), as assessed by α -Syn, α -Syn S129p and Thioflavin staining. The obtained data by Kordower et al. and Li et al. supporting the idea of cell to cell transfer of α -Syn *in vitro* and *in vivo*, lead to the assumption of an intercellular (interneuronal) spreading of PD disease pathology

Recently, several studies with cell culture and animal models have found evidence for transcellular spreading and induction of aggregation of α -Syn (Hansen et al. 2011, Rey et al. 2013, Ulusoy et al. 2013, Luk et al. 2014, Recasens et al. 2014).

Fig. 2 displays a short overview of possible mechanisms for the intercellular (interneuronal) transmission of α -Syn including tunnelling nanotubes (Tnt), active and passive secretion of α -Syn or extracellular vesicles (EVs). Tnts are thin extensions of cell membranes that are able to connect cells over long distances. It is known that these tubes can develop by subsequent membrane fusion, during cell division, or via Actin mediated overlapping from one cell to another cell (Angot et al. 2010). However, in contrast to Huntington (Costanzo et al. 2013), α -Syn has never been observed in Tnts. Another possibility is the uptake of free interstitial α -Syn, which is released after either active secretion or by passive release from a dying neuron followed by uptake through a healthy neuron. Recently, Ulusoy et al. have shown that interneuronal spreading of α -Syn is an active process which requires living neurons (Ulusoy et al. 2015). This makes a passive release from dying neurons a less likely mechanism. Alternatively, α -Syn could be released within EVs from one cell and could be taken up by another. This could explain the directional spreading of disease pathology because EVs can carry targeting signals for cellular delivery. In addition, they could efficiently transfer large amounts of α -Syn.

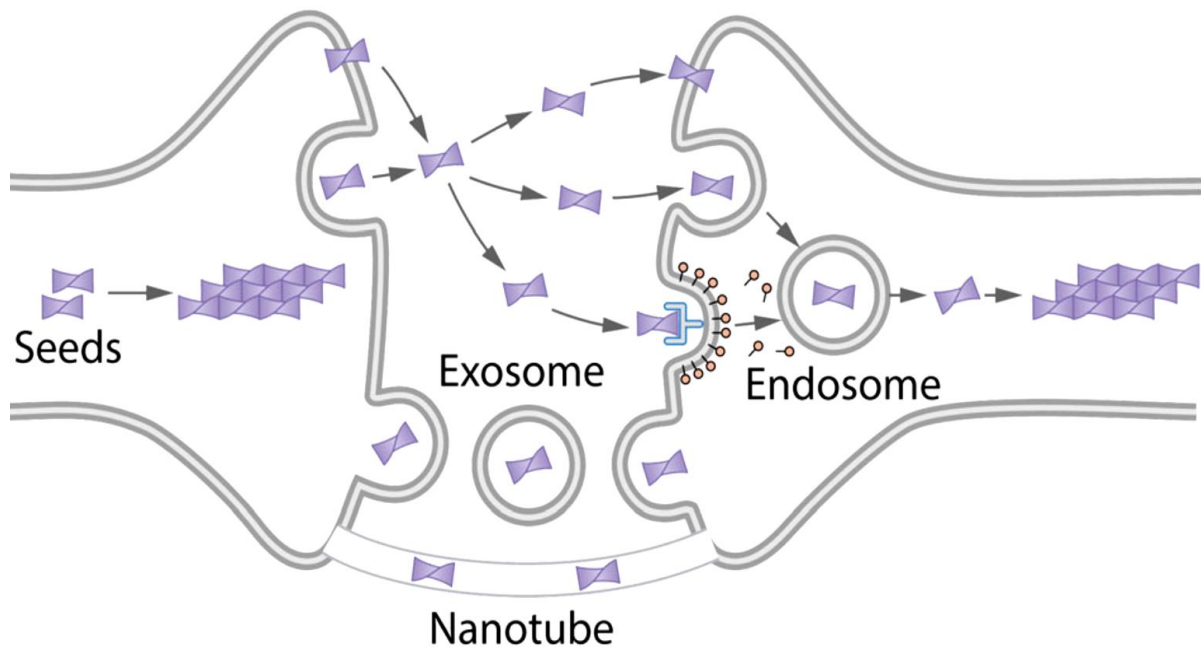


Fig. 2: Possible mechanisms for the intercellular transmission of α -Synuclein

Potential seeds of α -Syn can be released to the extracellular space within exosomes (extracellular vesicles) or either in a free form. Seeds which are released within vesicles can later fuse with the plasma membrane of another neuron and release the seeds, which can further act as seeds for additional α -Syn molecules. Seeds which are not bound to membranes of vesicles might be able to directly penetrate plasma membranes of a recipient cell. Proteins could be additionally transferred by tunnelling nanotube from one neuron to another. Adapted and modified from (Goedert *et al.* 2014).

1.4. Extracellular vesicles

The communication between cells is essential for all eukaryotic organisms. Eukaryotic cells are divided in various cellular compartments, which consist of membrane enclosed organelles. Cells are in constant contact with their environment and with other cells. This exchange of information can be mediated via direct contact or via the transfer of secreted signal molecules, like cytokines, chemokines and the uptake of secreted molecules from other cells. (Keller *et al.* 2006, Raposo *et al.* 2013). In the last decades another mechanism has been intensively discussed, the intracellular communication via transfer of extracellular vesicles from one cell to another. A variety of different extracellular vesicles are known today. Extracellular vesicles include microvesicles, exosomes and apoptotic bodies (Holme *et al.* 1994, Hess *et al.* 1999, Cocucci *et al.* 2009, György *et al.* 2011). Microvesicles or shedding vesicles have a diameter of 40-1000 nm and are derived by shedding directly from the plasma membrane. In contrast, exosomes are vesicles with a diameter of 40 nm-100 nm which are formed by inwardagination of the limiting membrane of late endosomes, giving rise to intraluminal vesicles (ILVs). The ILV filled endosomes are then termed multivesicular endosomes. Upon their fusion with the plasma membrane, ILVs are released to the extracellular space as exosomes. They were first described to be released during reticulocyte differentiation (Harding *et al.* 1983, Pan *et al.* 1983, Harding *et al.* 1984, Pan *et al.* 1985). (Johnstone *et al.* 1987). Based on morphology or biochemical properties it is not possible to distinguish between exosomes and microvesicles (Raposo *et al.* 2013). Therefore, there is now a consensus to term these vesicles extracellular vesicles (EV). EVs are released by a variety of different cells and are present in different body fluids including semen (Park *et al.* 2011, Aalberts *et al.* 2012), blood (Caby *et al.* 2005), urine (Pisitkun *et al.* 2004) and CSF (cerebrospinal fluid) (Vella *et al.* 2008).

1.4.1. Morphology and composition of extracellular vesicles

Morphology

Extracellular vesicles can be analysed via electron microscopy, where they occur in a typical cup-shaped morphology with a lipid bilayer in a diameter of 50 - 100 nm, which is consistent with the observed morphology of intraluminal vesicles inside (ILVs) of MVBs (multivesicular bodies) (Fauré *et al.* 2006). Extracellular vesicles can be purified from conditioned cell culture medium and a variety of biological fluids via ultracentrifugation approach at 100.000 x *g* (Théry *et al.* 2006).

With this ultracentrifugation protocol it is possible that other small vesicles with a similar size might simultaneously be collected. To validate the purity of the extracellular vesicle preparation subsequent methods may be used. Thus, a sucrose density gradient is often used to obtain a relatively purer preparation of EVs. In a sucrose density ultracentrifugation approach organelles derived from the Golgi apparatus, or the ER, protein aggregates and several other contaminations, show different and specific floating behaviors, which allows for the accurate separation of potential contaminations from the exosomal fraction. It is known that in sucrose gradients EVs in the size range of 40-100 nm are floating at densities of 1.13 - 1.19 g/mL (Raposo *et al.* 1996, Zitvogel *et al.* 1998, Théry *et al.* 2006). In contrast, contaminations derived from the ER are found to float at densities of 1.18 - 1.25 g/mL (Théry *et al.* 2006), vesicles from the Golgi apparatus are known to float at densities around 1.05 - 1.12 g/mL (Théry *et al.* 2006) and big apoptotic bodies float at higher densities around 1.3 – 2 g/mL, depending on their size (Gutwein *et al.* 2005).

Composition of extracellular vesicles

The protein and lipid composition of EVs depends on the releasing cell. Fig. 3 provides an overview of proteins, nucleic acids and lipids which have been identified within EVs. Proteins which are responsible for MVB formation and involved in the ESRCT complex (endosomal complex required for transport) are highly abundant in EVs (e.g. Alix and Tsg101) (van Niel *et al.* 2006). Another important group of proteins which are also associated with EVs in lipid rafts are so called Flotillins (Parolini *et al.* 2009).

Extracellular vesicles also contain heat shock proteins (e.g. like Hsp70 and Hsp90), which are known to permit peptide loading on major histocompatibility complex MHC-I and MHC-II (Gastpar *et al.* 2005). Notably, histocompatibility complexes are found to be highly enriched in exosomes that are released by parental cells from the immune system (Théry *et al.* 2001a, Théry *et al.* 2001b). Furthermore EVs are enriched in Integrins and Tetraspanins, like CD9, CD81, CD82 and CD63 (Schorey *et al.* 2008).

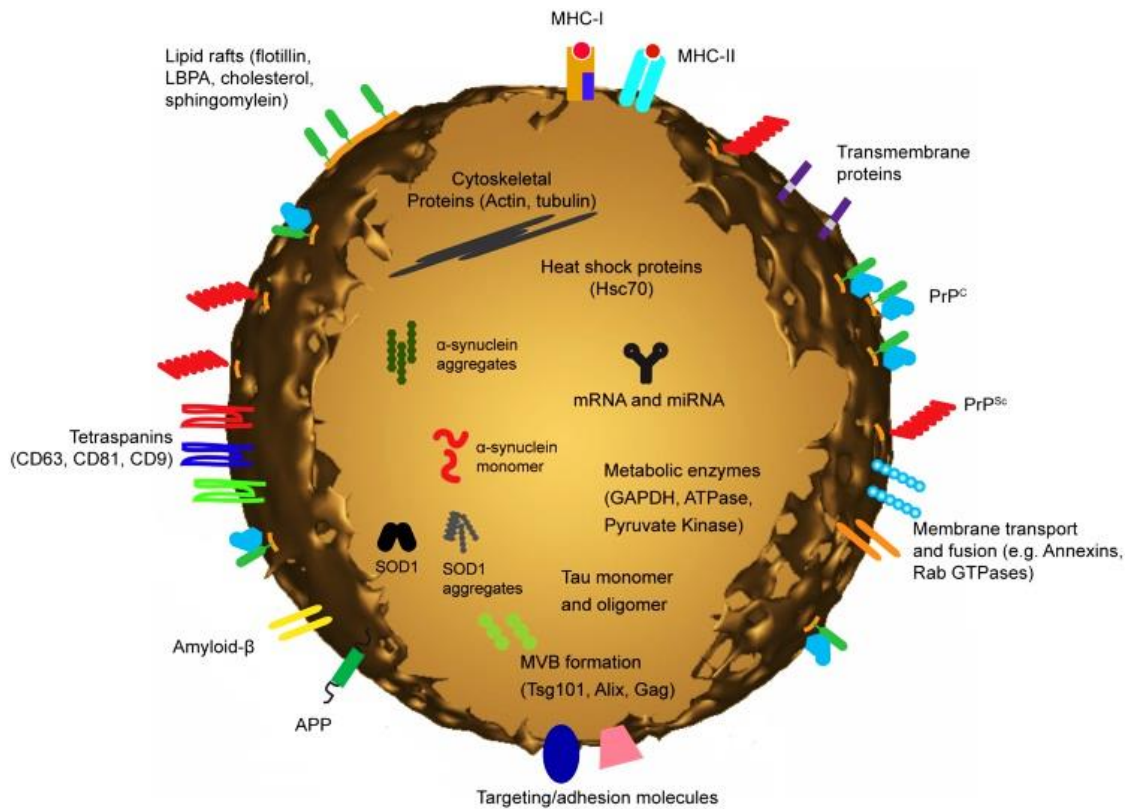


Fig. 3: Schematic view of the protein and lipid composition of exosomes

Common overview of proteins and lipids which can be reside within exosomes or attached to the outer membrane. Exosomes contain a huge quantity of proteins depending in their releasing parental cell types. Additionally they also contain nucleic acids, like different RNA species. In addition to general proteins which are involved of the formation of MVBs, exosomes can also contain proteins that are associated with neurodegenerative diseases, like PD, AD and prion diseases as well. Adapted from (Bellingham *et al.* 2012).

Different studies revealed that EVs are also highly enriched with different lipid molecules. EVs contain high amounts of cholesterol, sphingomyelin, ceramides, diglyceride, phosphatidylcholine, phosphatidylethanolamine and phosphatidylserine (Wubbolts *et al.* 2003, Laulagnier *et al.* 2004, Subra *et al.* 2007, Brouwers *et al.* 2013) as well as lipid-rich microdomains (de Gassart *et al.* 2003). The EV marker protein Flotillin-2 is known to be associated with cholesterol-rich membrane microdomains. Several studies demonstrated that EVs can also carry different RNA species, like messenger RNAs (mRNAs) and micro RNA (miRNAs) (Ratajczak *et al.* 2006, Valadi *et al.* 2007, Hunter *et al.* 2008, Rabinowits *et al.* 2009, Michael *et al.* 2010).

1.4.2. Biogenesis of extracellular vesicles

Exosomes

Exosomes are generated in cells within the endosomal system which is composed of primary endocytic vesicles, early and late endosomes and lysosomes (Mellman 1996). During endosome maturation an accumulation of vesicles occurs inside the late endosomes. These vesicles are formed by inward budding of the limiting membrane and are termed intraluminal vesicles (ILV). Late endosomes filled with ILVs are also called multivesicular bodies (MVBs) (Fevrier *et al.* 2004a). The MVBs can later fuse with the plasma membrane and ILVs can be released to the extracellular space as exosomes (Fig. 4). An alternative pathway is the fusion of MVBs with lysosomes for subsequent degradation of ILVs (Luzio *et al.* 2010). Based on morphology and biophysical properties, exosomes cannot be distinguished from shedding vesicles/microvesicles which bud from the plasma membrane. Therefore, we will use the term extracellular vesicles (EVs) throughout the text.

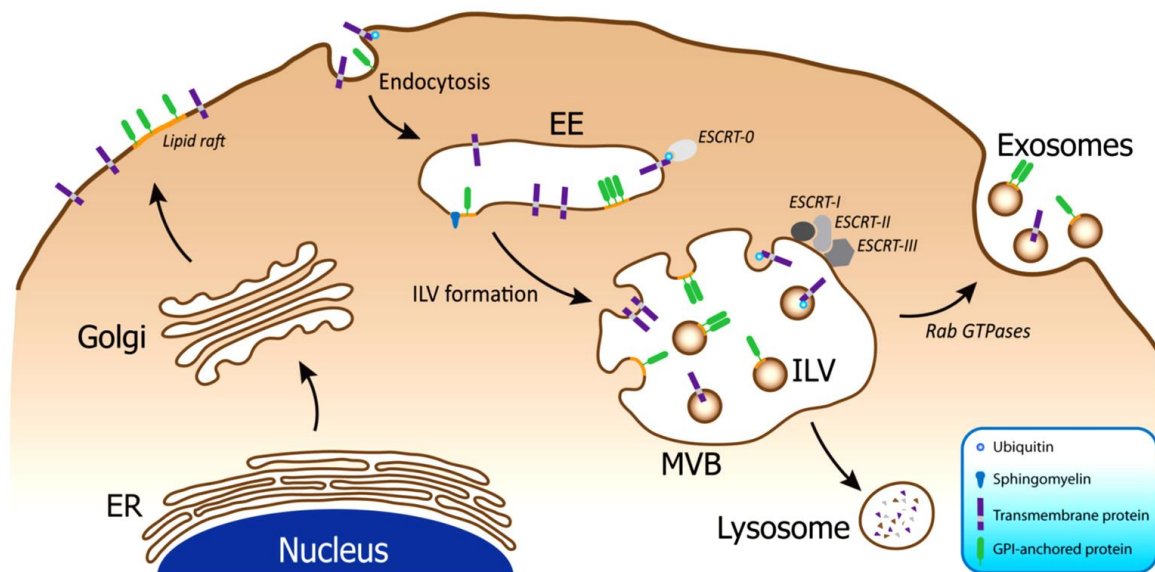


Fig. 4: Biogenesis of extracellular vesicles

Exosomes are formed within the endosomal system by inward invagination of the limiting membrane of late endosomes. This gives rise to intraluminal vesicles. The late endosome which is filled with intraluminal vesicles is then called multivesicular body. After fusion of the multivesicular body with the plasma membrane, these vesicles are released to the extracellular space as exosomes. Additionally MVBs can also fuse with lysosomes for the degradation of their cargo content. The sorting of proteins into exosomes and the biogenesis of exosomes requires the ESCRT-complexes 0 to III. Later the attachment of the MVBs and the resulting release of exosomes require several Rab GTPases. Adapted from (Bellingham *et al.* 2012)

ESCRT dependent sorting of proteins

So far, no consensus sequence for protein sorting into EVs has been identified. Posttranslational modification by monoubiquitination has been shown to direct the sorting of these proteins to the ESCRT machinery (Babst 2011, Piper *et al.* 2011). The ESCRT consists of subcomplexes 0, I, II and III. According to Hurley and Co-workers (2008), the ESCRT complexes 0-II are responsible for the recognition and sorting of ubiquitinated proteins to ILVs. Subsequent budding of vesicles from the plasma membrane is driven by the ESCRT-III complex (Hurley 2008, Hurley 2010).

The protein hepatocyte growth factor-regulated tyrosine kinase substrate (Hrs) is able to bind mono-ubiquitinated proteins and subsequently forms a complex with the proteins Signal-transducing adaptor molecule (STAM), clathrin (Raiborg *et al.* 2003) and Esp15. HRS binds via its FYVE domain to the endosome specific lipid phosphatidylinositol-3-phosphate (PI(3)P) and is therefore localized to early and late endosomes (Misra *et al.* 1999). Later the ESCRT-I is recruited and the protein Tsg101 is supposed to form a complex with ubiquitinated cargo proteins, which subsequently binds the protein Alix/AIP, leading to the recruitment of ESCRT-II. The binding of ESCRT-II initiates the oligomerisation of small coiled proteins and finally the recruitment of ESCRT-III. This complex is then responsible for the binding of the de-ubiquitinating enzyme Doa4, which removes the ubiquitin tag from the cargo proteins and finally initiates membrane budding to form ILVs. At the end of this sorting process the activity of the AAA-ATPase Vps4 is responsible for the final fission and disassembly of the ESCRT-complexes (Babst *et al.* 1998, Raiborg *et al.* 2003, Yeo *et al.* 2003, Fevrier *et al.* 2004a, Babst 2005, Keller *et al.* 2006). Recent observations revealed that ubiquitination of cargo proteins may be not the only determining factor for an interaction with the ESCRT machinery. For instance, the ESCRT-dependent sorting of the T-cell co-receptor CD4 or the delta opioid receptor DOR are not dependent on ubiquitination (Shields *et al.* 2011). It is, however, unclear, whether this reflects an ubiquitin independent ESCRT interaction. It is possible that both proteins bind to ubiquitinated interaction partners which mediate ESCRT dependent sorting. Thus, it is still not known whether ubiquitin-independent sorting mechanisms to the ESCRT-pathway exist. Recently, Villarroja-Beltri and co-workers demonstrated that the sumoylated heterogeneous nuclear ribonucleoprotein A2B1 (hnRNPA2B1), is able to interact with specific miRNA motifs. This interaction regulated the loading of these miRNAs into exosomes. Interestingly, it was shown that hnRNPA2B1 is sumoylated in EVs (Villarroja-Beltri *et al.* 2013). Based on these finding it is possible that the small ubiquitin like modifier (SUMO) could act as an ubiquitin-independent sorting determinant for the ESCRT-pathway.

ESCRT-independent sorting of proteins

ESCRT-independent sorting into extracellular vesicles was first shown for the Melanosomal protein Pmel17 (de Gassart *et al.* 2003, Theos *et al.* 2006) via a luminal domain dependent pathway (Theos *et al.* 2006). Contrary to these findings, it has been shown that the tetraspanin CD63 is involved in the endosomal sorting of PMEL during melanogenesis, in a ESCRT-dependent and independent manner as well (van Niel *et al.* 2011). Other mechanisms of ESCRT-independent sorting include interaction with tetraspanins and a ceramide-dependent pathway. Trajkovic and co-workers showed in 2008 that the ESCRT proteins Alix and Tsg101 were not involved in the sorting of the proteolipid protein (PLP). In contrast they observed that the EV release of PLP is mediated by ceramide-induced inward budding of intraluminal vesicles. Ceramide is known to have a cone-shaped morphology, which may favour the membrane invagination of late endosomal membranes to form ILVs (Trajkovic *et al.* 2008). Other studies found higher order oligomerisation to play a role in the sorting of proteins for EV release (Fang *et al.* 2007).

1.4.3. Secretion of extracellular vesicles

It has been shown that different Rab proteins are able to regulate the EV release from different types of cells. (Ostrowski *et al.* 2010). The secretion of EVs into the extracellular space is finally driven by the fusion of MVBs with the plasma membrane. It is known that this process possibly involves different SNARE proteins (Soluble N-ethylmaleimide-sensitive factor attachment protein receptors) (Pelham 2001). According to the literature, vesicular SNAREs (v-SNAREs), are localised to MVBs and are able to interact with target SNAREs (t-SNAREs). Both can form a membrane bridging complex and this complex can mediate the membrane fusion (Chaineau *et al.* 2009). As reported by Fader and co-workers in 2009, the v-SNARE complex was responsible for the fusion of MVBs with the plasma membrane in an erythroleukemia cell line ((TI-VAMP/VAMP7) vesicle associated membrane protein) (Fader *et al.* 2009).

1.4.4. Function of extracellular vesicles

Originally, it was assumed that EVs serve to discard obsolete proteins such as cytoplasm and plasma membrane during reticulocyte maturation (Johnstone *et al.* 1987). It has now become increasingly clear that EVs are involved in a variety of physiological processes, including intercellular communication (Colombo *et al.* 2014). Different studies indicate that tetraspanins alone or together with Integrins can mediate specific target cell delivery of EVs (Rana *et al.* 2011, Rana *et al.* 2012). EVs can either be internalized by endocytic uptake or direct fusion with the plasma membrane (Raposo *et al.* 2013). In addition to protein transfer, EVs are also able to deliver nucleic acids, thereby leading to changes in protein expression. E.g., Valadi and Co-workers described the transfer of mRNA from murine to human mast cells via exosomes and the subsequent translation of mouse protein in the recipient human mast cells (Valadi *et al.* 2007). *In vivo* evidence of a functionally active transfer of small RNAs and miRNAs mediated by EVs was described (Pegtel *et al.* 2010, Zomer *et al.* 2010). EVs are released by immune cells and can modulate inflammatory response (Braicu *et al.* 2015). For example, EVs are released by antigen presenting cells (APCs), like B-lymphocytes and dendritic cells which carry factors for T-Cell stimulation and MHCs, finally leading to T-cell activation (Raposo *et al.* 1996). (Wolfers *et al.* 2001, Giri *et al.* 2008, Théry *et al.* 2009, Walker *et al.* 2009). Other functions of EVs include morphogenesis (Sheldon *et al.* 2010, Gross *et al.* 2012, Luga *et al.* 2012, Beckett *et al.* 2013), e.g. in *Drosophila melanogaster* EVs were supposed to be associated with Wnt signalling and in signal transduction (Beckett *et al.* 2013).

In addition to their physiological functions, EVs take part in multiple pathological processes, including cancer metastasis (Braicu *et al.* 2015) EVs may play a role in neurodegenerative diseases. It is known that several proteins which are related to neurodegenerative disease are released within EVs. For instance, prions (Fevrier *et al.* 2004b), β -amyloid peptide (Rajendran *et al.* 2006) and α -Syn (Emmanouilidou *et al.* 2010) and it is possible that EVs related to these proteins are involved in disease propagation via the interaction with recipient cells (Raposo *et al.* 2013).

1.5. SUMOylation

SUMO (small ubiquitin like modifiers) proteins are ubiquitously expressed in all eukaryotic cells and can be conjugated to other proteins. SUMO modification is associated with regulation of gene transcription, cell cycle, DNA repair and protein localisation (Melchior 2000, Johnson 2004, Ulrich 2005).

1.5.1. The family of small ubiquitin like modifiers SUMO

Small ubiquitin like modifiers (SUMO-1 to SUMO-4) are a protein family that shares about 20% sequence homology to Ubiquitin. SUMO can be attached to lysine residues of various target proteins (Gareau *et al.* 2010). It is known that SUMO proteins are widely expressed in eukaryotic organisms. Interestingly, some lower organisms like yeast, *D. melanogaster* or *C. elegans* only encode one single SUMO gene (Geiss-Friedlander *et al.* 2007). In contrast, plants and vertebrates have several SUMO genes. The human genome encodes for several SUMO proteins (SUMO-1 to SUMO-4) (Melchior 2000, Guo *et al.* 2004). It has been shown that the SUMO proteins, SUMO-1 to SUMO-3 are widely expressed. Contrarily to SUMO-4, which has been shown to be mainly expressed in kidney, spleen and lymph nodes (Guo *et al.* 2004). The isoforms of SUMO-2 and SUMO-3 share a 97 % sequence homology to each other, and 50 % homology to SUMO-1. For all three isoforms different functions have been described (Saitoh *et al.* 2000, Rosas-Acosta *et al.* 2005, Vertegaal *et al.* 2006). In their conjugatable form SUMO-2 and SUMO-3 only differ in three aa residues in their N-terminus, therefore both isoforms are summarized to the subfamily SUMO-2/3 (Hay 2005). The physiological role of SUMO-4 is not uncovered till now, but it has been shown that SUMO-4 differs from the other SUMO-isoforms (Owerbach *et al.* 2005). Recently it has been shown that SUMO-4 is able to inhibit NFκB transcriptional activity (Hwang *et al.* 2012). In contrast to the other SUMO forms, SUMO-4 bears a proline residue in its C-terminus instead of a glutamine. Therefore, it seems that SUMO-4 is unable to form covalent isopeptide bonds with substrate proteins which prevent the maturation to a conjugatable form (Owerbach *et al.* 2005).

Interestingly, a flexible N-terminal stretch of 10-25 aa is a common feature in all SUMO isoforms. This stretch is not found in other Ubiquitin-related proteins and is supposed to be essential for SUMO chain formation (Tatham *et al.* 2001). A large number of SUMO conjugation target proteins can act as transcription factors or act as other nuclear proteins which can be involved in gene expression or DNA integrity (Gareau *et al.* 2010). Changes in levels of SUMO conjugation to other proteins can therefore be expected to have a major impact on the fate of cells.

1.5.2. The SUMOylation pathway

SUMOylation depends on the formation of an isopeptide bond between the C-terminal Glycine (Gly) residue of SUMO and the ϵ -amino group of a Lysine (Lys) residue in the target protein. SUMOylation as well as ubiquitination are dependent on an enzymatic cascade, which involves an E1-activating enzyme, an E2-conjugation enzyme and an E3-ligation enzyme (Fig. 5). Interestingly, SUMO-1 and SUMO-2/3 conjugation is driven by the identical enzymatic pathway (Tatham *et al.* 2001). The SUMOylation process is a reversible process, which primarily takes place at consensus motifs in the target proteins. This common consensus motif is defined as Ψ -K-X-[D/E], at which Ψ can be any large hydrophobic residue (I, V or L), K is defined as the target lysine, X can be any residue and D/E are aspartate or glutamate residues (Rodriguez *et al.* 2001, Sampson *et al.* 2001).

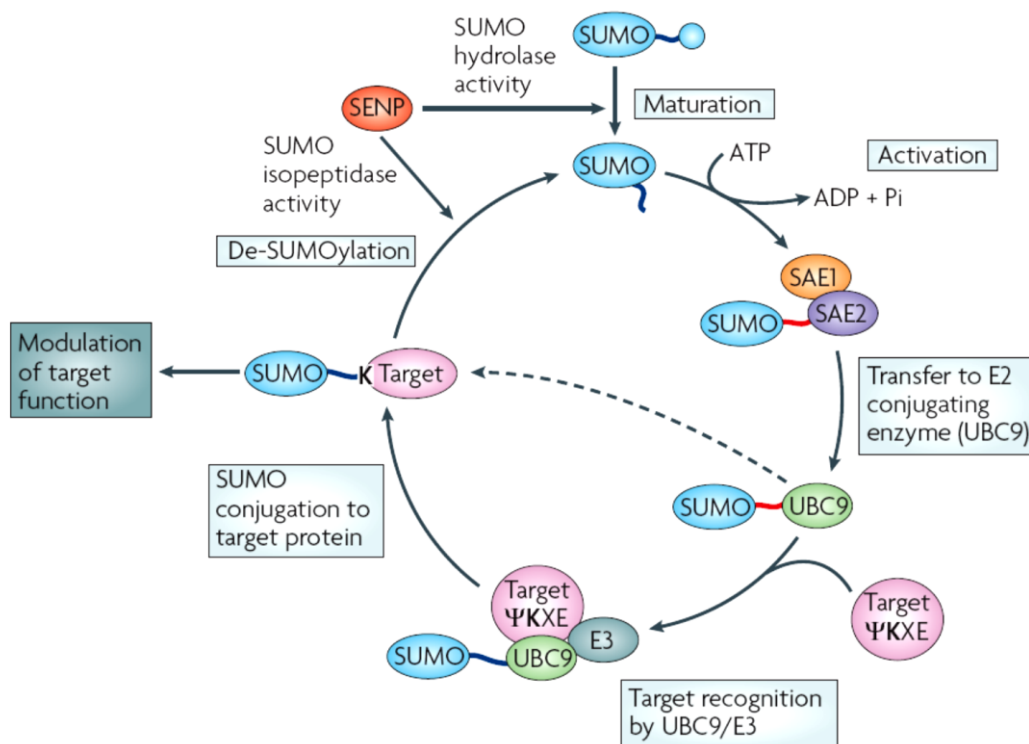


Fig. 5: Schematic representation of the SUMO cycle

SUMO-1 and SUMO-2/3 are first synthesized as precursor proteins and matured by specific SUMO proteases (SENPs), indicating the C-terminal Gly-Gly motif of SUMO. Subsequently SUMO is activated by the E1-activating enzyme, driven by the hydrolysis of ATP. Activated isoforms of SUMO are transferred to the E2-conjugating enzyme Ubc9. At the end of the cascade an isopeptide bond is formed between the ϵ -amino group of the acceptor lysine and the C-terminal carboxyl group of SUMO. Sumoylation can be reversed due to the activity of specific isopeptidase of the SENP family. Adapted from (Martin *et al.* 2007).

Briefly, SUMO precursor's proteins can be activated via the E1 activating enzyme (Desterro *et al.* 1999, Gong *et al.* 1999), via the hydrolysis of ATP.

Subsequent of this reaction, SUMO is transferred to the E2-activating enzyme, termed Ubc9 (Desterro *et al.* 1997, Johnson *et al.* 1997, Lee *et al.* 1998), which results in the formation of a thioester bond (Hay 2005) and finally in the conjugation of SUMO to the substrate, mediated by the E3-conjugating enzyme.

1.5.2.1. Enzymes involved in the SUMOylation process

The E1 activating and the E2 conjugating enzymes are identical in all SUMO paralogues and are also structurally comparable with the E1 and E2 enzymes involved in ubiquitination (Hochstrasser 2009). Enzyme Sae1 is known known to catalyse the formation of a thioester bond between Sae2 and the C-terminus of SUMO, which is driven by the hydrolysis of ATP (Lois *et al.* 2005). SUMO is now activated and can be transferred to Ubc9, the E2 enzyme in the SUMOylation process, which is driven by an intermolecular thiol transfer (Lois *et al.* 2005). Interestingly, the transfer of SUMO from Ubc9 to target proteins can also mediated via two ligase independent mechanisms. Firstly, Ubc9 can directly recognize the consensus motif Ψ -K-X-[D/E]. Secondly, SUMO target proteins can contain SUMO interacting motifs (SIM) (see section 1.5.2.2) to mediate the conjugation to SUMO on their own (Meulmeester *et al.* 2008, Zhu *et al.* 2008). Another group of enzymes that are involved in the SUMOylation process are so called SUMO ligases or E3 ligating enzymes. These enzymes are known to catalyse conjugation of SUMO to the lysine residue in the target protein (Wilkinson *et al.* 2010). It has been shown that there are three different groups of E3 ligases which can be involved in the SUMOylation pathway. So called SP-RING-finger like E3 ligases are known to function as adaptor proteins and are able to directly bind Ubc9 and the SUMO target protein (Johnson *et al.* 2001, Takahashi *et al.* 2001). In vertebrates these ligase are known as protein inhibitor of activated STAT (PIAS) (Hochstrasser 2001). In mammals five different PIAS proteins are discovered so far (Palvimo 2007). A second group of E3 ligases is defined as a nuclear pore protein and termed as Ran binding protein 2 (RanBP2) (Pichler *et al.* 2002). It has been shown that RanBP2 is able to raise the activity of Ubc9, but does not directly interact with the target protein (Reverter *et al.* 2005).

Another important group of enzymes which is involved in the SUMOylation process are sentrin specific proteases (SENPs). These enzymes are involved in the processing of SUMO peptides and in the de-conjugation process of SUMOylated target proteins (Hay 2007). In mammals six different SENPs enzymes are identified so far (Mukhopadhyay *et al.* 2007).

1.5.2.2. Non covalent SUMO binding mediated by SIM

SUMO can also bind to other proteins non-covalently. This interaction is mediated by a short conserved SUMO-interaction motif (SIM) in the SUMO binding protein. The SIM motif is composed of a hydrophobic core, which is flanked N-or C terminally by acidic residues or serine residues, respectively (Minty *et al.* 2000, Song *et al.* 2004, Hannich *et al.* 2005, Hecker *et al.* 2006). The SIM motif in SUMO-2 has been identified in a groove between the α -helix and the β -sheet and includes amino acids Q30, F31 and I33 (Hecker *et al.* 2006, Sun *et al.* 2007). Mutations of these residues to alanines abrogate the interaction of SUMO-2 with SIM domains (Meulmeester *et al.* 2008, Zhu *et al.* 2008).

1.5.3. **SUMOylation in neurodegenerative diseases**

SUMO modification has been suggested to be involved in a variety of neurodegenerative disease (Dorval *et al.* 2007a). In the last decades it becomes more and more evident that SUMOylation plays an important role and is associated with different neurological disorders, like PD, AD and Huntington's disease (HD).

1.5.3.1. SUMOylation in Alzheimer's disease

AD is the most common age related neurodegenerative disorder and is characterised by extracellular plaques composed of $a\beta$ and neurofibrillary tangles, consisting of hyper-phosphorylated tau (Wilkinson *et al.* 2010). It has been shown that both proteins are potential substrates for SUMOylation (Gocke *et al.* 2005, Dorval *et al.* 2006, Zhang *et al.* 2008). Li and co-workers observed that SUMO-2 decreases the $a\beta$ production (Li *et al.* 2003). In contrast, Dorval and co-workers showed increased $a\beta$ generation upon SUMO-3 overexpression which is independent of SUMO conjugation and might be mediated by indirect effect of SUMO-3 on APP and BACE expression levels (Dorval *et al.* 2007b). For the protein Tau, another key-player in AD, it has been shown that this protein can be SUMOylated by SUMO-1 at aa Lys 340. (Dorval *et al.* 2006). Importantly, SUMOylation at K340 inhibits tau degradation through deregulation of tau phosphorylation and ubiquitination, thereby facilitating its assembly into fibrils (Luo *et al.* 2014)

1.5.3.2. SUMOylation in Huntington's disease

The best characterised polyQ disorder is Huntington's disease (HD). This disease is caused by the expansion of a polyQ repeat in the N-terminus of the Huntingtin (Htt) protein (Gil *et al.* 2008). PolyQ disorders are dominantly inherited disorders with variations in the age of onset of the disease, which depends on the lengths of polyQ repeats (Walker 2007). It has been shown that a pathogenic fragment of Htt can be SUMOylated by SUMO-1 and as well as is ubiquitinated at the lysine residue in the N-terminus of the Htt protein (Steffan *et al.* 2004). SUMOylation stabilizes the pathogenic fragment of Htt (Httex1p) and is able to reduce its ability to form aggregates. In a *D. melanogaster* disease model of HD SUMOylation of the pathogenic Htt fragment increases neurodegeneration, contrarily to ubiquitination that has been shown to decrease neurotoxicity (Steffan *et al.* 2004). In a transgenic *Drosophila* model which is expressing both SUMO deficient and ubiquitination deficient mutations of Htt, a reduced Htt toxicity has been observed. These findings indicate that SUMOylation and ubiquitination of Htt are involved in the stabilising of toxic Htt species and that the balance between both modifications is disturbed in HD (Steffan *et al.* 2004).

1.5.3.3. SUMOylation in Parkinson's disease

In PD α -Syn is preferentially SUMOylated by SUMO-1 and to a lesser extent by SUMO-2/3 (Dorval *et al.* 2006). The influence of SUMOylation on α -Syn aggregation and toxicity, especially the formation of fibrils, under *in vitro* conditions has been shown by Krumova and co-workers (Krumova *et al.* 2011). They have shown by several approaches that SUMOylation of α -Syn inhibits neurotoxic fibril formation of α -Syn (Krumova *et al.* 2011). In addition, SUMOylation-deficient mutants of α -Syn showed a higher toxicity in mouse models, compared to wt α -Syn (Krumova *et al.* 2011). SUMO-1 has also been shown to be a component of Lewy bodies in brain tissue of patients with DLB and MSA (Pountney *et al.* 2005). Additionally, Parkin non-covalently interacts with SUMO-1, *in vitro* and *in vivo* (Um *et al.* 2006). This interaction results in the auto-ubiquitination and in the nuclear localisation of Parkin (Um *et al.* 2006). In addition SUMOylation of the protein DJ-1 has also been described (Shinbo *et al.* 2006). DJ-1 is known as a regulator for the expression of several genes which are linked to the cellular response to oxidative stress conditions (Taira *et al.* 2004). Oxidative stress conditions are known to induce the loss of dopaminergic neurons in PD (Jenner 2003).

SUMOylation of α -Synuclein

By mass spectrometry of SUMOylated α -Syn Krumova *et al* identified eleven lysine residues of α -Syn which serve as SUMO acceptor sites (Krumova *et al.* 2011). Nevertheless, only two lysine residues K96 and K102 are counting for more than 50% of the α -Syn SUMOylation. Mutations of these lysine residues (K96R K102R) impairs SUMOylation to the same extent as a D98A E104A double mutation, which disrupts the consensus sequence for the recognition of adjacent SUMO receptor lysines. These finding are consistent with the observations of Sapetschnig and colleague. They showed that SUMO acceptor sites requires the acidic residues for efficient SUMOylation (Sapetschnig *et al.* 2002).

Furthermore, Krumova *et al.* found that the ubiquitination status of α -Syn is unaffected by mutated K96 and K102 (Krumova *et al.* 2011)

2. Materials and Methods

2.1. Materials

2.1.1. Chemicals and Consumables

Unless stated otherwise, all chemicals which were used in this study were purchased from AppliChem (Darmstadt, Germany), Merck KGaA (Darmstadt, Germany) or Sigma Aldrich Chemie GmbH (Munich, Germany). Cell culture media, supplements, sera and antibiotics were purchased from PAA Laboratories GmbH (Pasching, Austria), GE Healthcare (Chalfont Buckinghamshire, UK) and Gibco® by Life Technologies (Darmstadt, Germany). Consumables which were used in cell culture, molecular biology and biochemistry analysis were purchased from Starlab GmbH (Hamburg, Germany), Eppendorf AG (Hamburg, Germany), Greiner Bio-One GmbH (Frickenhausen, Germany) or Falcon (Becton Dickinson Labware Europe, Le Pont de Claix, France).

2.1.2. Cell lines and primary cells

2.1.2.1. Cell lines

Cell lines used in this study are specified in Table 1.

Table 1: Cell lines

Name	Cell type	Obtained from
N2a	Mouse neuroblastoma cell line	(Schubert <i>et al.</i> 1969)
Oli-neu	Mouse oligodendrocyte precursor cell line	J. Trotter, University of Mainz, Germany
HEK	Human embryonic kidney cell line (HEK 293)	(Graham <i>et al.</i> 1973a, Graham <i>et al.</i> 1973b, van der Eb 1973)
<i>E. coli</i> (DH5α)	chemically competent <i>E.coli</i> strain	Invitrogen Darmstadt, Germany

2.1.2.2. Primary cells

Primary cortical neurons were prepared from E16.5 NMRI mouse embryos (for details see section 2.2.2.1).

2.1.3. Antibodies

Primary antibodies that were used in this study are specified in Table 2. Secondary fuorophore- or horseradish peroxidase (HRP) conjugated were purchase from Invitrogen (Darmstadt, Germany) and Dianova (Hamburg, Germany).

Table 2: Primary Antibodies

Antibody	Host species	Application	Obtained from
Myc (clone 9E10)	Mouse	WB	Sigma-Aldrich St. Louis, MO, USA
Myc (clone 9B11)	Mouse	WB, IF	Cell Signaling Danvers, MA, USA
Flotillin-2	Mouse	WB	BD Biosciences Heidelberg, Germany
α -Synuclein	Mouse	WB, IF	Invitrogen Darmstadt, Germany
Alix/AIP1	Mouse	WB	BD Biosciences Heidelberg, Germany
Alix(clone 3A9)	Mouse	WB	GeneTex Inc., Irvine, CA, USA
TSG-101	Mouse	WB	Santa Cruz Dallas, TX, USA
CD63	Mouse	WB	BD Biosciences Heidelberg, Germany
Beta Amyloid (6E10)	Mouse	WB	Covance Inc., Princeton, NJ, USA
GluR 2/3	Rabbit	WB	Chemicon Limburg, Germany
GluR 1	Rabbit	WB	Chemicon (Limburg, Germany)
Calnexin	Rabitt	WB	Sigma-Aldrich St. Louis, MO, USA
GFP	Rabitt	WB, IF	Invitrogen Darmstadt, Germany
Ubc9	Rabbit	WB	Santa Cruz Biotechnology Inc., Dallas, TX, USA

2.1.4. Nucleotide constructs

2.1.4.1. Previously published plasmids

Plasmids which were kindly provided by other laboratories are listed in Table 3.

Table 3: Previously published plasmids

Plasmid	Obtained from
pEYFP-N1	Clonetech, Mountain View, CA, USA
Rab5Q79L GFP	M. Zerial, MPI-CBG, Dresden, Germany
pcDNA3.1- Δ N- α -Synuclein	(Karube <i>et al.</i> 2008)
pcDNA3.1-Myc-SUMO-2	(Krumova <i>et al.</i> 2011)
pcDNA3.1-Myc-SUMO-2 Δ GG ¹	(Krumova <i>et al.</i> 2011)
pEYFP-SUMO-1	(Krumova <i>et al.</i> 2011)
pEYFP-SUMO-1 Δ GG ¹	(Krumova <i>et al.</i> 2011)
pcDNA3.1- Myc- α -Synuclein	(Krumova <i>et al.</i> 2011)
pcDNA3.1-Myc- α -Synuclein 2KR ²	(Krumova <i>et al.</i> 2011)
pcDNA3.1-Myc- α -Synuclein 2AA ³	(Krumova <i>et al.</i> 2011)
pTE1E2S1	(Uchimura <i>et al.</i> 2004)
pT7.7	P. Lansbury Cambridge, MA, USA
α -Synuclein pHGLuc1 (S1)	(Outeiro <i>et al.</i> 2008)
α -Synuclein pHGLuc2 (S2)	(Outeiro <i>et al.</i> 2008)
pcDNA3.1-Myc- α -Synuclein-SUMO-2 Δ GG	K. Eckermann Neurology UMG Göttingen, Germany
pcDNA3.1-GFP-SUMO-2 Δ GG	K. Eckermann Neurology UMG Göttingen, Germany
pcDNA3.1-Myc-SUMO-2 Δ GG cleft ⁴	K. Eckermann Neurology UMG Göttingen, Germany
pcDNA3.1-Myc-SUMO-2 Δ GG cleft+loop ⁵	K. Eckermann Neurology UMG Göttingen, Germany

pcDNA3.1-Ubiquitin-SUMO-2 Δ GG	K. Eckermann Neurology UMG Göttingen, Germany
pR4-PLP-Myc	J. Trotter, University of Mainz, Germany
pcDNA3.1-MLV Gag-GFP	W. Mothes, Yale University New haven, CT, USA
GFP-VPS4dn (E233Q)	P. Woodman, University of Manchester, UK
GFP-VPS4	P. Woodman, University of Manchester, UK
pShuttleCMV YFP-APP ^{sw}	P. Keller, MPI-CBG Dresden, Germany
YFP-APP ^{sw} -SUMO-2 Δ GG	K. Eckermann Neurology UMG Göttingen, Germany

¹ C-terminal deletion mutant that cannot be conjugated

² bearing the double mutation K96R K102R

³ bearing the double mutation D98A E104A

⁴ bearing following mutations Q30A F31A K32A I33A L42A Y46A

⁵ bearing following mutations H16A Q30A F31A K32A I33A H36A L42A Y46A D62A

SUMO-2-luciferase construct (SUMO-2-S3) was created by cloning the amino-terminal fragment of humanized Gaussia Luciferase including the same linker as used in S2 into BamHI/EcoRI sites of pcDNA3. SUMO-2 was subsequently subcloned into EcoRI/XhoI sites.

2.1.4.2. Self constructed plasmids

PcDNA3.1-GFP-SUMO-2 Δ GG Δ SIM was generated by site directed mutagenesis to introduce the triple amino acid point mutation Q30A F31A I33A. Mutagenesis was performed according to the manufactures protocol (Quick Change Site-Directed Mutagenesis Kit, Agilent Technologies, Waldbronn, Germany).

2.1.4.3. siRNA constructs

To down regulate expression of Alix/AIP1 or TSG-101, the following siRNAs were used as specified in Table 4.

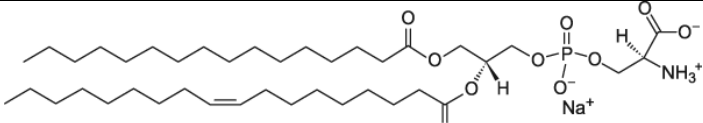
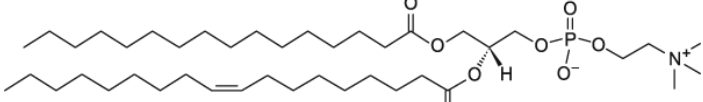
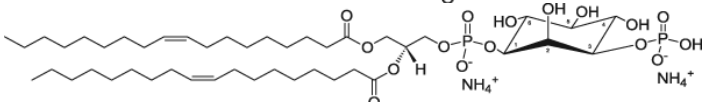
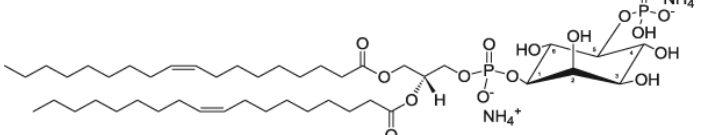
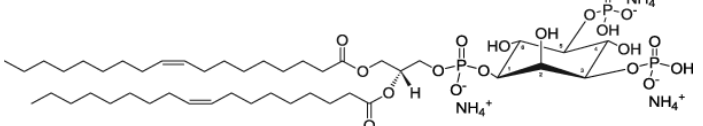
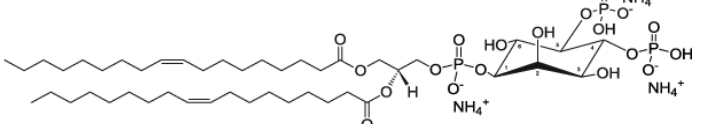
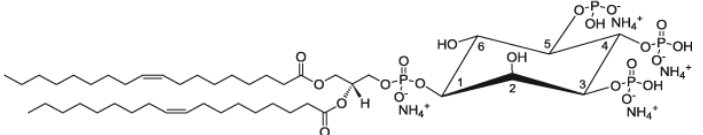
Table 4: siRNA constructs

Target	Target sequence 5'-3'	Reference
Alix mouse	AAGAACCTGGATAATTGATGAA	Qiagen GmbH, Hilden, Germany
TSG-101 mouse	CACTGTATAAACAGATTCTAA	Qiagen GmbH, Hilden, Germany
Ubc9 human (UBE2I)	CAAAAAAUCCCGAUGGCACUU	GE Dharmacon, Lafayette, CO, USA

2.1.5. Phospholipids

Phospholipids which were used in this study are specified in Table 5.

Table 5: Phospholipids

Lipid	structure	Reference
POPS		Avanti Polar Lipids Alabaster; AL, USA
POPC		Avanti Polar Lipids Alabaster; AL, US)
PI(3)P		Avanti Polar Lipids Alabaster; AL, US)
PI(5)P		Avanti Polar Lipids Alabaster; AL, USA
PI(3,5)P ₂		Avanti Polar Lipids Alabaster; AL, USA
PI(4,5)P ₂		Avanti Polar Lipids Alabaster; AL, USA
PI(3,4,5)P ₃		Avanti Polar Lipids Alabaster; AL, USA

2.1.6. Buffer and Solutions

2.1.6.1. Phosphate buffered saline (PBS)

PBS was prepared according to (Sambrook *et al.* 2001).

10x PBS (1 L)

80.0 g	NaCl
2.0 g	KCl
14.4 g	Na ₂ HPO ₄
2.4 g	KH ₂ PO ₄

To obtain 1x PBS, 10x PBS was diluted 10 times with bi-distilled H₂O and the pH was adjusted to 7.4.

2.1.6.2. Tris buffered saline (TBS)

TBS was prepared according to (Sambrook *et al.* 2001)

10x TBS (1 L)

80.0 g	NaCl
2.0 g	KCl
30.0 g	Tris

To obtain 1x TBS, 10x TBS was diluted 10 times with bi- distilled H₂O and the pH was adjusted to 7.4.

2.1.6.3. HEPES/sucrose stock solution

HEPES/sucrose stock solution was prepared according to (Théry *et al.* 2006).

1x HEPES/sucrose (1 L)

4.8 g	Hydroxyethylpiperazine-N-2-ethanesulfonic acid (HEPES), (\cong 20 mM)
856 g	Protease-free sucrose, (\cong 2.5 M)

The pH was adjusted to 7.4.

2.1.6.4. Homogenisation-buffer (HB)

320 mM Sucrose
1 mM EDTA (Ethylenediaminetetraacetic acid)
20 mM HEPES

The pH was adjusted to 7.0 and Complete protease inhibitor (Roche Diagnostics GmbH, Mannheim, Germany) was added according to the manufactures protocol.

2.1.6.5. CHAPS lysis buffer

1x lysis buffer (1 L)

10 g 3-[(3-cholamidopropyl)dimethylammonio]-1-propanesulfonate (CHAPS), ($\pm 1\%$)
6.1 g Tris(hydroxymethyl)aminomethane (Tris), (± 50 mM)
1.5 g EDTA, (± 5 mM)

The pH was adjusted to 8.0.

2.1.6.6. Protein loading buffer

5x loading buffer

10 % Glycerol
50 mM Tris-HCl
2 mM EDTA
2 % SDS
144 mM β -Mercaptoethanol
0.05 % Bromophenol blue

The pH was adjusted to 6.8.

2.1.6.7. Resolving gel buffer

90.8 g Tris, (\pm 1.5 M)

The pH was adjusted with HCl to 8.8.

2.1.6.8. Stacking gel buffer

30.3 g Tris, (\pm 0.5 M)

The pH was adjusted with HCl to 6.8.

2.1.6.9. 10x Running buffer

143 g Glycine

30.3 g Tris

10 g Sodium dodecyl sulfate (SDS)

To achieve 1x running buffer, 10x running buffer was diluted 10 times with bi-distilled H₂O.

2.1.6.10. 10x Transfer buffer

143 g Glycine

30.3 g Tris

2.1.6.11. 10x Transfer buffer

100 mL 10x Transfer buffer

200 mL Methanol

To achieve the final volume 1 L, 1x transfer buffer was filled up with bi-distilled H₂O.

2.1.7. Media and sera

2.1.7.1. Commercial media

Table 6 illustrates commercially available media, sera and additives used in this study.

Table 6: Commercial media and solutions

Medium/Solution	Obtained from
Dulbecco's Modified Eagle Medium (DMEM)	PAA Laboratories GmbH, Pasching, Austria
Fetal Calf Serum (FCS)	PAA Laboratories GmbH, Pasching, Austria
GlutaMAX™-I supplement	gibco® by LifeTechnologies, Darmstadt, Germany
Hanks' Balanced Salt Solution (HBSS)	gibco® by LifeTechnologies, Darmstadt, Germany
Opti-MEM + GlutaMAX™-I	gibco® by LifeTechnologies, Darmstadt, Germany
Penicillin/Streptomycin (Pen/Strep) 100x	gibco® by LifeTechnologies, Darmstadt, Germany
The <i>TransIT</i> ®-LT1 Reagent	Mirus Bio LLC, Madison, USA
Phosphate Buffered Saline (PBS)	PAA Laboratories GmbH, Pasching, Austria
LB medium + LB agar plate	AppliChem GmbH Darmstadt, Germany
B27-Supplement 50x	gibco® by LifeTechnologies, Darmstadt, Germany
0.25 % Trypsin-EDTA 1x	gibco® by LifeTechnologies, Darmstadt, Germany
0.05 % Trypsin-EDTA 1x	gibco® by LifeTechnologies, Darmstadt, Germany
Oligofectamine™ Reagent	LifeTechnologies, Darmstadt, Germany
MEM 10x	gibco® by LifeTechnologies, Darmstadt, Germany
Sodium Pyruvate 100 mM, 100x	gibco® by LifeTechnologies, Darmstadt, Germany
Sodium Bicarbonate Solution 7.5 %	gibco® by LifeTechnologies, Darmstadt, Germany

2.1.7.2. General growth medium

General growth medium was used in this study to cultivate mouse neuroblastoma cells (N2a) and human embryonic kidney cells (HEK 293). For preparation of serum free medium, no fetal calf serum was added.

General growth medium (500 ml)

- 5 mL GlutaMAX™-I supplement, 200 mM
- 5 mL Penicillin/Streptomycin (Pen/Strep), 5000 U/5000 µg
- 50 mL Fetal calf serum

in Dulbecco's Modified Eagle Medium (DMEM) with 4.5 g/L glucose.

2.1.7.3. SATO-medium

SATO-medium was used to cultivate Oli-neu cell line. For preparation of serum free medium, no horse serum was added.

SATO-medium (100 ml)

- 1 mL Insulin-Transferrin-Selenium-A Supplement ITS-A, 100x
- 1 mL Putrescine dihydrochloride, stock 10 mM in DMEM
- 10 µL Progesterone, stock 2 mM in ethanol
- 10 µL Triiodothyronine (Calbiochem/Merck KGaA, Darmstadt, Germany),
5 mM stock in ethanol
- 13 µL L-Thyroxine (Calbiochem/Merck KGaA, Darmstadt, Germany),
4 mM stock in 0.26 N NaOH, 25% ethanol
- 1 mL GlutaMAX™-I supplement, 200 mM
- 1 mL Penicillin/Streptomycin, 5000 U/5000 µg
- 5 mL Horse serum

in Dulbecco's Modified Eagle Medium (DMEM) with 4.5 g/L glucose.

2.1.7.4. MEM-B27

MEM-B27 was used in this study to cultivate primary cortical neurons from E16.5 NMRI mouse embryos.

MEM-B27 (250 ml)

- 15 mL 10x MEM
- 7.25 mL Sodium- Bicarbonate
- 7.5 mL 20% Glucose
- 25 mL Sodium-Pyruvate
- 2,5 mL Penicillin/Streptomycin (Pen/Strep), 5000 U/5000 µg
- 2,5 mL GlutaMAX™-I supplement, 200 mM
- 5 mL B27-Supplement

The final volume of 250 mL was adjusted with bi-distilled H₂O.

2.1.8. Commercial kits

Commercial Kits that were used in this study are listed in Table 7.

Table 7: Commercial Kits

Kit	Application	Obtained from
NucleoBond Xtra Midi Kit Quick Change Site- Directed Mutagenesis	Plasmid DNA-Isolation Point mutagenesis	Machery-Nagel, Düren, Germany Agilent Technologies, Waldbronn, Germany

2.1.9. Software

Software that was used in this study is specified in Table 8.

Table 8: Software

Software	Application	Source
ImageJ	Image processing and analysis	http://rsbweb.nih.gov/ij/
MS Office Exel 2007	Spreadsheet analysis	Microsoft GmbH, Berlin, Germany
MS Office Word 2007	Text processing	Microsoft GmbH, Berlin, Germany
EndNote X5	Citization/Bibliographie	Thomson Reuters, New York City, NY, USA
Leica Confocal Software, 2.61	Acquisition of confocal images	Leica Microsystems, Mannheim, Germany
NanoSight Tracking Analysis Software 2.3	Tracking and analysis of EVs	NanoSight, Amesbury, UK

2.2. Methods

2.2.1. Molecular biology methods

2.2.1.1. Site-directed mutagenesis

To introduce amino acid point mutations into the SIM domain of the SUMO-2 protein, site-directed mutagenesis was performed using Stratagene QuickChange™ Site-Directed Mutagenesis Kit (see Table 7). This method is based on site-directed mutagenesis using double stranded DNA templates (Braman *et al.* 1996).

2.2.1.2. Transformation of Escherichia coli (*E. coli*)

To amplify plasmid DNA constructs in bacteria, the chemo-competent *E. coli* strain “Library efficiency@DH5α™” (Table 1) was used. For transformation 45 µL of competent cells were thawed for 10 min on ice. Afterwards, 100 ng from the plasmid DNA of interest were added to the cells and incubated on ice for 30 min followed by a heat shock at 45°C for 42 s. After recovery on ice for 2 min, 600 µL of S.O.C medium was added and the cells were incubated for 1h at 37°C with agitation. In order to select single transformants, cells were plated on LB- Agar plates with the appropriate antibiotics (100 µg/ml ampicillin or 50 µg/ml kanamycin) and incubated over night at 37°C.

2.2.1.3. Plasmid DNA isolation from *E. coli*

To enlarge the amount of plasmid DNA from transformed *E. coli* at a medium scale, a single colony was picked from a LB-Agar plate and transferred to 150 mL of antibiotics supplemented LB medium. The culture was incubated for 16-20 h at 37°C with 200 rpm. Afterwards, cells were harvested by centrifugation for 10 min at 6000 rpm and 4°C. Plasmid DNA was isolated with the NucleoBond Xtra Midi Kit (see Table 7), according to the manufactures protocol.

2.2.1.4. Determination of DNA concentration

The concentration of plasmid DNA in the final solution was measured by a NanoDrop 2000 Spectrophotometer (PEQLAB Biotechnologie GMBH, Erlangen, Germany).

2.2.1.5. Expression and purification of sumoylated α -Synuclein

The expression and purification of human sumoylated wild-type α -Syn was previously described (Krumova *et al.* 2011). Briefly, BL21 competent *E.coli* cells were co-transformed with the tricistronic plasmid pTE1E2S1, which codes for the expression of SUMO-1 and the E1 and E2 enzymes of the SUMOylation pathway (Uchimura *et al.* 2004), and the pT7.7 encoding for human wild-type α -Syn (courtesy of the P. Lansbury laboratory, Harvard Medical School, Cambridge, MA). After enzymatic degradation of DNA, the bacterial extracts were heat precipitated at 95 °C for 10 min and the supernatant was subjected to column chromatography (GE Healthcare Äkta system) with a sequence of 3 columns: Q Shepharose fast flow, HiLoad 26/600 Superdex 200, and Mono Q 4.6/100 PE. Fractions of sumoylated α -Synuclein were combined and concentrated with an Amicon Ultracel Filter (10 kDa, Millipore), and purity assessed by polyacrylamide gel electrophoresis (PAGE) and electrospray ionization mass spectroscopy (ESI-MS). The protein concentration was estimated using a molar extinction coefficient at 280 nm of 9080 M⁻¹·cm⁻¹.

2.2.1.6. Expression of recombinant SUMO-2 for NMR

SUMO-2 was cloned into pET11 vector and expressed as previously described (Pichler *et al.* 2002). For N¹⁵ labelling of SUMO-2 proteins, bacterial cells were grown in 1 L LB at 37°C until the culture reached an optic density (OD600) of 0.6. Bacteria cultures were then centrifuged and resuspended in 500 ml standard Minimal M9 media containing 3 g glucose. After 30 min incubation, 1 g N¹⁵H₄Cl was added to the medium, Cells were grown for 1 h at 37°C, before induction with 1mM IPTG. SUMO purification was performed as described, except that for gel-filtration analysis a buffer containing 20mM NaH₂ PO₄/Na₂ HPO₄ pH 6.8, 100 mM KCl, 2 mM DTT was used.

2.2.2. Cell culture

All cell culture work was carried out according to security level S1 safety rules. Work was executed under sterile conditions, involving antiseptic cleaning of the equipment with 70% ethanol, UV- treatment and sterile filtration of all media and solutions with a 0.22 µm polyethersulfone (PES) filter (Corning Inc., Corning, NY, USA).

2.2.2.1. Growth and maintenance of cells

In general, cells were grown at 37°C and 5.0% (7.5% for primary neurons) CO₂ in humidified incubators. Specific cultivation procedures are described below. For collection of EVs cells were cultured in 10 cm plastic dishes, with general growth medium in the absence of serum.

Oli-neu cell line

The oligodendrocyte precursor cell line Oli-neu was grown in SATO medium (see section 2.1.7.3). The cells were grown on 75 cm² cell culture flasks or 10 cm petri dishes which were previously coated with poly-L-lysine (PLL, 30 mg/L, Sigma, St. Louis, MO, USA) for at least 30 min or overnight. Thereafter, dishes were washed 3 times with PBS. For passaging of Oli-neu cells was executed 1:6 every 2-3 days after a confluence of 70- 90% was reached. For passaging, cells were washed off with cultured medium to bring them in suspension.

Mouse neuroblastoma (N2a) and human embryonic kidney (HEK293) cell lines

The N2a and HEK293 cell lines were grown in general growth medium (see section 2.1.7.2). These cells were grown on 75 cm² cell culture flasks, 10 cm petri dishes, 6-well plates or on coverslips which were coated with PLL. Passaging of both cell lines were conducted 1:4 every second day after a confluence of 80-90% was reached. For passaging, cells were washed once with PBS and trypsinized with 3 mL of 0.25% trypsin/EDTA (see Table 6) for approximately 3 min until cells were detached. Afterwards, 10 mL of general growth medium was added to inhibit trypsin activity. The cells were used up to a passage 30.

Mouse primary cortical neurons

Primary cortical neurons were prepared from E16.5 NMRI mouse embryos and cultured on PLL coated coverslips or petri dishes, in serum free MEM-B27.

2.2.2.2. Cryoconservation of cells

Freezing of cells

To store cells for a long term period, cells were cultured on a 75 cm² cell culture flask, to a confluence of 80-90%. Cells were then cultured as described above (see section 2.2.2.1). Afterwards, the cell suspension was centrifuged at 900 rpm for 10 min and the pellet was resuspended in 1.6 mL freezing medium (50% FCS and 10% DMSO in DMEM). Thereafter, the suspension was mixed gently and transferred into a Nalgene® sterile Cryogenic vial (Thermo Fisher Scientific, Waltham, MA, USA). The vials were transferred into a Nalgene® Cryo 1°C Freezing Container (Thermo Fisher Scientific, Waltham, MA, USA) which allows a slow freezing at a temperature dropping point of 1°C/min in a -80°C freezer. For permanent storage, cells were stored in liquid nitrogen.

Thawing of cells

Cryoconserved cells were taken out of liquid nitrogen and immediately incubated in a 37°C water bath for thawing. Rapidly after the medium was defrosted the cell suspension was carefully and slowly resuspended. Then the suspension was transferred into 10 mL pre-warmed general growth medium. Afterwards the suspension was centrifuged at 900 rpm for 10 min and the pellet was resuspended in pre-warmed medium and plated in a 75 cm² cell culture flask. Growing cells were further passaged according to their cell type as described in section 2.2.2.1.

2.2.2.3. Transfection of plasmids

Introduction of plasmid DNA to mammalian cell lines was done via *TransIT®- LT1* (Mirus Bio LLC, Madison, USA). At the time of transfection the cells were grown to a confluence of 70-80%. The plasmid DNA and the transfection reagent were added to 600 µL Opti-MEM (see Table 6), mixed gently and incubated at room temperature for 30-45 min.

Based on various vessel sizes, the transfection protocol used in this study was specified in Table 9. After incubation, the mixture was added drop wise to the cells, the vessel was shaken gently and the cells were kept under cultivation conditions for 8-12 h.

Table 9: Transfection protocols

Reagent	12 well plate	6 cm dish	10 cm dish
Opti-Mem	100 µL	300 µL	600 µL
TransIT	3 µL	9 µL	18 µL
Plasmid DNA	1 µg	3 µg	6 µg

2.2.2.4. RNA interference

To down regulate protein expression, siRNA was introduced into N2a cells. SiRNA was delivered to N2a cells by Oligofectamine (see Table 6) and cells were transfected 36 h later with the plasmids of interest, followed by medium exchange after 8 h and collection for extracellular vesicles. As a control, cells were mock transfected with oligofectamine reagent in the absence of siRNA.

2.2.2.5. Collection of extracellular vesicles

In general, after 8-16 h of transfection cells were washed three times with PBS and EVs derived from Oli-neu/N2a cells were collected at least for 16 h in serum free medium to eliminate any contaminations with serum derived exosomes.

2.2.2.6. Luciferase activity assay

HEK293 cells were cultivated as described in section 2.1.2.1 and transfected with α -Synuclein and SUMO-2-luciferase constructs (α -Syn fused to full length gaussia luciferase (syn pHGluc); C-or N-terminal fragments of split pHGluc fused to α -Syn (syn-S2) or SUMO-2 (SUMO-2-S3)). After 16 h of transfection the cells were washed with PBS and the general growth medium was replaced by medium without sera and phenol red to collect EVs for 48 h. Thereafter, vesicles were prepared as described in section 2.2.3.1. Cells were washed with PBS and lysed in PBS using sonication. Luciferase activity from protein complementation was measured using same the amounts of total protein from both cell lysates and EV fractions in an automated plate reader at 480 nm. Afterwards the cell permeable substrate coelenterazine (40 μ M;PJK GmbH, Kleinbittersdorf, Germany) was added with a signal integration time of 2 seconds.

2.2.2.7. Membrane preparation

Cells were washed twice with ice cold PBS and collected into 200 μ L homogenization buffer (20 mM Na-HEPES, 1mM EDTA, 0.32 M sucrose, pH 7.0). The cells were mechanically disrupted by 10 times pipetting up and down through a yellow pipette tip and finally 10x through a 27G needle. Cells were centrifuged at 4,000 rpm for 5 min at 4 °C. The postnuclear supernatant was then ultracentrifuged with 196,000 x g for 30 min at 4 °C, followed by a washing step with PBS. The pellet containing membrane fraction and cytosol were resolved in sample buffer and subjected to SDS-PAGE and Western blotting.

2.2.3. Extracellular vesicle purification and analysis

2.2.3.1. Ultracentrifugation

Conditioned growth medium from cultured cells was collected as described in section 2.2.2.5. To purify EVs, an adapted protocol from (Strauss *et al.* 2010) was applied. Conditioned medium was collected and subjected to subsequent centrifugation steps performed at 4°C, 3,500 x *g* for 10 min, 2 times at 4,500 x *g* for 10 min, 10,000 x *g* for 30 minutes and 100,000 x *g* with a TLA 100.3 rotor (Beckman-Coulter, *k*-factor 60.6) for 60 min. Afterwards, the EV pellet was washed once with PBS (at 100,000 x *g* for 60 min) before resuspended in protein loading buffer (see section 2.1.6.6). For the quantification of extracellular protein release, postnuclear supernatants of cell lysates that were gained by scraping the cells in 1% CHAPS lysis buffer (see section 2.1.6.5) and EV fractions were subjected to Western Blot analysis. The ratio of EV protein versus cellular protein levels was calculated by Image J analysis.

For the preparation of EVs from human cerebrospinal fluid 5 ml cerebrospinal fluid was used for Western blot analysis. The samples were collected from consent informed patients. The analysis of patient cerebrospinal fluid was approved by the ethical committee of the Medical Faculty, University Medicine Göttingen (IRB 02/05/09).

2.2.3.2. Sucrose gradient ultracentrifugation

For a cleaner purification, a 100,000 × *g* pellet containing EVs were prepared as described above and resuspended in 400 µL of 0.25 M sucrose in 10 mM HEPES, pH 7.4. Afterwards, the suspension was pulled 5 times through a 26 g needle to separate potential big clusters of EVs. The extracellular vesicle-sucrose suspension was then layered on top of a discontinuous sucrose density gradient consisting of 8 layers with 400 µL each as listed in Table 10. The gradient was then centrifuged for 18 h and 200,000 x *g*, at 4°C in a Sw 60 Ti or a Sw 41 Ti rotor (Beckman Coulter GmbH, Krefeld, Germany) to separate vesicles according to their density (see Table 10). After centrifugation 8 fractions were recovered and diluted 1:6 with PBS. Thereafter, the diluted fractions were centrifuged for 1 h and 100.000 *g* at 4°C and the resulting pellet was resuspended in 15 µL sample buffer and subjected to Western Blot analysis.

Table 10: Sucrose density gradient

Molarity of Sucrose [M]	Corresponding density [g/cm ³]	Sucrose stock solution (2.5 M in 20 mM HEPES) for 2.5 mL [mL]	20 mM HEPES for 2.5 mL [mL]
0.25	1.03	0.25	2.25
0.57	1.07	0.57	1.98
0.89	1.11	0.89	1.61
1.21	1.16	1.21	1.29
1.53	1.20	1.53	0.97
1.86	1.24	1.86	0.64
2.18	1.27	2.18	0.32
2,50	1.32	2.5	0

2.2.3.3. Nanoparticle tracking analysis (NTA)

N2a cells were cultured as described in section 2.2.2.1 and transfected with *TransIT*®-LT1 (Mirus Bio LLC, Madison, WI, USA) according to the manufacturer's protocol. 8 h after transfection cells were washed with PBS and incubated in FCS-free DMEM for 16 h. Then 200 µl of culture medium was collected and centrifuged at 4°C, 5000 rpm and for 10 min to remove cell debris. All samples were carried out at 1:1 dilution with PBS. For particle size determination and particle concentration, nanoparticle tracking analysis (NTA) was performed with a NanoSight LM10 instrument (NanoSight, Amesbury, United Kingdom). This experimental set up consists of a conventional optical microscope with a high resolution camera, which uses a (<60 mW) 532 nm laser light to illuminate particles within a size of 50-1000 nm. The diluted samples were introduced into the sample chamber of the NanoSight LM10 analysis unit. While the particles in the laser beam undergo Brownian motion a video of these particle movements is recorded.

The NanoSight Tracking Analysis Software 2.3 then allows the automatic tracking of these particles and determines the particle concentration and the size distribution of the particles. Three videos with duration of 30s and a camera level of 11 were recorded for each sample. For the analysis the detection threshold was set to 10 and at least 800 tracks were analysed for each video. The concentration of vesicles smaller than 120 nm was analysed, all bigger vesicles were excluded from the analysis.

2.2.4. Protein biochemistry

2.2.4.1. SDS-PAGE

For protein separation according to their molecular weight, under denaturing conditions, sodium dodecyl sulfate polyacrylamide gel electrophoresis (SDS-PAGE) (Laemmli 1970) was performed by using the Bio-Rad Mini-PROTEAN® Tetra electrophoresis system (Bio-Rad Laboratories GmbH, Munich, Germany). The Bio-Rad Mini-PROTEAN® Tetra casting system was used to prepare two layered polyacrylamide gels. Composition of the upper stacking gel and the lower resolving gel are specified below in Table 11 and Table 12.

Table 11: Stacking gel (4%)

Chemicals	1x	2x	3x	4x
H ₂ O	1.21 mL	2.42 mL	3.63 mL	4.48 mL
Stacking buffer	500 µL	1 mL	1.5 mL	2 mL
Acrylamide (37.5:1)	540 µL	1.08 mL	1.62 mL	2.16 mL
10% SDS	20 µL	40 µL	60 µL	80 µL
APS	20 µL	40 µL	60 µL	80 µL
TEMED	3 µL	6 µL	9 µL	12 µL

Table 12: Resolving gel (12%)

Chemicals	1x	2x	3x	4x
H ₂ O	1.66 mL	3.32 mL	4.98 mL	6.64 mL
Resolving buffer	1.3 mL	2.6 mL	3.9 mL	5.2 mL
Acrylamide (37.5:1)	2.04 mL	4.08 mL	6.12 mL	8.16 mL
10% SDS	50 µL	100 µL	150 µL	200 µL
APS	50 µL	100 µL	150 µL	200 µL
TEMED	2 µL	4 µL	6 µL	8 µL

For loading on the gel, samples (EVs and cell lysates) were mixed with denaturing protein loading buffer (see section 2.1.6.6) and incubated for 5 min at 95°C. For the detection of PLP-myc protein, samples were incubated only at 55°C for 10 min to avoid assembly of multimers. After loading the sample were separated at 100 V for approximately 90 min. To estimate the molecular weights of the analyzed proteins, the protein marker PageRuler® Plus Prestained Protein Ladder (Fermentas, St. Leon- Rot, Germany), was used for every run.

2.2.4.2. Western blotting

After completion of gel electrophoresis, proteins were subjected to Western blot (Towbin *et al.* 1979). For the Western blot procedure a Mini-Trans Blot cell set up (Bio-Rad Laboratories GmbH, Munich, Germany), according to the manufacturer's protocol, was used. By this procedure, proteins were transferred from a SDS-polyacrylamide gel onto a Whatman® Protran Nitrocellulose Transfer Membrane (Whatman GmbH, Dassel, Germany), at 100 V for 55 min at 4°C.

After the protein transfer a blocking step in 4% (w/v) non-fat milk powder (AppliChem, Darmstadt, Germany) in 1% PBS was applied, for 30 min at room temperature to avoid nonspecific binding of immunoglobulins. Thereafter, the membrane was incubated with primary antibodies in 0.05% PBST (Tween-20 in PBS) in dilutions according to Table 2, for 10-12 h at 4°C. After washing three times for 15 min a specific secondary horse-radish peroxidase (HRP) coupled antibody was added to the membrane (1:2000 in PBST for EV fractions and 1:4500 in PBST for cell lysates) and incubated for 1 h at RT and washed 3 times for 25 min. Subsequently, detection of HRP coupled antibodies was achieved by an enhanced chemiluminescent reaction (Haan *et al.* 2007). Briefly, proteins were visualized by using ECL Western Blotting Substrate 1 and 2 (Thermo Fisher Scientific Inc., Rockford, IL, USA) in equal volumes. Through, the enzymatic activity of the peroxidase, light was emitted. The signal of the light was then captured on X- Ray Films (CL-XPosure™ Film, Thermo Fisher Scientific, Rockford, IL, USA) and the films were scanned and analyzed for light intensities by ImageJ (see Table 8).

2.2.4.3. FCS/SIFT measurements

For this assay the expression and purification of α -Syn and sumoylated α -Syn was performed as described previously (Krumova *et al.* 2011). The labelling of both proteins with Alexa Fluor-647-O-succinimidylester (Molecular Probes®, USA) was carried out as described previously (Giese *et al.* 2005). Green labelled small unilamellar Dipalmitoyl-sn-glycero-3-phospho-choline lipid vesicles (DPPC-SUV) were generated as described previously (Högen *et al.* 2012). Scanning for intensely fluorescent targets (SIFT) and Fluorescence correlation spectroscopy (FCS) measurements for the quantification of α -Syn vesicle binding were performed with an Insight Reader (Evotec-Technologies) with dual colour excitation at 488 and 633 nm as described before (Högen *et al.* 2012). All measurements were carried out after an incubation period of at least 30 min of DPPC-SUV with labelled α -Syn. For equilibrium conditions, measurements were performed at least 2 h after addition of unlabelled non-sumoylated α -Syn.

2.2.4.4. Electrochemiluminescence assay for quantification of α -Synuclein

For the quantification of α -Syn in cell lysates and EVs, derived from primary neurons, a slightly modified electrochemiluminescence assay was used (Kruse *et al.* 2012). Briefly, the antibody MJF-1, clone 12.1 (kindly provided by Dr. Liyu Wu, Epitopics Burlingame, USA), was coated on standard 96-well Multi-Array plates (Meso Scale Discovery, Gaithersburg, USA) and incubated over night at 4°C. All additional steps were performed at room temperature. The plates were washed three times with 150 μ L PBS + 0.05 % Tween-20. Subsequent blocking was performed with 150 μ g BSA (Meso Scale Discovery, Gaithersburg, USA) for 1 h with gently shaking at 300 rpm. A serial four-fold dilution of recombinant α -Syn (kindly provided by Dr. Omar el- Agnaf, United Arab Emirates University, Al Ain, United Arab Emirates), starting at 25.000 pg/ml, was used to prepare a standard curve. After washing as indicated above, 25 μ L of standards and samples were applied per well in duplicates. To secure a successful binding of the antibody to the samples, the plates were shaking for 1 h at 700 rpm and then washed again as indicated above. Afterwards addition of 25 μ L of Sulfo-TAG labelled anti α -Syn clone 42 (BD Transduction Laboratories, Heidelberg, Germany) was added to achieve a final concentration of 1 μ g/mL and incubated for 1 h at 700 rpm. Three washing steps followed, before 150 μ L of 2 x Read Buffer (Meso Scale Discovery, Gaithersburg, USA) was applied to each well and the plates were measured in a Sector Imager 6000 (Meso Scale Discovery, Gaithersburg, USA). The final data analysis was performed using MSD Discovery Workbench 3.0 Analysis Toolbox.

2.2.4.5. Labelling of SUMO-2 with the ESPIT dye MFM

SUMO-2 was labelled at its single cysteine (Cys) 52 with the ESPIT (excited state intramolecular proton transfer) probe MFM (Shvadchak *et al.* 2011). To uncover the Cys 52, SUMO-2 was pre-treated with 1 mM DTT and a buffer exchange to 25mM $\text{PO}_4\text{-Na}$, pH 6.5, without any sulfhydryl groups. Afterwards the protein concentration was measured and adjusted between 200 μ M and 350 μ M, followed by the addition of the MFM dye (1-4 mg/mL) in 1-2 times excess and an incubation period for 12-24 h with gently mixing at 4°C. Finally, 10 times excess of N-Methylmaleimide in DMSO was added and incubated for 30min in the same conditions as before. This step is necessary to block any remaining free Cys groups. For purification the labelled protein was applied to a gravity PD 10 column (GE Healthcare Ltd., Little Chalfont, Buckinghamshire, UK) and eluted with the same buffer, while collecting fractions of 5-10 drops. The fractions were checked for absorbance with a NanoDrop (PEQLAB Biotechnologie GmbH, Erlangen, Germany), pooled into one tube, aliquoted in small volumes and flash frozen in liquid N_2 . The labelled protein was stored at -20°C.

2.2.5. Lipid biochemistry

2.2.5.1. Preparation of Small Unilamellar Vesicles (SUVs)

Small Unilamellar Vesicles (SUVs) were prepared by sonication as described previously (Huang *et al.* 1974), (Storch *et al.* 1986), (Falomir-Lockhart *et al.* 2011). Briefly, the composition of SUVs based on mixtures of POPC, POPC and PIPS (Avanti Polar Lipids, Inc., Alabaster, AL, USA). The relative molar compositions and approximate charge densities were as follows (POPC, 100; [0], POPC:POPS, 90:10; [-0.1], POPC:POPS:PI(3)P 85:10:5; [-0.13], POPC:POPS:PI(5)P 85:10:5; [-0.14]; POPC:POPS:PI(3,5)P₂ 85:10:5; [-0.2]; POPC:POPS:PI(4,5)P₂ 85:10:5, [-0.2] and POPC:POPS:PI(3,4,5)P₃, 85:10:5, [-0.25]).

At first the lipids were mixed from their chloroform stocks, in molar ratios indicated above, in clean glass balloons, followed by drying the mixture under a gently stream of nitrogen. Afterwards the dry lipid mixture was resuspended in a specific volume of buffer (25 mM HEPES, 100 mM KCl, pH 7.26) and transferred to a falcon tube and sonicate in an ice water bath at least for 30 min, until the solution appeared translucent.

After a 1 h centrifugation at 4°C and maximum speed, the vesicles were stored at least 5°C above the transition temperature of the lipid mixture and used within 10 days of their preparation. The vesicles were quantified by determining the inorganic phosphorus (Gomori 1942).

2.2.5.2. Membrane binding assay of SUMO-2

The measurements of labelled SUMO-2-MFM with SUVs were performed with a new 96 well microplate slope assay (to be published elsewhere). This assay offers several advantages compared to conventional fluorescence assays as lipids are added to proteins. Thereby, e.g. emission and scattering from lipids, photo-bleaching effects during the sequential addition of lipids and waste of material are avoided.

The strategy of “slopes” takes advantage of the maximal sensitivity of a titration performed with lipid concentrations in excess varied around the anticipated value of the dissociation constant K_d . The slopes measured for a small number of protein concentrations are plotted versus the lipid concentrations, from which K_d and the fluorescence enhancement factor are calculated from the relation: $\text{slope} = f_0[1+(fe-1) \alpha]$, where f_0 is the slope corresponding to 0 lipid concentration and fe is the (enhanced) fluorescence of the bound protein relative to that of the free protein. Some major advantages of this assay are: the parallel readout in a microplate reader, the possible bottom readout with a small optical path length and therefore minimal scattering effects. Additionally, it is enough to use a minimal amount of reagents, endpoint determinations, that means no photo-bleaching effects.

Solutions of SUMO-2-MFM (100 nM, 200 nM and 300 nM) were prepared with 7 different SUV concentrations (0-120 μ M) in 25 mM HEPES, 100 mM KCl, pH 7.26. Afterwards 100 μ l of these 48 mixtures were added in duplicates to a 96 well quartz microplate (Hellma Analytics, Müllheim, Germany). After an incubation period of at least 10 min at room temperature, the fluorescence was recorded at 540 nm in BMG Pherastar plate reader (BMG Labtech, Ortenberg, Germany). The recording was applied with a bottom readout, well scan mode with a 10 x 10 matrix, a well scan diameter of 5 mm and with 25 flashes per well. Wells without lipid and/or protein were included to the data sets in order to establish blank values and the lipid contributions to the measured signal. Finally the data were analyzed with procedures implemented in Mathematica (Wolfram Research).

2.2.6. NMR spectroscopy

In order to study membrane binding of SUMO-2 NMR spectroscopy was performed. Thus 200 μ M of 15 N-labelled SUMO-2 in 20 mM $\text{NaH}_2\text{PO}_4/\text{Na}_2\text{HPO}_4$, pH 6.8, 100 mM KCl, 1 mM DTT was titrated with increasing concentrations (8, 16 and 32 mM) of DHPC (1,2-dihexanoyl-*sn*-glycero-3-phosphocholine). ^1H , ^{15}N -HSQC spectra were acquired at 600 MHz and 22 $^\circ\text{C}$ on a triple resonance room temperature probe with 16 transients, 2084 x 256 total points and widths of 8418 x 2129 Hz (^1H x ^{15}N). Carrier frequencies were set to the water resonance for ^1H and to 117 ppm for ^{15}N . Resonance assignments were taken from BMRB entry 11267. The normalized weighted average chemical shift difference for the amide proton and nitrogen were calculated according to $\Delta\delta$ (HN) = $[\Delta\delta_{\text{H}}^2 + (0.2 \cdot \Delta\delta_{\text{N}})^2]^{1/2}$.

2.2.7. Immunocytochemistry

2.2.7.1. Immunofluorescence staining

Proteins were labeled with specific primary antibodies and fluorophore-labeled secondary antibodies to determine their localization in cultured N2a cells. All steps of the staining protocol were carried out at RT. N2a cells were grown on PLL-coated glass coverslips, washed once with PBS and fixed then with PFA (Paraformaldehyde) (4 % PFA in PBS, pH 7.4) for 25 min. Thereafter coverslips were washed three times with PBS and cells were permeabilized in 0.1 % (v/v) Triton X-100 (in PBS), that allows the antibodies to enter the cell. Subsequently the cells were washed immediately three times and covered with 100 % blocking solution (see below) for 35 min to avoid unspecific binding of the antibodies.

Primary antibodies (see Table 2) were diluted in 10 % blocking solution and incubated with the cells in a dark and humidity chamber for 1 h at RT. After three washing steps with 1 x PBS for 5 min, cells were incubated with fluorophor-conjugated secondary antibodies in 10 % blocking solution for 1 h, again in a dark and humidity chamber. Thereafter, the cells were washed 3 times with 1 x PBS for 5 min and once with bi-distilled H₂O to remove remaining salt traces, followed by mounting the glass coverslips onto glass slides with a drop of mowiol (see below) and dried overnight. For long term period the slides were kept in the dark and stored at 4°C.

100 % Blocking solution

2 % BSA

2 % FCS

0.2 % Gelatin, from cold water fish skin

add 10 mL 10 x PBS

Fill up to 100 mL with bi-distilled H₂O. The solution was aliquoted to 5 mL and stored at -20°C.

Preparation of 16 % paraformaldehyde (PFA)

For the preparation of 16 % paraformaldehyde (PFA) solution, 16 g PFA (AppliChem GmbH, Darstadt, Germany) was mixed with 70 mL bi-distilled H₂O and dissolved by heating to 60°C. Thereafter 2-3 pellets NaOH were added, resulting in a noticeable cooling of the solution, followed by the addition of 10 mL 10 x PBS and the chilling to room temperature. Finally the pH was adjusted to 7.4 and the solution was filled up to 100 mL with bi-distilled H₂O. The solution was separated to 3 mL aliquots and stored at -20°C.

Preparation of mowiol solution

To prepare the mounting solution, 2.4 g mowiol (GmbH, Darstadt, Germany) and 6 g glycerol were mixed and incubated at room temperature for 2 h with gentle agitation. Thereafter, 12 mL 0.2 M Tris/HCl (pH 8.5) were added and the solution was mixed under heating to 50°C. A subsequent centrifugation step at 5,000 x g secure the clearance of the solution, followed by the addition of the anti-fading reagent 1,4-Diazabicyclo[2.2.2] octan (DABCO) in a final concentration of 24 mg/ml (Sigma-Aldrich St. Louis, MO, USA). Finally the mowiol solution was aliquoted and stored at -20°C.

2.2.8. Microscopy

2.2.8.1. Confocal microscopy

To visualize and record the localization of proteins, which were stained with fluorescent antibodies, in PFA fixed cells, confocal microscopy was applied. The images were acquired with a Leica DMIRE2 microscope with a 63 x oil-immersion objective and a Leica TCS SP2 AOBS confocal laser scanning setup (Leica Microsystems, Darmstadt, Germany).

2.2.8.2. Electron microscopy

EVs were prepared from cerebrospinal fluid and culture medium as described in section 2.2.3.1. The 100,000 x g pellet was fixed with 4% PFA and was adsorbed to glow-discharged Formvar-carbon-coated copper grids by floating the grid for 10 min on 5 µl droplets on Parafilm. The grids were negatively stained with 2% uranyl acetate containing 0.7 M oxalate, pH7.0, and imaged with a LEO EM912 Omega electron microscope (Carl Zeiss, Jena, Germany). Digital micrographs were obtained with an on-axis 2048 x 2084 CCD camera (Proscan GmbH, Scheuring, Germany). (Electron microscopic imaging of EVs was kindly performed by Dr. Wiebke Möbius, MPI for experimental medicine, Göttingen).

2.2.9. Image processing and statistical analysis

2.2.9.1. Quantification of extracellular vesicle secretion

To compare the relative EV release, EV pellets and the corresponding cell lysates were subjected to Western blotting as described in section 2.2.4.1 and 2.2.4.2. After developing of the Western blot membranes on X-ray films (CL-XPosure™ Film, Thermo Fisher Scientific, Rockford, IL, USA), the films were scanned and analysed with ImageJ software for the signal intensity of protein bands on the X-ray films. As a degree of EV release, the ratio of signal intensities of EVs versus corresponding cell lysates was calculated from at least 4-13 independent experiments.

2.2.9.2. Statistical analysis

Data were statistical analysed with MS Office Excel 2007 (Microsoft Deutschland GmbH, Berlin, Germany). For descriptive statistics, mean and standard error of the mean (SEM) of a data set were calculated and illustrated with MS Office Excel 2007. For the comparison of two independent groups with normal distribution of sample sets and equal variance, the parametric Student's t-test was used. A data group which displays a p-value less than 0.05 was regarded as significantly different.

3. Results

Most of these results have been published in:

Extracellular vesicle sorting of α -Synuclein is regulated by sumoylation

Marcel Kunadt, Katrin Eckermann, Anne Stuendl, Jing Gong, Belisa Russo Katrin Strauss, Surya Rai, Sebastian Kügler, Lisandro Falomir Lockhart, Martin Schwalbe, Petranka Krumova, Luis M. A. Oliveira, Mathias Bähr, Wiebke Möbius, Johannes Levin, Armin Giese, Niels Kruse, Brit Mollenhauer, Ruth Geiss-Friedlander, Albert C. Ludolph, Axel Freischmidt, Marisa S. Feiler, Karin M. Danzer, Markus Zweckstetter, Thomas M. Jovin, Mikael Simons, Jochen H. Weishaupt, Anja Schneider

Acta Neuropathol DOI 10.1007/s00401-015-1408-1

The results displayed in Fig. 9 A, Fig. 10 A, Fig. 11, Fig. 13, Fig. 17 and Fig. 18 were first performed by Surya Rai, a former master student under the supervision of Prof. Dr. Anja Schneider. In the course of this thesis, the experiments were repeated to increase the number of performed experiments and to improve the significance.

3.1. α -Synuclein is released in extracellular vesicles

In neurodegenerative diseases extracellular vesicles (EVs) have been proposed to be potential carriers of misfolded proteins and thereby may be responsible for the spreading of the disease pathology (Aguzzi *et al.* 2009). In this study we aimed to investigate how α -Syn is sorted into EVs.

3.1.1. α -Synuclein is released in extracellular vesicles derived from N2a cells

For the preparation of EVs, the conditioned medium was collected and subjected to subsequent centrifugation steps (see section 2.2.2.5 and section 2.2.3.1). In a final ultracentrifugation step at 100.000 x g for 1 h, EVs were pelleted as previously described (Trajkovic *et al.* 2008). We further refer to this 100.000 x g pellet as EV pellet (P100). The P100 and the cell lysate of the corresponding secreting parental cells were subjected to Western blot analysis and probed with an antibody against α -Synuclein. As shown in Fig. 6 A α -Syn was enriched in the P 100.

As a positive control the EV fraction and the corresponding lysates were also stained with the EV marker proteins Alix (AIP-1) and Flotilin 2 (Flot-2). In addition to the signal for α -Syn we also found intense signals for both EV marker proteins, Alix and Flot-2 in the P100. A contamination of the P100 with cellular compartments, membrane particles or other vesicles than EVs could be excluded by the absence of a signal for cellular compartments, like the ER marker protein Calnexin (Fig. 6 A).

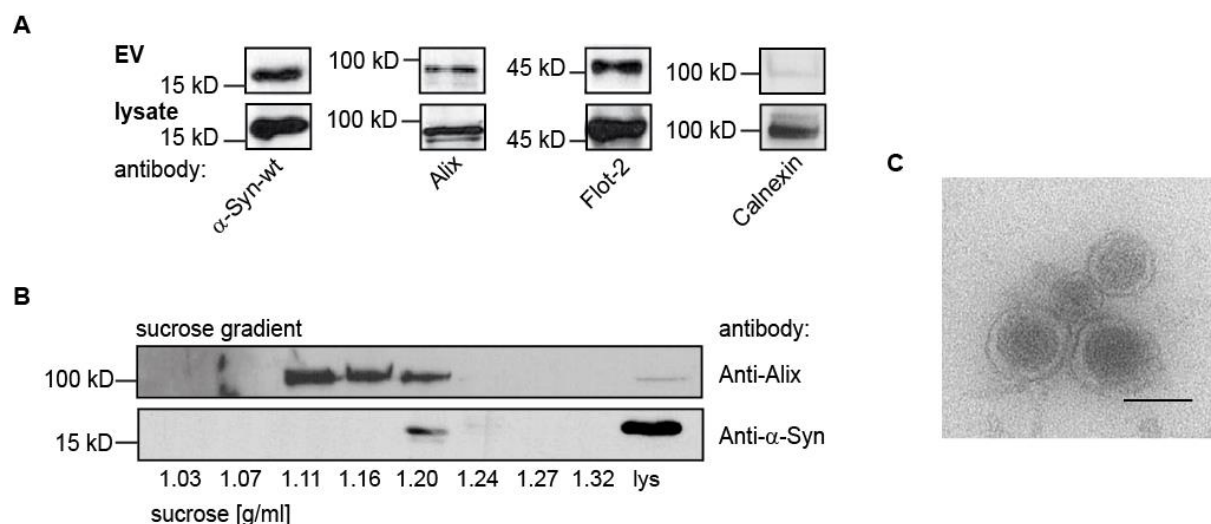


Fig. 6: α -Synuclein is released in extracellular vesicles derived from N2a cells

(A) Cultured medium of N2a cells was collected and subjected to subsequent centrifugations steps to clear the medium from cell debris, dead cells and macrovesicles with 1 x 10 min at 3500 x g, 2 x 10 min at 4500 x g and 1 x 30 min at 10,000 x g. In a final centrifugation step the EVs were pelleted. The whole EV pellet and 10 μ l of the corresponding cell lysates were subjected to Western Blot analysis. The P100 pellet is immune positive for α -Syn and the EV marker proteins Flot-2 and Alix, but negative for the ER marker Calnexin. **(B)** For a broader purification the P100 was loaded on top of a sucrose gradient (1.03-1.32 g/mL) and ultracentrifuged for 16 h at 200,000 x g. The collected fractions were ultracentrifuged again and the pellets as well as the corresponding lysates were subjected to Western Blot analysis and immune stained against α -Syn and Alix. The detected signals corresponded to known densities for EVs ranging from 1.11 to 1.20 g/mL. **(C)** EVs derived from N2a cells were processed to electron microscopy and showed their typical cup shaped morphology (scale bar 100 nm).

In another experiment we subjected the P100 to sucrose density ultracentrifugation, to get a higher purity level of the EV fraction as well as to further characterise the previous P100. The gradient was centrifuged at 200,000 x g for 16 h. After the ultracentrifugation step 8 fractions, corresponding to densities between 1.03-1.32 g/mL (0.25-2.5 M), were collected and diluted 1:6 with PBS. These fractions were processed to Western Blot analysis and immunostained for α -Syn and for the EV marker protein Alix. As shown in Fig. 6 B signals were detected for α -Syn in the fraction of 1.20 g/mL and for Alix in fractions of 1.11, 1.16 and 1.20 g/mL.

This is in line with the previous described flotation behaviour of EVs (Fauré *et al.* 2006, Théry *et al.* 2006). To visualize EVs we subjected the 100.000 x g pellet to electron microscopy and negatively stained the pellets with 1 % uranyl acetate. We found the typical cup shaped morphology (Simons *et al.* 2009) with diameter between 50 nm and 100 nm, as previously observed by transmission and cryo-electron microscopy (Conde-Vancells *et al.* 2008) (Fig. 6 C). Taken together, these data demonstrate that α -Syn is released within EVs derived from N2a cells and that we are able to recover material with our EV purification protocol.

3.1.2. α -Synuclein is localized in extracellular vesicles *in vivo*

It is not known whether α -Syn is present in EVs *in vivo*. To address this issue we firstly analysed whether α -Syn is present in EVs in the human central nervous system (CNS). Therefore, we prepared EVs from cerebrospinal fluid (CSF) after the written informed consent was given of patients with PD. Analysis of patient CSF was approved by the ethical committee of the Medical Faculty, University Medicine Goettingen (IRB 02/05/09). The CSF was subjected to a series of centrifugation steps to clear the CSF from cell debris with 1 x at 3500 x g for 10 min (P3), 2 x at 4500 x g for 10 min (P4), 1 x at 10.000 x g for 30 min (P10) and a final 100.000 x g ultracentrifugation step (P100). Pellets of each centrifugation step and the EV pellet (P100) were subjected to Western blot analysis and probed with Flot-2 and Calnexin antibodies. As shown in Fig. 7 A Flotillin 2 was enriched in the EV fraction and a contamination of the 100,000 x g pellet could be excluded by immunostaining for the ER marker Calnexin.

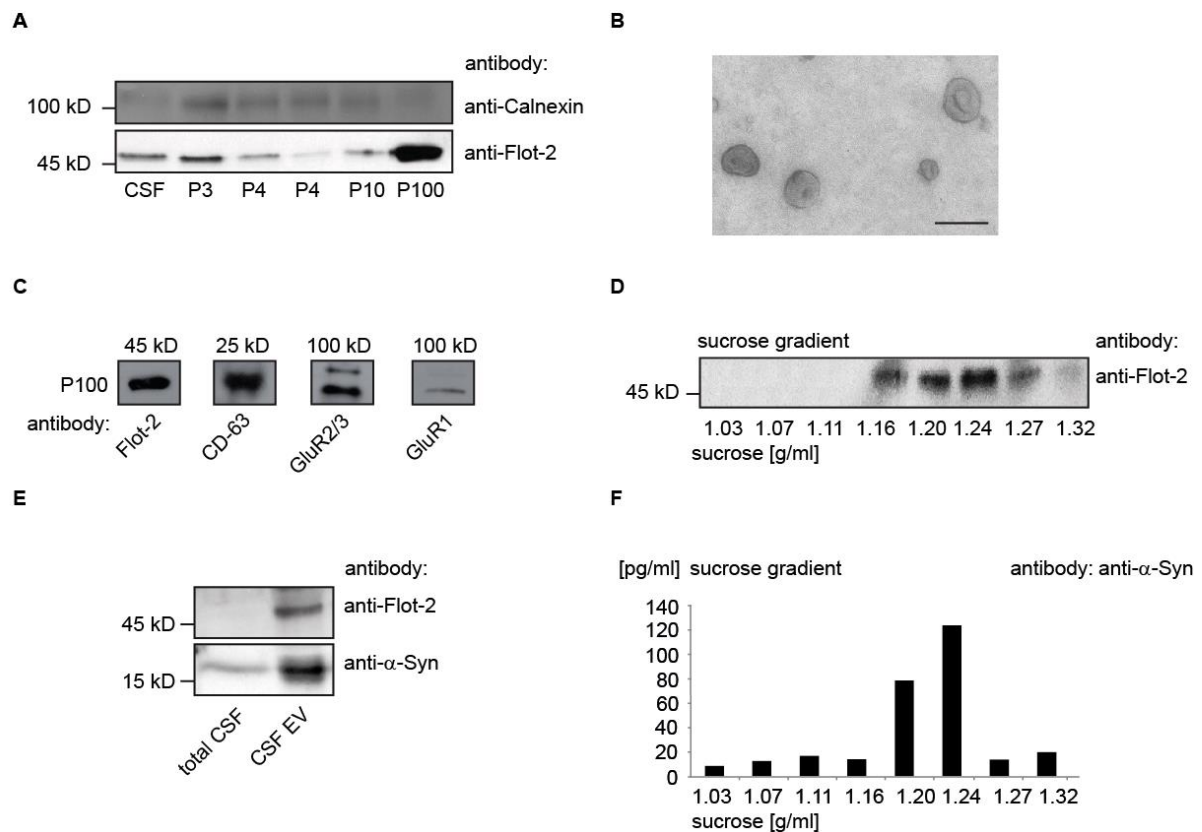


Fig. 7: Characterization of extracellular vesicles in cerebrospinal fluid

(A) Cerebrospinal fluid was processed to a series of centrifugation steps and each fraction as well as the P 100 was immunostained in Western blot. **(B)** Part of the P 100 was negatively stained with 1 % uranyl acetate and the EVs were visualized by electron microscopy (scale bar 100 nm). **(C)** Immunostaining of 100.000 x g pellets against various microsomal and EV marker proteins. **(D)** Discontinuous sucrose density gradient (0.25 M-2.5 M) was analysed by Western Blot for the presence of Flot-2. **(E)** EVs were prepared from 5 mL CSF and 20 μ L of total CSF and the corresponding 100.000 x g pellet were subjected to Western blot analysis. One representative blot out of 3 different patient samples is shown. **(F)** A 100,000 x g pellet of a Parkinson dementia CSF sample was loaded on a discontinuous sucrose gradient (0.25 M-2.5 M) and α -synuclein was quantified in each fraction via an electrochemiluminescence assay.

Electron microscopy of the resulting P100 revealed 50-100 nm structures with the typical cup shaped morphology for EVs (Fig. 7 B). The 100.000 x g pellet was also enriched for EV marker protein CD63 as well as for the Glutamate Receptors- 1, -2 and -3. This latter indicates that CSF EVs are at least partially derived from the central nervous system. Microsomal proteins such as the ER marker Calnexin and the trans golgi network (TGN) protein γ -Adaptin were absent (data not shown), thus excluding microsomal contamination of the EV preparation (Fig. 7 C). On a sucrose gradient Flotillin-2 positive EVs showed a consistent floating behaviour as supported by previously published results (Baietti *et al.* 2012). Flotillin-2 was enriched at a density of 1.16-1.24 g/mL (Fig. 7 D).

To elucidate whether α -Syn is enriched in the P100 of CSF in comparison to total cerebrospinal fluid, we processed total CSF and the corresponding 100.000 x g pellet to Western blot analysis and the samples were immunostained for α -Syn. As shown in Fig. 7 E, the 100,000 x g pellet revealed an enriched α -Syn signal compared to total CSF. In addition we performed a sucrose density ultracentrifugation experiment with a 100,000 x g pellet of a Parkinson's disease CSF sample. In this experiment EVs of CSF samples were isolated and the resulting 100.000 x g pellet was subjected to a discontinuous sucrose gradient, consisting of 8 different layers (0.25 M-2.5 M, see section 2.1.6.3). Subsequent detection of α -Syn by an electrochemiluminescence assay (see section 2.2.4.4) revealed flotation behaviour of CSF derived α -Syn, similar to the EV marker protein Flotilin-2 (Fig. 7 F). Taken together, all these findings indicate, that α -Syn associated EVs are present in the CNS *in vivo*

3.1.3. α -Synuclein is predominantly localized in the lumen of EVs

We next wanted to clarify whether α -Syn is either localized in the lumen of EVs or rather attached to the outer membrane. To this end, we transiently transfected N2a cells with a wild-type α -Syn plasmid and EVs were prepared from cultured medium and processed to subsequent centrifugations steps, as described previously in section 2.2.3.1. The P100 was resuspended in PBS and divided into two equal parts. One part was digested with trypsin and the other only with PBS as a control. The silver gel shows degradation bands for the trypsin treated P100 pellet compared to the non-trypsinized control (PBS treated) (Fig. 8 A). Western Blot analysis showed that the content of the bona fide intraluminal protein Flotilin-2 and α -Syn was unaltered by trypsin treatment, which indicates that α -Syn is localised in the lumen of EVs (Fig. 8 B).

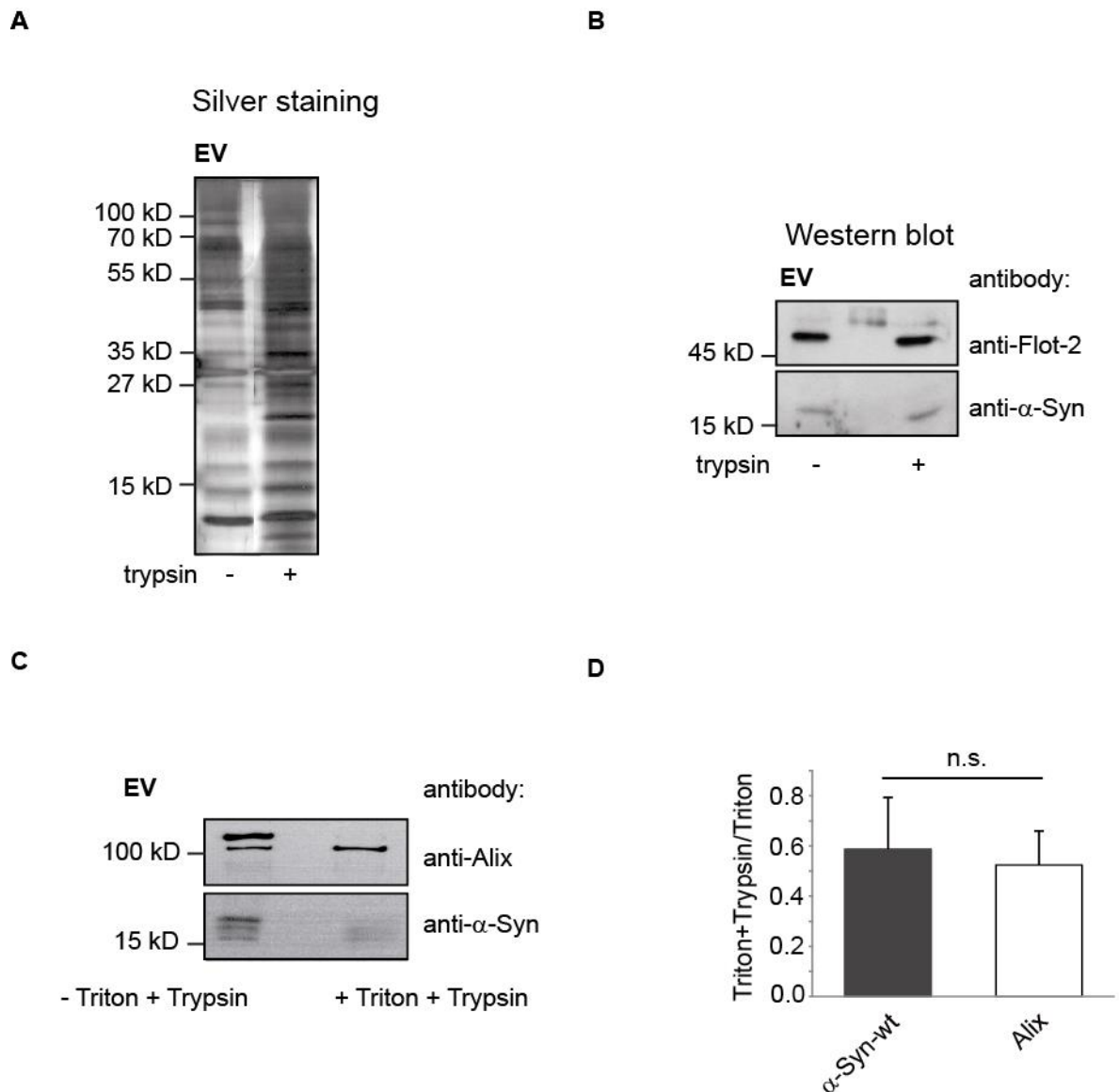


Fig. 8: α -Syn is localised in the intraluminal compartment of extracellular vesicles

(A) The 100.000 $\times g$ pellets were digested in 0.0125 % and incubated for 5 min at 37°C (right lane). As a control the other half of the pellet was incubated in PBS under the same conditions as used for the trypsin treatment. Trypsination reaction was stopped by adding sample buffer. The efficiency of the reaction was controlled by SDS-PAGE and silver staining of the gel. **(B)** Western Blot analysis of not- trypsinized (left) and trypsinized (right) EVs. The membrane was immunostained against Flotilin-2 and α -Syn. **(C)** EV Pellets were resuspended in PBS and 0.00084 % Trypsin and incubated either in the presence (right lane) or in the absence (left lane) of 1 % Triton X-100 for 3 min at 37°C. Samples were analyzed by Western Blot for staining against Alix and α -Syn. **(D)** The level of degradation was quantified by calculating the ratio under trypsin plus triton condition versus trypsin without triton condition. Values are given as mean + SEM, n.s. = not significant.

To further investigate whether α -Syn is attached to the outer membrane or resides within the lumen of EVs, we performed the same experiment as described above, but incubated the pellet either in the absence or presence of 1 % Triton (to disrupt the membrane of EVs).

The reaction was stopped by adding sample buffer (see section 2.1.6.6) and the probes were subjected to Western blot analysis and stained again Alix (AIP1) which also resides in the lumen of EVs and for α -Syn.

In contrast to the treatment without 1 % Triton, α -Syn was degraded to a similar extent as Alix when the EV pellet was trypsinized in the presence of 1 % Triton (Fig. 8 C+D).

Taken together, the trypsin digestion in the absence and in the presence of 1 % Triton revealed that α -Syn resides within the EVs rather than being attached to the outer membrane.

3.2. The extracellular release of α -Synuclein is regulated by membrane binding

To answer the question how α -Syn is targeted into the lumen of EVs, we hypothesised that cytosolic proteins such as α -Syn need to bind to the limiting membrane of late endosomes. Therefore, we hypothesized that membrane binding should have an impact on the EV release of α -Syn. Membrane binding of α -Syn involves the binding of amino acids 3-25 (Bartels *et al.* 2010, Bodner *et al.* 2010).

Therefore, we transiently transfected N2a cells with an N-terminal deletion construct of α -Syn, lacking the amino acids 2-19 (Karube *et al.* 2008, Bartels *et al.* 2010). To determine the membrane binding affinity of a Δ N-truncated version of α -Syn, we scraped the cells in a homogenisation buffer (see section 2.1.6.4) and mechanically disrupt them by passing through a 27G needle. In order to remove cell and nuclei debris we processed the suspension to a subsequent centrifugation step at 4000 rpm and 4°C for 5 min. A final ultracentrifugation step at 196,000 x *g* for 30 min at 4°C was necessary to separate cytosolic and membrane fractions. Finally, both fractions were subjected to Western blot analysis. The membrane pellets and the corresponding cytosolic fractions were immunostained with an antibody against α -Syn.

As present in Fig. 9 A, the membrane binding propensity of the N-terminally deletion construct of α -Syn was significantly decreased, compared to an α -Syn wt construct in transiently transfected N2a cells. To control the separation of cytosolic and membrane fractions, the blot membranes were probed with an antibody against Glycerinaldehyd-3-phosphat-dehydrogenase (GAPDH) as a cytosolic marker or against β 5-Integrin as a membrane marker (Fig. 9 B and C).

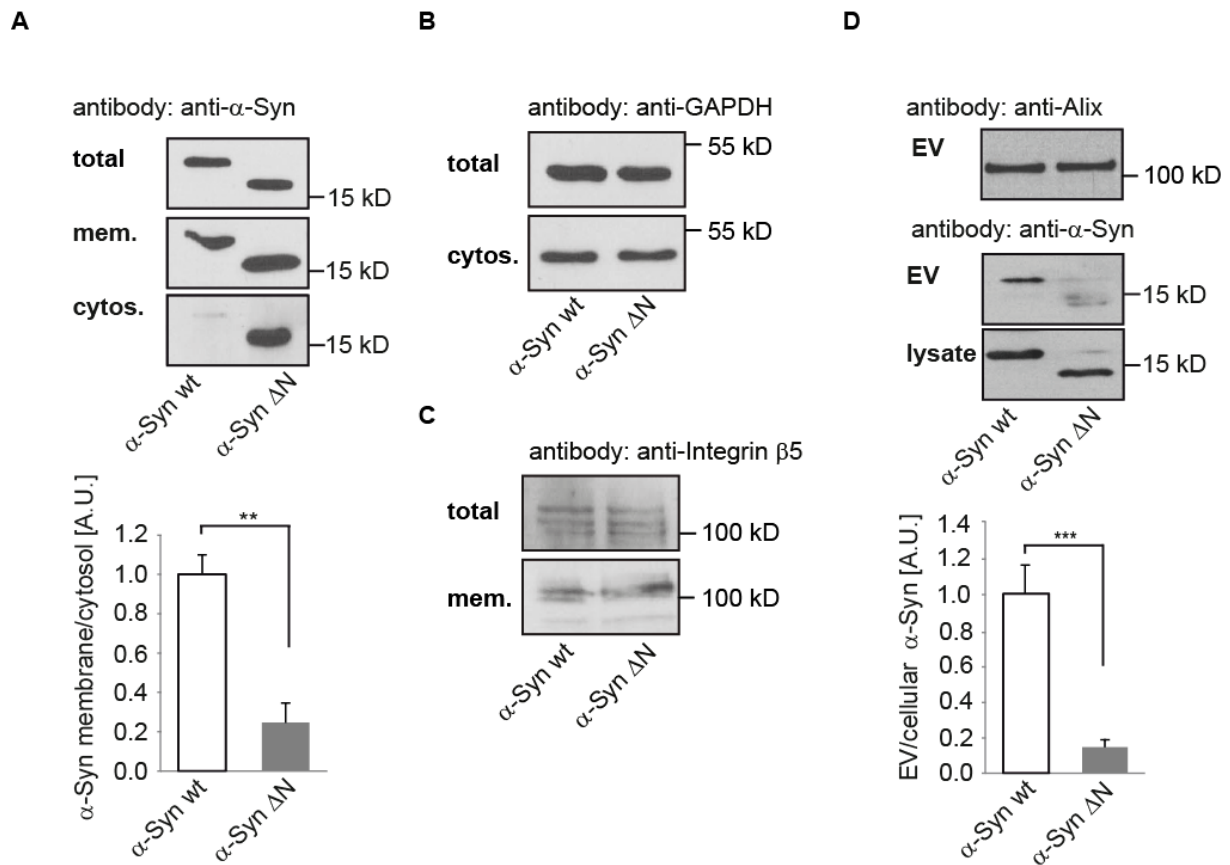


Fig. 9: Membrane binding regulates release of α -Synuclein within extracellular vesicles

(A) Plasmids encoding for α -Syn wt and the N-terminally truncated version (Δ N) of α -Syn were transiently transfected in N2a cells. The cells were scraped, mechanically disrupted and subjected to different centrifugation steps to separate membrane and cytosolic fractions. Complete membrane pellet and a proportion of the cytosolic supernatant were processed to Western blot analysis (top). To quantify the ratio of membrane associated α -Synuclein, the ratio of protein intensity in the membrane fraction versus protein intensity of the cytosolic fraction was determined (bottom). Values are given as mean + SEM from $n = 8$ experiments; ** indicates $p < 0.005$. (B+C) The blots in (A) were re-probed with an antibody against GAPDH as a cytosolic marker and against β 5-Integrin as a membrane marker, respectively. (D) N2a cells were transfected with the same constructs as in (A). EVs were prepared from cultured medium of N2a cells and the ratio of EVs to the corresponding cell lysate protein was quantified upon Western blot analysis (top) and signal intensity was measured with ImageJ (bottom). As a positive control for EVs, the membrane was re-probed with an antibody against the extracellular marker protein Alix. (A+D) Results are given as mean + SEM from $n = 8$ independent experiments; *** indicates $p \leq 0.001$; student's 2-side t-test.

Next, we wanted to know whether membrane binding indeed regulates the release of α -Syn within EVs. Therefore we transfected N2a cells with the N-terminal deletion construct of α -Syn. To quantify the EV release of α -Syn we collected and prepared vesicles as described in sections 2.2.2.5 and 2.2.3.1. To determine the EV release of both constructs, we subjected the EV pellet and the corresponding parental cell lysates to Western blot analysis and probed the membrane with an antibody against α -Syn.

As shown in Fig. 9 D (upper panel), the N-terminal deletion construct of α -Syn was largely excluded from the EV fraction in comparison to the α -Syn wt construct. Altogether, this data demonstrates that membrane binding is required for the sorting of α -Syn into EVs.

3.3. SUMOylation regulates membrane binding and extracellular vesicle release of α -Synuclein

We hypothesized that SUMOylation might regulate the release of α -Syn by modulating the binding of α -Syn to lipid membranes. In a previous study the two major SUMOylation sites in α -Syn (K96 and K102) were described to be in close proximity to the membrane interacting α -helical regions of α -Syn (Krumova *et al.* 2011). We wondered whether SUMOylation of these sites might modulate its interaction of with lipid membranes.

3.3.1. SUMOylation modulates membrane binding of α -Synuclein

We transiently transfected N2a cells with myc- α -Syn constructs either bearing the K96R K102R double mutation at both sumoylation sites which account for more than 50 % of protein's SUMO modification, further referred to as 2 KR mutant, or the D98A E104A double mutation, further referred to as 2 AA mutant, which disrupts the consensus sequence for sumoylation (Krumova *et al.* 2011).

After transfection, N2a cells were mechanically disrupted followed by a subsequent centrifugation step to remove cell and nuclei debris. The postnuclear supernatant was then processed to an ultracentrifugation step to separate membrane pellet and cytosolic supernatant. Thereafter, SDS-PAGE and subsequent Western Blot analysis was performed, to investigate the membrane binding of both SUMO-deficient mutants.

As displayed in Fig. 10 A we found that the membrane binding of both SUMO-deficient mutants (α -Syn 2KR and α -Syn 2AA) was significantly attenuated when compared to a myc- α -Syn wt construct. To verify if the separation of cytosolic and membrane fractions was successful, we re-probed the membrane with an antibody against GAPDH, as a positive control for the cytosolic fraction and with an antibody against β 5-Integrin as well, as a positive control for the membrane fraction (Fig. 10 B and C).

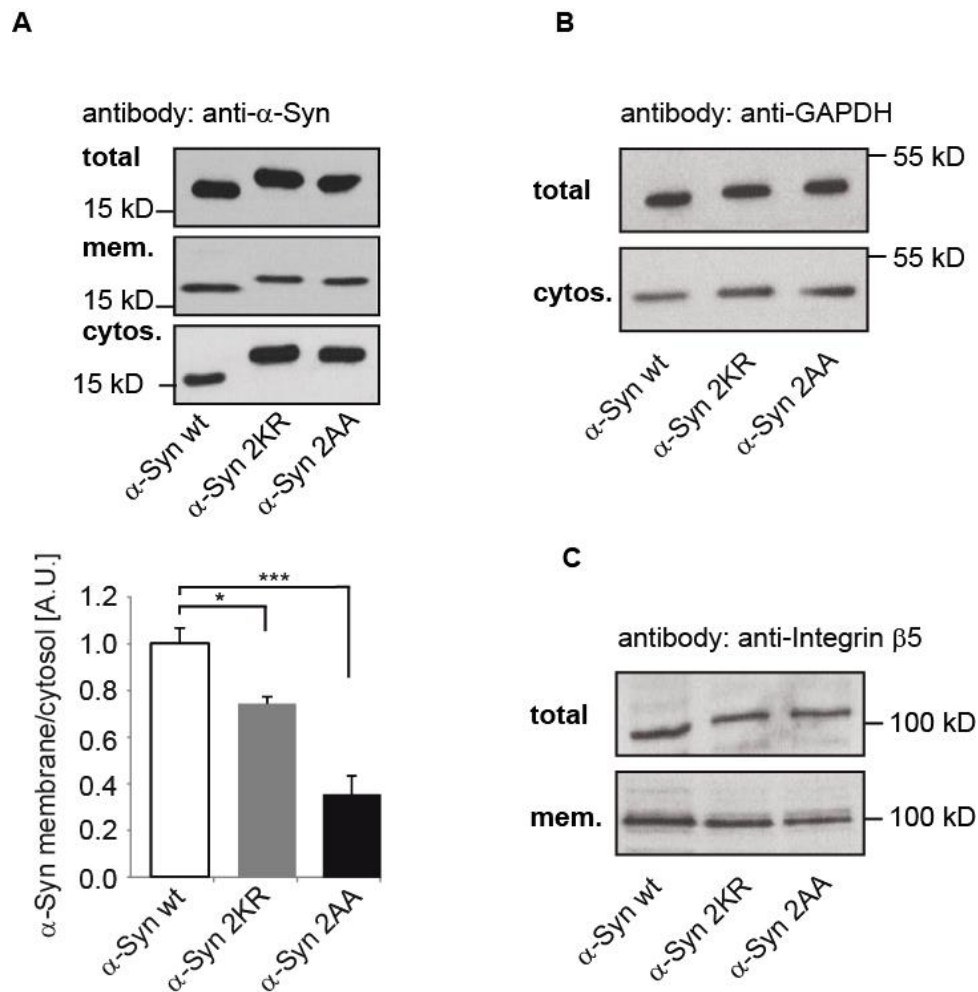


Fig. 10: Membrane binding of SUMO- deficient α -Syn mutants 2 KR and 2 AA

(A) N2a cells were transiently transfected with the indicated α -Syn mutant constructs and a wt construct of α -Syn. Cells were scraped and resuspended in homogenisation buffer and mechanically disrupted by passing through a 27G needle. A final 196,000 $\times g$ step leads to a separated membrane and to cytosolic fraction as well. Membrane pellets and the corresponding cytosolic supernatant were analysed by Western blotting (left) and immunostained against α -Syn. For quantification of membrane binding the ratio of α -Syn signal intensity in membrane pellets versus signal intensity in the cytosolic supernatant were determined (left, bottom). (B+C) The blots in (A) were re-stained with antibodies against GAPDH as a cytosolic marker and against β 5-Integrin as a membrane marker. All Values are given as mean + SEM from $n = 12$ experiments for α -Synuclein wild-type, $n = 12$ experiments for 2 KR and $n = 12$ experiments for 2 AA with α -Syn wt normalized to 1. * indicates $p \leq 0.05$, *** indicates $p \leq 0.001$; student's 2-side t-test.

Having confirmed that both SUMOylation sites in α -Syn at aa 96 and 102 are required for the binding of α -Syn to lipid membranes, we designed a myc- α -Syn SUMO fusion construct, mimicking SUMO modification and bearing a Δ GG mutation, which prevents the SUMO conjugation to other proteins and to SUMO itself. After transient transfection, membrane pellets as well as cytosolic supernatants of transfected cells were subjected to Western blotting and probed against α -Syn. As shown in Fig. 11 A, membrane binding of an α -Syn SUMO fusion protein was markedly increased in N2a cells, compared to the wild-type protein of α -Syn (Fig. 11 B).

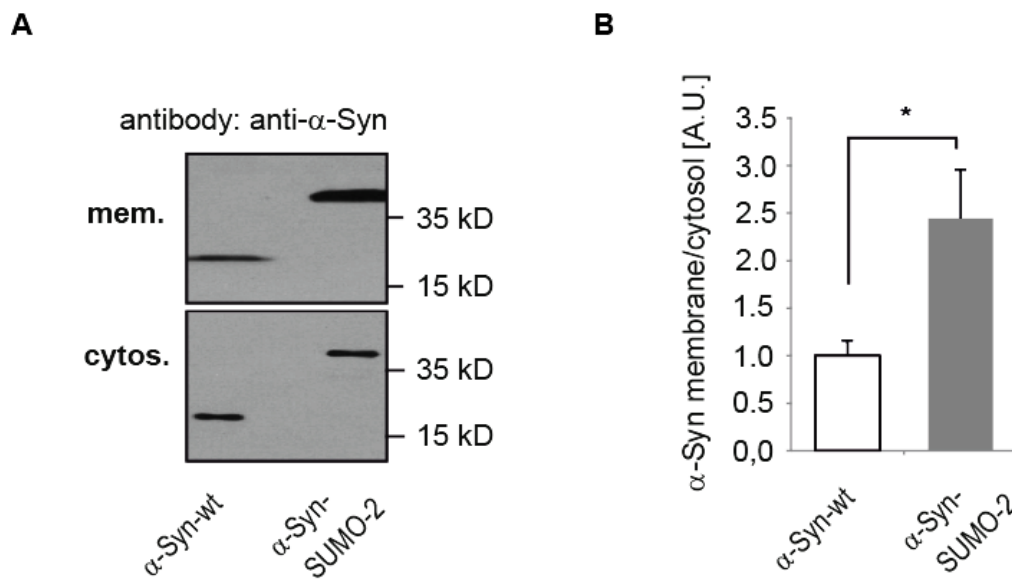


Fig. 11: Membrane binding of a myc- α -Syn-SUMO fusion construct

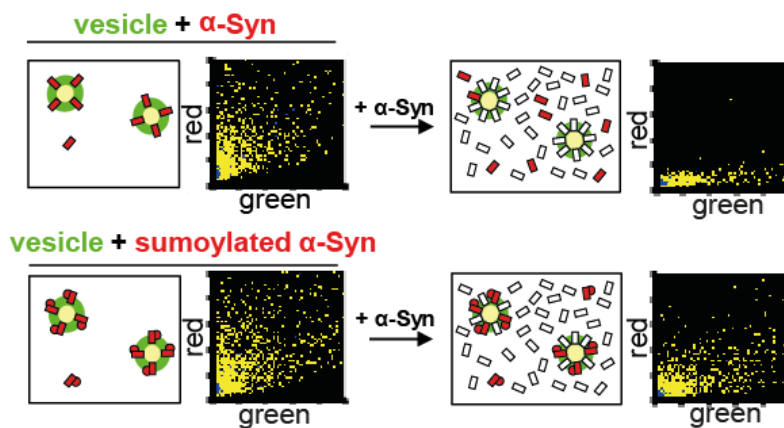
(A) Plasmids which are either encoding for α -Syn wt or for α -Syn-SUMO-2 Δ GG-fusion construct were transfected in cell line N2a. The membrane pellet and the cytosolic supernatant were processed to SDS-PAGE and subsequent analysed by Western blot and membranes were probed with an antibody against α -Synuclein. **(B)** For quantification of membrane binding, the ratio of protein intensity of the membrane pellet versus the corresponding cytosolic supernatant was determined (right). All values are given as the mean + SEM from $n = 6$ experiments, and the mean for α -Syn wt was normalized to 1; * indicates $p \leq 0.05$; student' 2-side t-test.

Our collaboration partner Prof. Giese (Dept. of Neuropathology and Prion Research, Ludwig-Maximilians University Munich) employed fluorescence correlation spectroscopy (FCS)-scanning for intensely fluorescent targets (SIFT) (Giese *et al.* 2005, Högen *et al.* 2012) as a complementary method, aiming to confirm that the membrane binding propensity of α -Syn is regulated by SUMOylation. This method is based on a single particle analysis by adapting a method, derived from fluorescence correlation spectroscopy (Giese *et al.* 2005). This technique is also used for the efficient analysis of protein aggregation in neurodegenerative diseases, like prion diseases and in Alzheimer's disease (AD) (Schwille *et al.* 1997, Pitschke *et al.* 1998, Post *et al.* 1998, Bieschke *et al.* 2000, Giese *et al.* 2000, Giese *et al.* 2004, Bertsch *et al.* 2005).

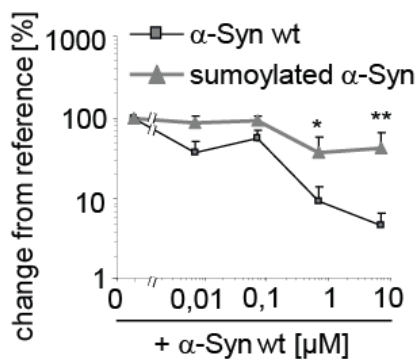
They used a two colour scanning set up with red and green fluorophores and two different excitation lasers together with recombinant α -Syn and recombinant sumoylated α -Syn (for purification method, see section 2.2.1.5), labelled with Alexa Fluor-647-O-succinimidylester (Giese *et al.* 2005) which competed for the binding of the green labelled small unilamellar Dipalmitoyl-*sn*-glycero-3-phospho-choline lipid vesicles (DPPC-SUV) (Högen *et al.* 2012).

The frequencies of specific combinations of green and red photon counts were recorded in a two-dimensional (2D) intensity distribution histogram Fig. 12 A. The fluorescence intensity data were calculated by summing up high intensity bins over a defined time period (Fig. 12 B right panel).

A



B



C

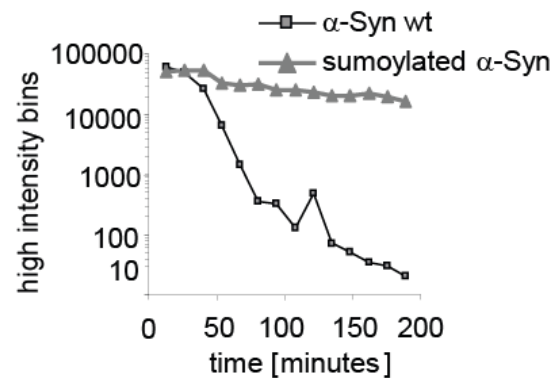


Fig. 12: SIFT assay for vesicle binding properties of sumoylated and non-sumoylated α -Syn

(A) Schematic figure of the assay and two-dimensional fluorescence intensity distribution histograms of SIFT recordings show binding of recombinant α -Syn (red bar) and sumoylated α -Syn (red bar with red dot) to DPPC-SUVs (green circle) and unlabelled non-sumoylated α -Syn (white bar). Red fluorescence intensity is given on the vertical axis and the green fluorescence intensity is given on the horizontal axis as photons/bin. (B) Dose response curve for the effect of non-labelled α -Syn on the vesicle binding of sumoylated and non-sumoylated α -Syn. Values are given as a + SEM normalized to reference (addition of buffer) of duplicate measurements of three parallel samples. (C) Time course of release of α -Synuclein and sumoylated α -Synuclein after addition of 7 μ M non-labelled α -Syn in a representative experiment.

No change in the distribution of particles could be observed in the absence of unlabelled, non-sumoylated α -Syn. In contrast to sumoylated α -Syn, non-sumoylated α -Syn is released from the lipid vesicles following addition of about 1000-fold excess of unlabelled α -Syn (see also Fig. 12 B left and right panel).

Following the addition of unlabelled non-sumoylated α -Syn, the release of labelled non-sumoylated α -Synuclein from the green labelled DPPC-SUVs, is also visible in the two-dimensional fluorescence intensity distribution histogram (Fig. 12 A upper right panel) This is in accordance with our results which show increased membrane binding of sumoylated α -Syn. Taken these data together one can conclude that SUMOylation of α -Syn promotes its binding to (lipid)-membranes.

3.3.2. Extracellular vesicle release of α -Synuclein is regulated by SUMOylation

To investigate whether SUMOylation might have an influence on the release of α -Syn within EVs, we determined the EV secretion of both SUMOylation deficient α -Syn mutants. To address this issue, N2a cells were transiently transfected with both SUMOylation deficient mutants of α -Syn. After an expression time for all constructs of 8 h, we changed the medium from DMEM (see section 2.1.7.2) with fetal calve serum, to medium without serum and collected EVs 16 h (see section 2.2.2.5). Collecting medium was subjected to subsequent centrifugation steps, including a final ultracentrifugation step, to pellet down EVs (see section 2.2.3.1). After preparation of EVs we subjected the P100 and the corresponding parental cell lysate to SDS-PAGE and subsequently to Western blot analysis. The membranes were probed for α -Syn and as a control for the EV marker protein Flotilin-2. As shown in Fig. 13 A, we were able to detect α -Syn in the EV fraction and in the lysates. Both SUMOylation deficient mutants were significantly reduced in the EV fraction, compared to α -Syn wt (Fig. 13 B). With nanoparticle tracking analysis (NTA), we investigated, whether the transfection of the different mutant versions of α -Syn, might change the total number of EVs released by the neuroblastoma cell line N2a. With this technique it is possible to analyse nanoparticles in real time. To determine the number of EVs, 200 μ L of cultured medium were taken and centrifuged for 5 min at 5.000 rpm. The supernatant was diluted 1:1 with PBS. NTA was performed with a NanoSight LM14 instrument, which consists of a conventional optical microscope with a high resolution camera, which uses a 532 nm laser to illuminate the nanoparticles. During the analysis the particles were illuminated by the laser beam, which results in Brownian motion of the illuminated particles.

The Brownian motion of the particles were then recorded by a high resolution camera and the analysis software of the device allows for an automatic tracking of these particles and determines both, the particle concentration and the size distribution of the recorded particles. In order to determine the concentration of released vesicles, we recorded 3 videos with duration of 30s and a camera level of 11, for each construct.

The detection threshold was set at 10 and at least 800 tracks were analysed for each video. The concentration of vesicles smaller than 120 nm was analysed, all larger vesicles were excluded from the analysis. We found no significant differences in the release of EVs between α -Syn wt and both SUMOylation deficient mutants (see Appendix, Table 13). This indicates that expression of α -Syn or its mutants does not interfere with the number of released vesicles.

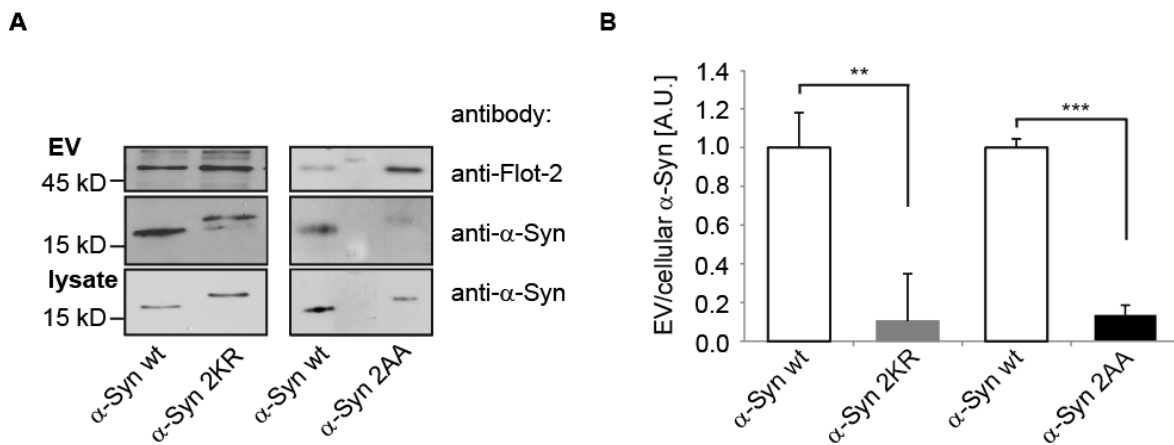


Fig. 13: Extracellular vesicle release of SUMOylation deficient α -Syn

(A) Western blot analysis of EVs and the corresponding parental cell lysate from N2a cells transfected with both sumoylation deficient mutants (2 AA and 2 KR) and α -Syn wt as well. Blots were scanned and the signal intensities of the bands were determined by ImageJ software analysis. **(B)** The quantification histogram shows the ratio of α -Syn wt (white bars left and right) which was normalized to 1, and the α -Syn mutant 2 KR (grey bar) and the α -Syn mutant 2 AA (black bar) intensities in EV pellets versus corresponding cell lysates. The EV release of both SUMOylation deficient mutants was impaired compared to α -Syn wt. The membranes of the EV fractions were additionally probed with an antibody against Flotilin-2, as an EV marker protein. All values are given as mean + SEM from $n = 6$ independent experiments; ** indicates $p < 0.01$, *** $p < 0.001$, student's 2-side t-test.

Additionally, primary cortical neurons were infected with an adeno-associated virus to express either α -Syn wt or the SUMOylation deficient mutant α -Syn 2 KR (Krumova *et al.* 2011). After 4 days of post-infection the cultured medium was collected and further processed to EV preparation as described in section 2.2.3.1 (notably, for this approach the P-100 was not resuspended in protein loading buffer, but rather in CHAPS lysis buffer (see section 2.1.6.5)) to further quantify the amount of α -Syn in the EV fraction and in the corresponding cell lysate by an electrochemiluminescence assay (Kruse *et al.* 2012).

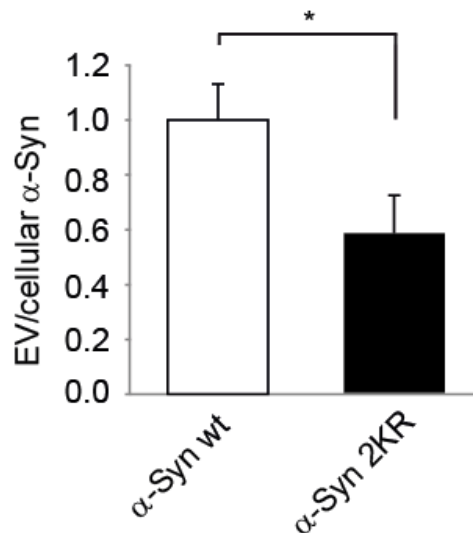


Fig. 14: Primary cortical neurons were infected with AAV to either express α -Syn-wt or the SUMOylation-deficient mutant α Syn-2 KR

Extracellular vesicles were prepared from cultured medium of primary cortical neurons and the amount of α -Syn was quantified in EV fractions and in the parental cell lysates by an electrochemiluminescence assay. The quantification histogram shows the calculated ratio of EVs versus cellular α -Syn for wild-type (white bar) which was normalized to 1, and the α -Syn mutant 2 KR (black bar). All values are given as mean + SEM from $n = 15$ independent experiments. * indicates $p < 0.05$; student's 2-side t-test.

The assay was performed in collaboration with Prof. Brit Mollenhauer and Dr. Niels Kruse, Dept. of Neuropathology, University Medical Center Göttingen. As shown in Fig. 14 we were able to detect a significant reduction of extracellular release of α -Syn 2KR mutant compared to α -Syn wt. In conclusion, this data from primary neurons confirms our findings obtained in the neuroblastoma cell line N2a. The results show that SUMOylation increases EV of α -Syn.

3.3.2.1. Silencing of Ubc9 decreases the release of α -Synuclein within extracellular vesicles

To further prove our conclusion that SUMOylation increases EV release of α -Syn, we silenced the SUMO E2 conjugating enzyme Ubc9 (UBE2I) by RNA interference and assessed its effect on the secretion of α -Syn in EVs. E2 enzymes are able to catalyse the attachment of ubiquitin and ubiquitin-like proteins (e.g. SUMO) to acceptor lysines of other proteins. This reaction is mediated directly or via specific E3 enzymes (Bernier-Villamor *et al.* 2002). Human embryonic kidney cells (HEK), were either treated with Ubc9 siRNA or mock treated for 36 hours. After 36 hours the cells were harvested. The cell lysate was subjected to Western blotting and the membrane was probed with antibodies against Ubc9 and Actin as a loading control to quantify the down regulation of Ubc9.

As presented shown in Fig. 15 A, Ubc9 protein levels were significantly decreased in the cells treated with siRNA against Ubc9 compared to mock treatment. To quantify the knockdown efficiency of the Ubc9 siRNA, we calculated the ratio of α -Syn to Actin protein levels. We normalized the ratio of Mock treated cells to 1. The quantification revealed a knockdown efficiency of approximately 80% for cells treated with siRNA against Ubc9 (Fig. 15 B). To determine the effect of Ubc9 down-regulation on EV release of α -Syn, HEK cells were treated with Ubc9 siRNA or mock treated 36 hours prior to transfection with α -Syn wt. After 8 hours post-transfection time, the cells were washed with PBS and the medium was changed to medium without FCS, to collect EVs for 16 hours. The EV containing medium was collected and purified by ultracentrifugation. The resulting pellets P100 and the corresponding cell lysates were subsequently analysed by western blot analysis with antibodies against α -Syn and Alix. Indeed, Ubc9 RNAi resulted in a significantly decreased secretion of α -Syn within EVs (Fig. 15 C+D). The total number of EVs was unaltered by the siRNA treatment, as indicated the by EV marker protein Alix (Fig. 15 C, upper panel).

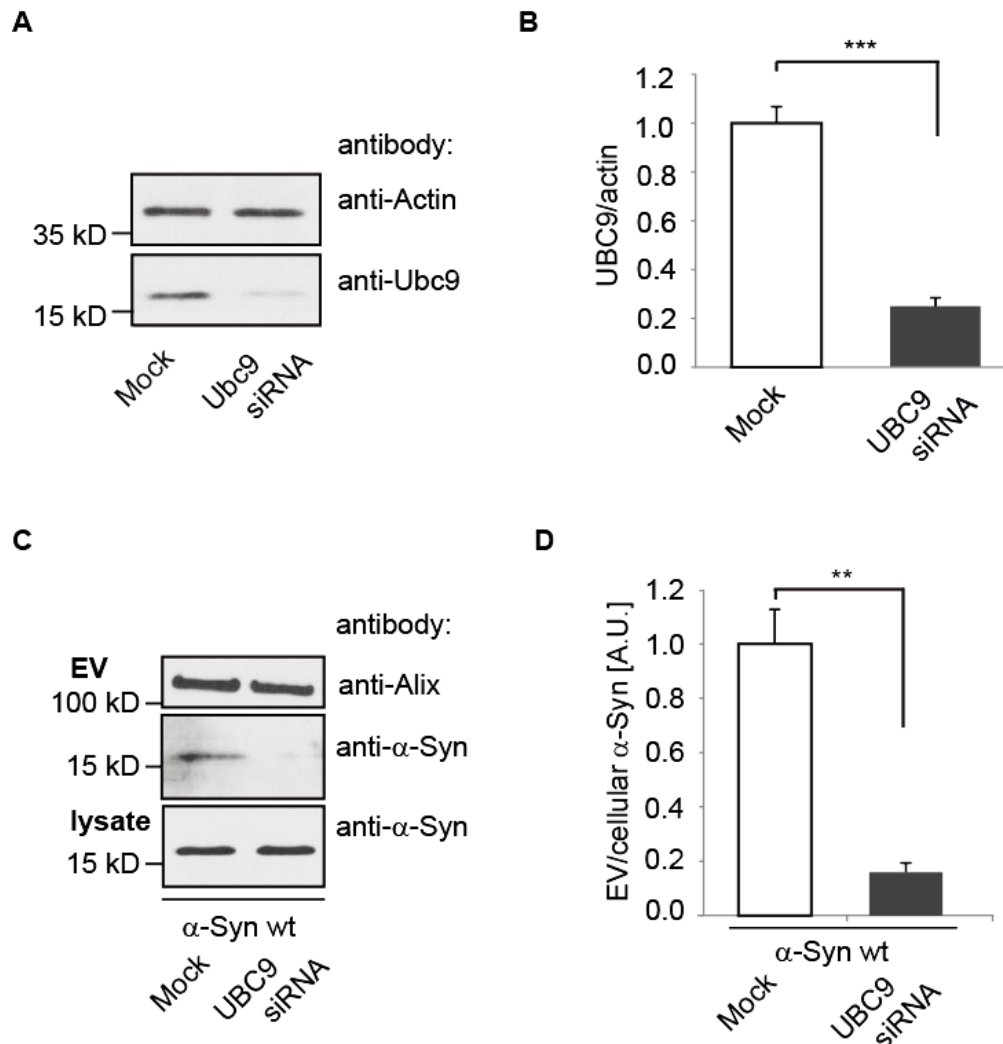


Fig. 15: Down-regulation of Ubc9 protein levels with siRNA

(A) Efficiency of siRNA-mediated down-regulation was quantified by Western blot analysis of cell lysates. Membranes were immunostained with antibodies against Ubc9 and Actin. **(B)** For the quantification of silencing efficiency, the ratio of Ubc9 to Actin was calculated. The silencing efficiency was around 80%. Results are given as mean + SEM, student's t-test with $n = 8$ individual experiments, *** $p < 0.0005$. **(C)** Western blot analysis of Ubc9 siRNA and Mock treated HEK cells. Membranes were immunostained with antibodies against α -Syn and Alix as a positive control for the purity of EV preparations. **(D)** The ratio of EV to cellular α -Syn was determined by calculating a ratio between Mock (white bar) and siRNA (grey bar) treated cells. All results are given as mean + SEM, ** indicates $p < 0.005$; Mock was normalized to 1; 2-side students t-test with $n = 6$.

3.3.2.2. α -Synuclein fusion with SUMO-2 increases the release of α -Synuclein within extracellular vesicles

To investigate, whether increased SUMOylation would promote EV release of α -Syn, N2a cells were transfected either with myc- α -Syn-wt or with myc- α -Syn-SUMO-2, mimicking constitutive SUMO modification. We then harvested the cell lysates and prepared EVs from the culture medium, which were subjected to SDS-PAGE and for Western blot analysis. We found that EV release of α -Syn-SUMO-2 was increased compared to α -Syn wt (Fig. 16 A and B). NTA analysis revealed no significant difference in the amount of secreted EVs in both conditions (see Appendix, Table 13).

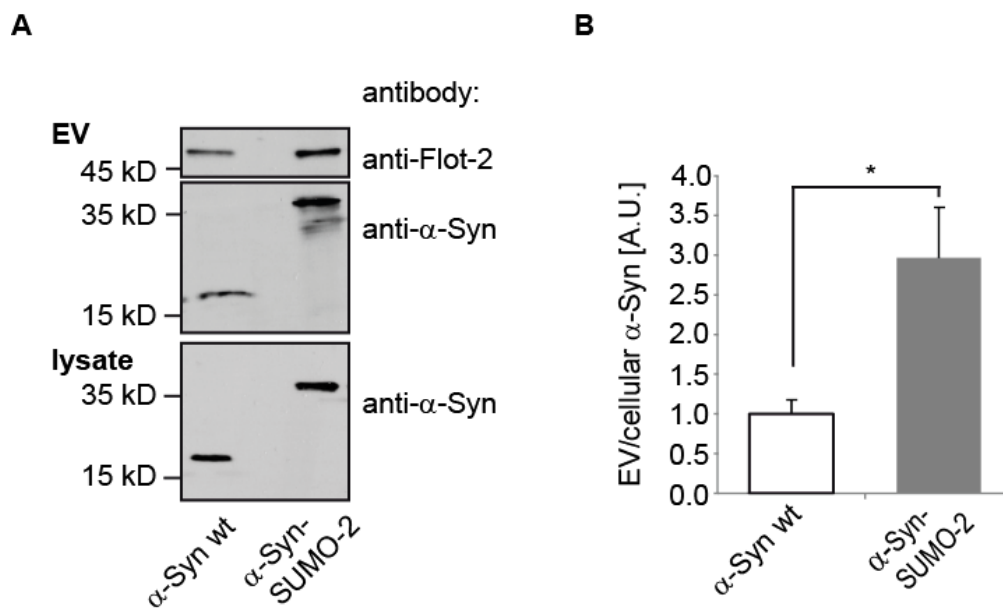


Fig. 16: SUMO-2 fusion increases extracellular vesicle release of α -Syn

(A) EVs and corresponding cell lysates were analysed by Western blotting and immunostained with an antibody against α -Syn. The membranes of the EV fractions were additionally probed with an antibody against Flotilin-2 as an EV marker protein. (B) For quantification of EV release, the signal intensity for α -Syn in the EV fraction, versus the signal intensity for α -Syn in the parental cell lysate was determined. The ratios were normalized to the wt and set to 1. All values are given as mean + SEM from $n = 8$ independent experiments; * indicates $p \leq 0.05$, in student's 2-side t-test.

3.3.2.3. Co-expression of SUMO-2 increases the release of α -Synuclein within extracellular vesicles

In a slightly different approach we co-expressed α -Syn with either wt SUMO-2 or a conjugation deficient SUMO-2 Δ GG mutation. EV pellets as well as parent cell lysates of co-transfected cells were subjected to Western blotting and the membranes were probed with an antibody against α -Syn (Fig. 17 A). Co-transfection of myc- α -Syn wt together with myc-SUMO-2 wt significantly increased the amount of α -Syn in EVs compared to co-expression of the conjugation-deficient SUMO mutant myc-SUMO-2 Δ GG (Fig. 17 B).

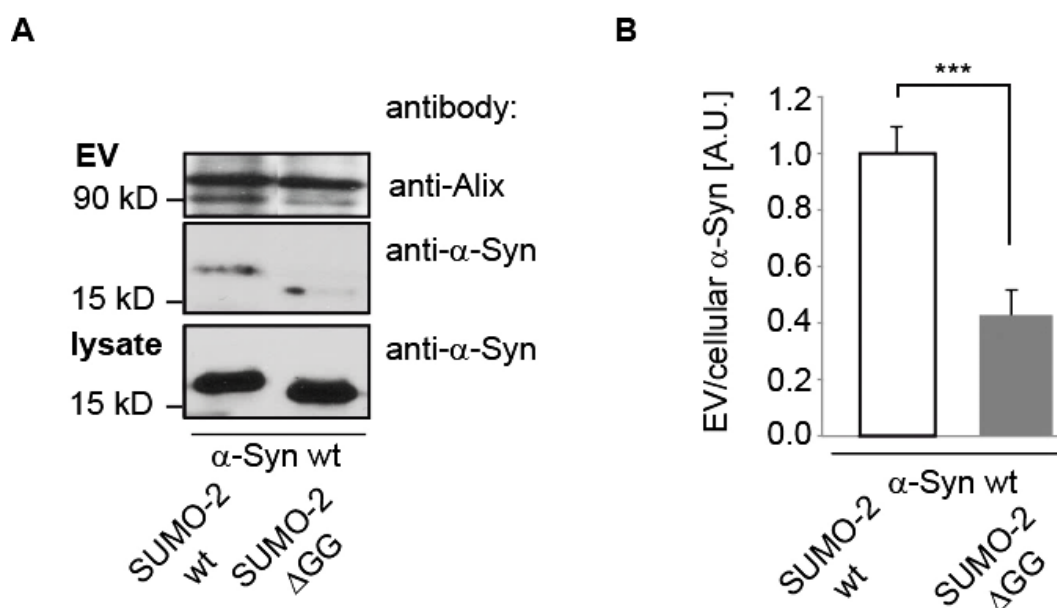


Fig. 17: Co-expression of SUMO-2 increases release of α -Syn with extracellular vesicles

(A) N2a cells were transiently co-transfected with plasmids either encoding for the mature SUMO-2 version (myc-SUMO-2 wt) or for the conjugation deficient mutant myc-SUMO-2 Δ GG. Extracellular vesicles were prepared and analysed together with the parental cell lysates by SDS-PAGE and were further processed to Western blot analysis. The EV fraction and the cellular fraction were immunostained against α -Syn and for quantification of signals subjected to signal intensity analysis via ImageJ software. **(B)** The histogram displays the calculated ratio between signal intensity of the extracellular fraction versus the corresponding cell lysate. (SUMO-2 wt is normalized to 1) All values are given as mean + SEM from $n = 10$ independent experiments. *** indicates $p \leq 0.001$; student's 2-side t-test.

By NTA analysis, no significant difference was observed in the amount of EVs by SUMO-2-wt or SUMO-2- Δ GG overexpression (see appendix, Table 13). Likewise, WB analysis of Flotillin-2 and Alix in the EV fractions revealed no differences between SUMO-2-wt and SUMO-2- Δ GG mutant co-expression (Fig. 18). This data indicates that SUMO expression does not increase the release of EVs per se but specifically the release of α -Syn with EVs.

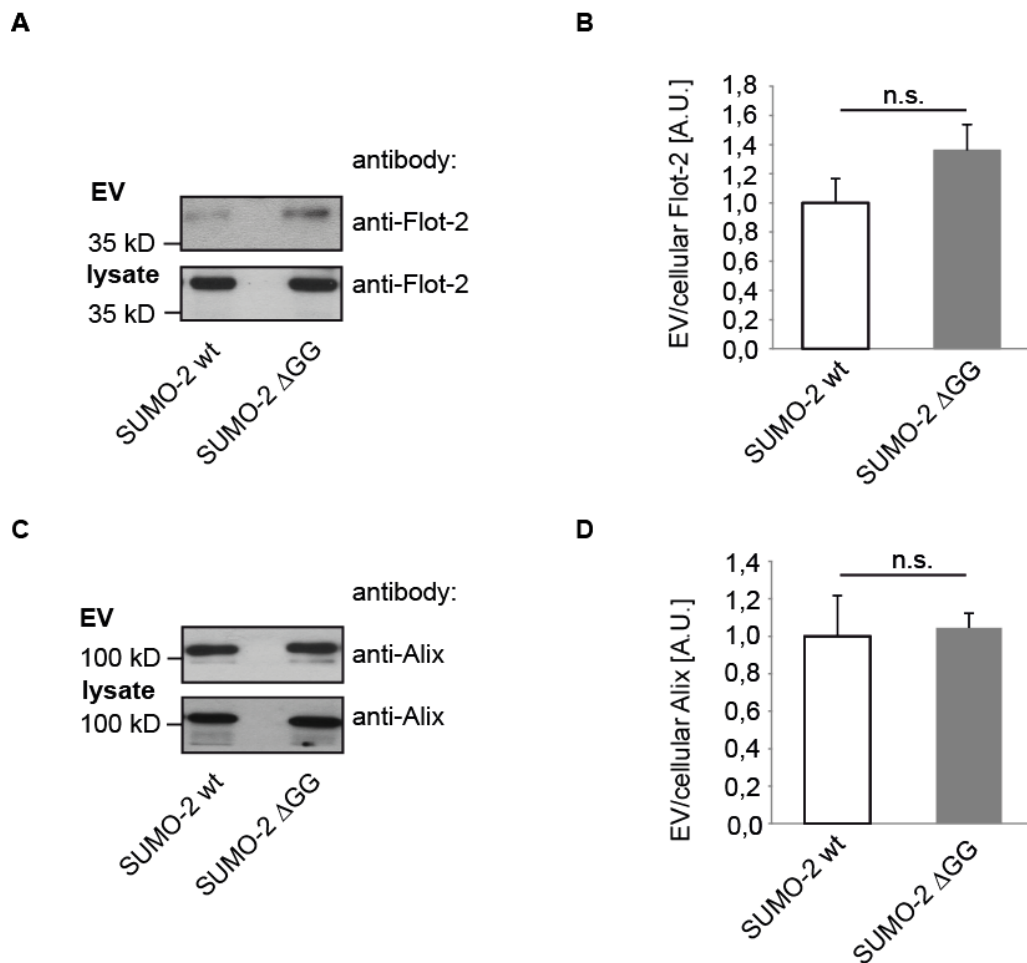


Fig. 18: Co-expression of SUMO-2 does not increase the production and release of extracellular vesicles itself

The neuroblastoma cell line N2a was co-transfected with α -Syn wt and either myc-SUMO-2 wt or the conjugation deficient mutant myc-SUMO-2 Δ GG. **(A)** EVs and the corresponding cell lysates were prepared and processed by Western blot analysis. Membranes were probed with an antibody against Flotilin-2. **(B)** The histogram shows the ratio of Flotilin-2 signal intensities of EV pellets versus cell lysates, of myc-SUMO-2 wt (white bar) and the conjugation deficient mutant myc-SUMO-2 Δ GG (grey bar). **(C)** Western blot analysis of EV pellets and the parental cell lysates that were stained with an antibody against Alix. The ratios of Alix signal intensities in the EV fraction versus cellular fractions were calculated. **(D)** The histogram displays no significant difference for the release of Alix positive EVs, when α -Syn was either co-transfected with myc-SUMO-2 wt (white bar), or the mutant myc-SUMO-2 Δ GG (grey bar). All values are given as mean + SEM of $n = 6$ independent experiments; n.s. = not significant; student's 2-side t-test.

In summary, our data show that membrane binding is required for EV release of α -Syn. SUMOylation of α -Syn increases membrane binding and also EV release, whereas SUMO deficient mutants of α -Syn show less membrane binding and decreased EV release (Fig. 19).

membrane binding deficient	membrane binding	release with EVs
α -Syn wt	++	++
α -Syn Δ N	-	-
sumoylation deficient		
α -Syn wt	++	++
α -Syn 2AA	-	-
α -Syn 2KR	-	-
SUMO fusion		
α -Syn wt	++	++
α -Syn-SUMO-2	+++	+++
SUMO co-transfection		
α -Syn wt + SUMO-2 wt	+++	+++
α -Syn wt + SUMO-2 Δ GG	++	++

Fig. 19: Summary of α -Syn membrane binding and release with extracellular vesicles

Schematic summary of α -Syn membrane binding (middle column) and release within extracellular vesicles (right column).

3.3.2.4. Isopeptidase activity in extracellular vesicles results in a rapid de-conjugation of SUMO

We could not detect sumoylated- α -Syn in EVs by Western blots analysis. It is known that SUMO modification is transient and can be rapidly removed by SUMO specific proteases (Shin *et al.* 2012).

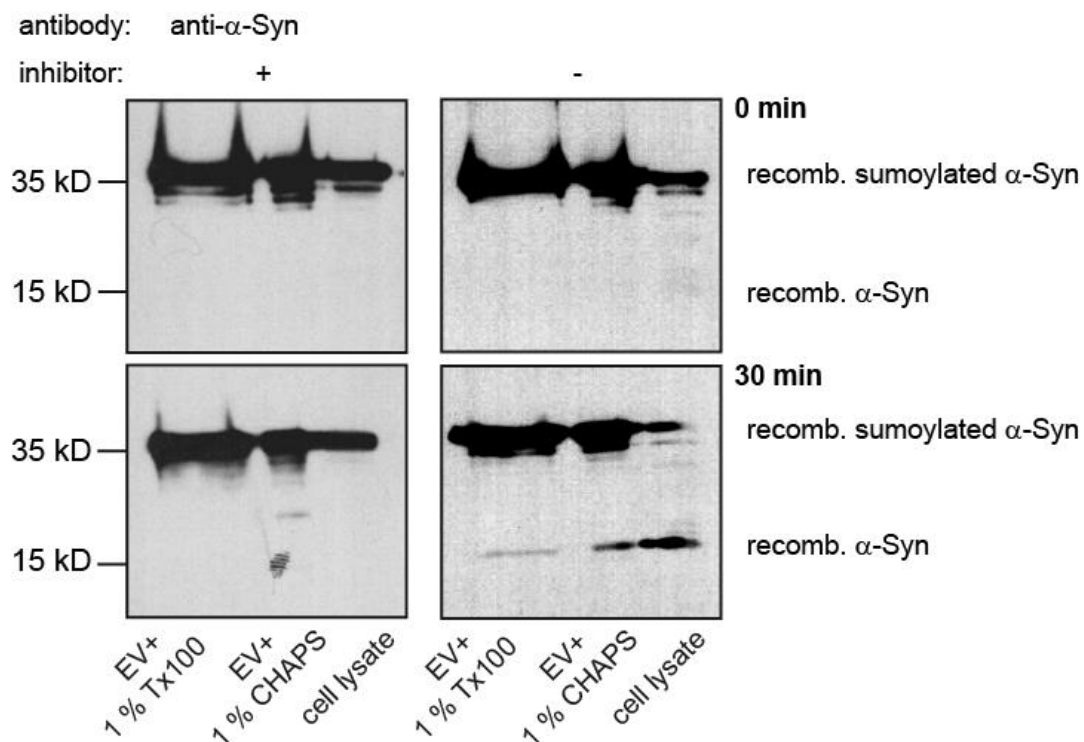


Fig. 20: Extracellular vesicles contain desumoylase activity

N2a cells were cultured for 24 h and the medium was changed to medium without FCS to collect EVs. After 24 h EVs were prepared and the corresponding cell lysates were prepared by scraping in 1 % CHAPS buffer. The vesicles were lysed with either 1 % Triton X 100 or 1 % CHAPS in the presence (left) or in the absence (right) of N-Ethylmaleimide, which is known to inhibit de-sumoylases (isopeptidases). Lysed EVs and cell lysates were incubated for 0 min (top panel) or 30 min (right) panel at 37°C with recombinant sumoylated α -Syn. The reaction was stopped by adding protein loading buffer. All samples were subjected to SDS-PAGE and subsequently analysed by Western blot with an antibody against α -Syn. One representative experiment, out of $n = 3$ is shown.

The enzymes responsible for the de-conjugation of SUMO in mammals include two ubiquitin-like-specific proteases in yeast, named Ulp1 and Ulp2 and six sentrin-specific proteases (SEN1, 2, 3, 5, 6 and 7) (Hay 2007, Yeh 2009). All members of the SENP and both Ulp proteases belong to the C48 family of cysteine proteases, by sharing a conserved catalytic His-Cys-Asp triad (Schulz *et al.* 2012). To investigate, whether an isopeptidase (de-sumoylase) activity in EVs results in de-conjugation of SUMO within EVs, we prepared EVs from N2a cells.

The prepared vesicles were either lysed in 1 % CHAPS or 1 % Triton X-100. The lysed vesicles and N2a cell lysate serving as a positive control were then incubated with recombinant sumoylated α -Syn at 37°C for 0 or 30 min in the presence or absence of 20 mM N-ethylmaleimide (NEM). NEM inhibits isopeptidases by forming a stable, covalent thioether bond with cysteine residues. The reaction was stopped by adding protein loading buffer (see 2.1.6.6) and the samples were subjected to Western blot analysis and probed with an antibody against α -Syn. After 0 min of incubation no de-sumoylated α -Syn was detected, neither in the presence or absence of NEM. After an incubation period of 30 min de-sumoylated α -Syn appeared in the absence of NEM while in the presence of NEM only sumoylated α -Syn was detectable. Taken together, we found an isopeptidase activity in EVs, which results in a rapid cleavage of SUMO from α -Syn (Fig. 20).

Since we were unable to detect sumoylated α -Syn by WB in EVs, we used a luciferase-based protein fragment complementation assay (Danzer *et al.* 2012), to detect sumoylated α -Syn in EVs. We used a bioluminescence protein-fragment complementation assay (Outeiro *et al.* 2008, Tetzlaff *et al.* 2008, Putcha *et al.* 2010). For this assay α -Syn was fused to full length *Gaussia princeps* luciferase (Remy *et al.* 2006) (syn pHluc), or to the amino-terminal or carboxy-terminal fragments of split pHluc (α -Syn-S2) or SUMO-2 (SUMO-2 S3). Close proximity of SUMO and α -Syn will result in complementation of split luciferase which can be quantified by luminescence.

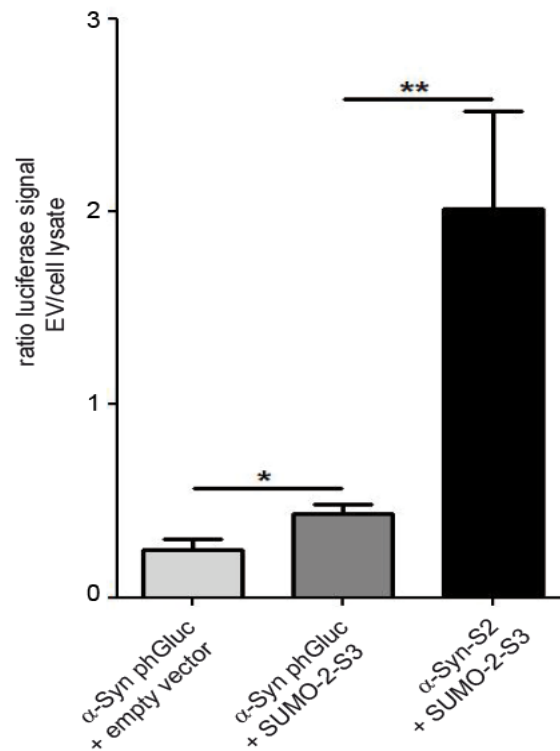


Fig. 21: Sumoylated α -Syn is enriched in extracellular vesicles

Constructs indicated above were transfected into HEK 293 cells. Cells were washed after 16 h post-transfection and PBS was replaced with serum- and phenol free media. After 48 h the medium was collected, EVs and cell lysates were prepared. Luciferase activity from protein complementation was measured using the same amount of total protein of the cell lysates and EV fractions. The ratio of luciferase activity signal was calculated for the EV fraction versus cell lysates. The histogram shows significant increase in luciferase activity when α -Synuclein fused to full length gaussia luciferase was co-expressed with SUMO-2 (dark grey bar) compared to the control, expressing only the aS-full length gaussia luciferase construct (light grey bar). The highest luciferase signal was obtained when C- or N-terminal fragments of split gaussia luciferase were fused to α -Synuclein (α -Syn-S2) or to SUMO-2 (SUMO-2-S3) (black bar). All values are given as mean + SEM of $n = 3$ independent experiments; student's 2-side t-test; * indicates $p \leq 0.05$ and ** indicates $p \leq 0.01$. Measurements and data analysis were performed by Marisa Feiler, Karin M. Danzer (Dept. of Neurology, Ulm University, Germany)

To address the question whether sumoylated α -Syn is enriched in EVs, we transfected either (a) α -Syn coupled to luciferase, (b) α -Syn coupled to luciferase plus Sumo-2 split luciferase or (c) α -Syn coupled to split luciferase plus SUMO-2 coupled to split luciferase into HEK 293 cells. EVs were prepared and cells were washed with PBS and lysed by sonication. The probes were subjected to luciferase measurements in an automatic plate reader at 480 nm. As shown in Fig. 21 only a low luciferase signal was obtained in EVs when α -Syn was fused to the full length construct of *Gaussia* luciferase (light grey bar). In contrast, co-transfection of α -Syn fused to full length *Gaussia* luciferase (α -Syn-phGluc), co-expressed with SUMO-2 (SUMO-2-S3), resulted in a significantly increased luciferase activity signal (dark grey bar). These findings indicate that α -Syn is targeted to EVs, when sumoylated to a higher degree.

In a similar fashion, when C-or N-terminal fragments of split luciferase were fused to α -Syn (α -Syn-S 2) or SUMO-2 (SUMO-2-S 3) and co-transfected into HEK 293 cells, only α -Syn which was modified by SUMO-2, resulted in a dramatic increase of luciferase signal (black bar). These findings indicate that sumoylated α -Syn is present and also enriched in EVs.

3.4. SUMOylation can act as sorting signal for the release within extracellular vesicles

Next, we wanted to clarify whether SUMOylation acts as a sorting signal for release within EVs. To answer this question we designed a GFP-SUMO-2- Δ GG fusion construct and as a positive control a GFP-Ub- Δ GG construct, both constructs bearing, as described above, the Δ GG mutation to prevent the conjugation of SUMO or Ubiquitin (Ub) to other proteins or themselves. We decided to use ubiquitin as a positive control, because it is known that mono-ubiquitination (Hicke *et al.* 2003, Haglund *et al.* 2005, Duncan *et al.* 2006, Huang *et al.* 2006) directs cargo for EV release. As a negative control we used GFP because as a cytosolic protein, GFP is excluded from extracellular vesicle release. We prepared EVs and corresponding cell lysates according to the previously described protocols (see section 2.2.3.1) from cultured medium of N2a cells. For further analysis we subjected cell lysates and EV fractions to SDS-PAGE and subsequently to Western blot analysis. The membranes were probed with an antibody against GFP. As shown in Fig. 22 A, GFP was nearly absent from the EV fraction GFP signal intensity was normalized to 1. Results of the quantification are displayed in the histogram in Fig. 22 B (right) indicating that the release of the GFP-Ub fusion protein within EVs (positive control) was increased up to 16-fold compared to GFP. In a similar fashion, the GFP-SUMO-2 fusion protein was released within EVs with an increase up to 6-fold compared to GFP, but to a lesser extent when compared to the GFP-Ub fusion protein.

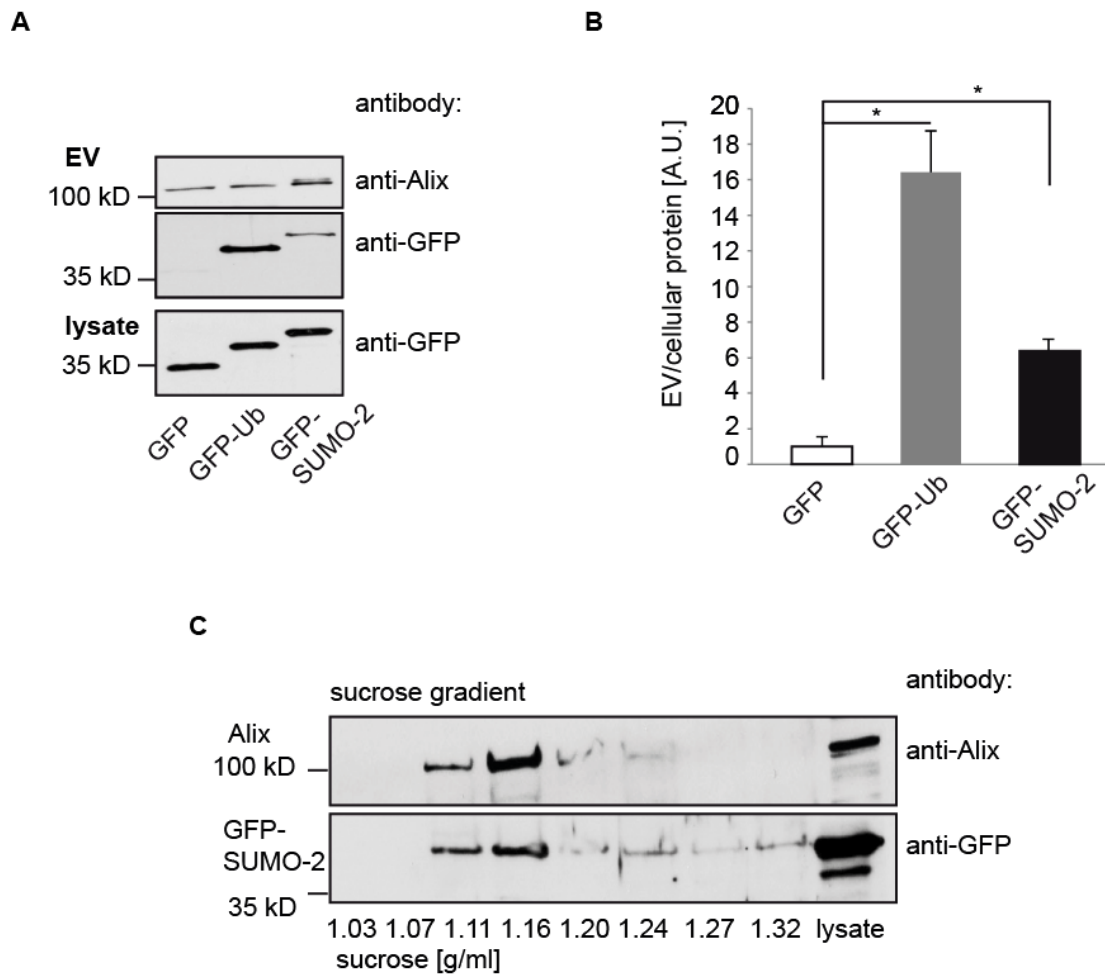


Fig. 22: SUMO-2 is released within extracellular vesicles

N2a cells were transiently transfected with GFP or GFP either fused to a conjugation deficient Ubiquitin mutant (GFP-Ub Δ GG) or to the conjugation deficient SUMO-2 mutant (GFP-SUMO-2 Δ GG). **(A)** EVs and the parental cell lysates were prepared and subjected to SDS-PAGE and further analysed by Western blotting. The membranes were probed with an antibody against GFP and the EV protein Alix, as an internal loading control. **(B)** The blots were scanned and analysed with ImageJ software, to calculate the ratios of GFP signal intensities in the EV fraction versus cellular fractions. The histogram displays an increase of EV release of GFP-Ub Δ GG (grey bay) up to 16-fold compared to GFP (white bar) and an increase of GFP-SUMO-2 Δ GG (black bar) up to 6-fold when compared to GFP. All values are given as mean + SEM of $n = 8$ independent experiments; student's 2-side t-test; * indicates $p \leq 0.05$. **(C)** N2a cells were transiently transfected with a construct encoding for the GFP-SUMO-2 fusion protein. EVs were prepared as described previously and the EV pellet was loaded for further purification on top of discontinuous sucrose gradient with a range of 1.03 g/mL to 1.32 g/mL. The gradient was centrifuged for 16 h at 200,000 $\times g$ and the 8 different layers were diluted 1:6 in PBS and re-centrifuged again at 100,000 $\times g$. The obtained pellets and one representative cell lysate were analysed by Western blot and membranes were stained against GFP and Alix.

To verify that SUMO-2 GFP is sorted into EVs, we additionally performed a sucrose gradient centrifugation. The P100 pellet was resuspended in 0.25 M sucrose and loaded on top of a discontinuous sucrose density gradient 0.25 M-2.5 M sucrose (1.03 g/mL - 1.32 g/mL). After centrifugation at 200,000 $\times g$ for 16 h, 8 fractions were collected corresponding to the densities indicated above, diluted 1:6 with PBS and subsequent re-centrifuged at 100,000 $\times g$ for 1 h.

For further analysis the 8 fractions were subjected to Western blotting and blot membranes were probed with an antibody against GFP and additionally against the EV marker protein Alix as a control. As presented in Fig. 22 C, we were able to detect GFP-SUMO-2 Δ GG positive exosomes floating at a density of 1.11 - 1.16 g/mL. A similar floating behaviour was observed for the EV marker protein Alix as shown in Fig. 22 C upper panel, which is consistent with previously described floating behaviour for EVs on sucrose gradients (Fauré *et al.* 2006, Théry *et al.* 2006).

3.4.1. SUMO-2 targets the cytosolic protein GFP to extracellular vesicle release

Next, we wanted to rule out the unspecific sorting of GFP-SUMO-2 into EVs mediated by the GFP-fusion. Thus, we transiently transfected N2a cells with SUMO-2 either fused to a GFP- or a myc-tag. We prepared EVs and parental cell lysates as described previously in this thesis and subjected the P100 and the corresponding cell lysate to SDS-PAGE and to a subsequent Western blot analysis with an antibody against GFP and the myc-tag (Fig. 23 A). The blots were scanned and the signal intensity was quantified by ImageJ. The ratio between the proteins in the EV fraction und the parent cell lysates was calculated. As shown in the histogram in Fig. 23 B, the release of either GFP-SUMO-2 (white bar) or myc-SUMO-2 (grey bar) within EVs was indistinguishable.

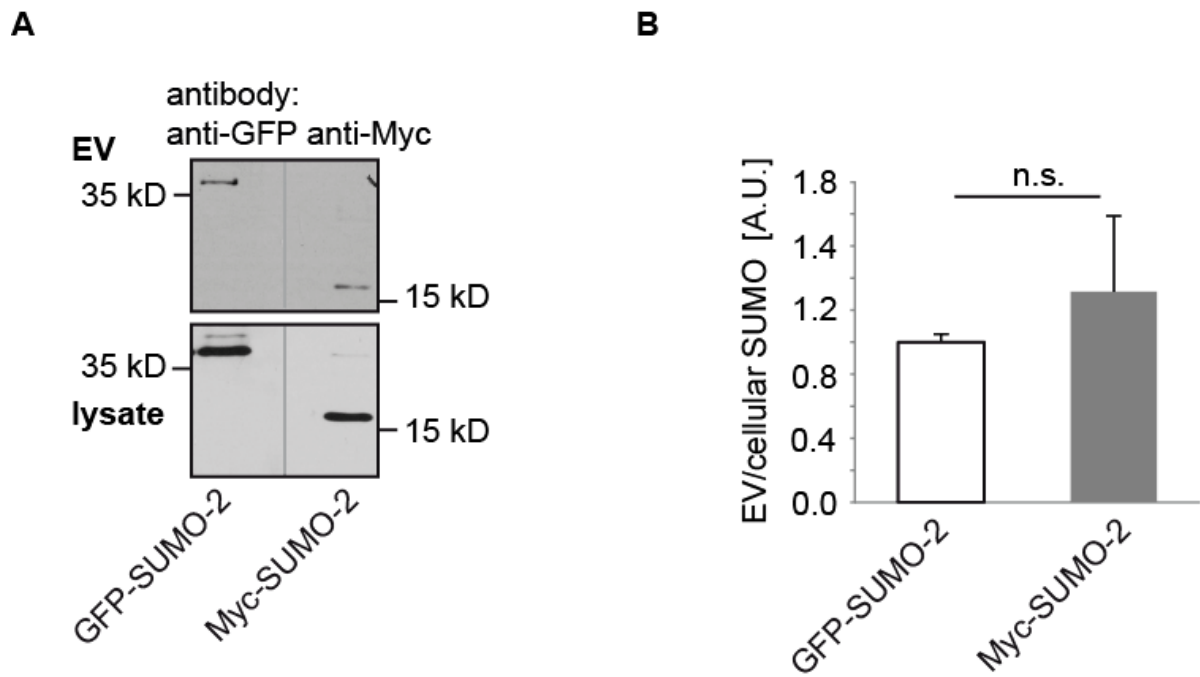


Fig. 23: SUMO-2 fusion leads to extracellular vesicle sorting of GFP

N2a cells were transfected with constructs either encoding for GFP-SUMO-2 Δ GG or myc-SUMO-2 Δ GG. **(A)** EVs and corresponding cell lysates (lys) were analysed by Western blot with antibody against the GFP-tag or the myc-tag (Please note that the EV and lysate blots were cut for incubation with either anti-GFP or anti-myc antibodies. Exposure times were identical). Blots were scanned and signal intensities of the bands were quantified. To determine the EV release of both constructs, ratios of SUMO-2 signal intensities in the EV fraction versus cellular fractions were calculated. **(B)** The histogram (right) displays no significant differences for the EV release of GFP-SUMO-2 Δ GG (white bar), compared to the EV release of a myc-tagged SUMO Δ GG (grey bar). All values are given as mean + SEM from $n = 6$ independent experiments; student's 2-side t-test; n.s. indicates not significant.

3.4.2. SUMO-1 also modulates extracellular vesicle sorting of the cytosolic protein GFP

After demonstrating that SUMO-2 can act as a sorting factor for EV release, we wondered whether SUMO-1 could also mediate sorting to EVs. We transiently transfected N2a cells with either GFP-SUMO-2- Δ GG or with GFP-SUMO-1- Δ GG construct. EVs as well as the corresponding cell lysates of transfected cells were processed for Western blot analysis and probed with an antibody against GFP. We found that the GFP-SUMO-1- Δ GG is sorted to EVs, albeit to a lesser extent as GFP-SUMO-2- Δ GG (Fig. 24 A).

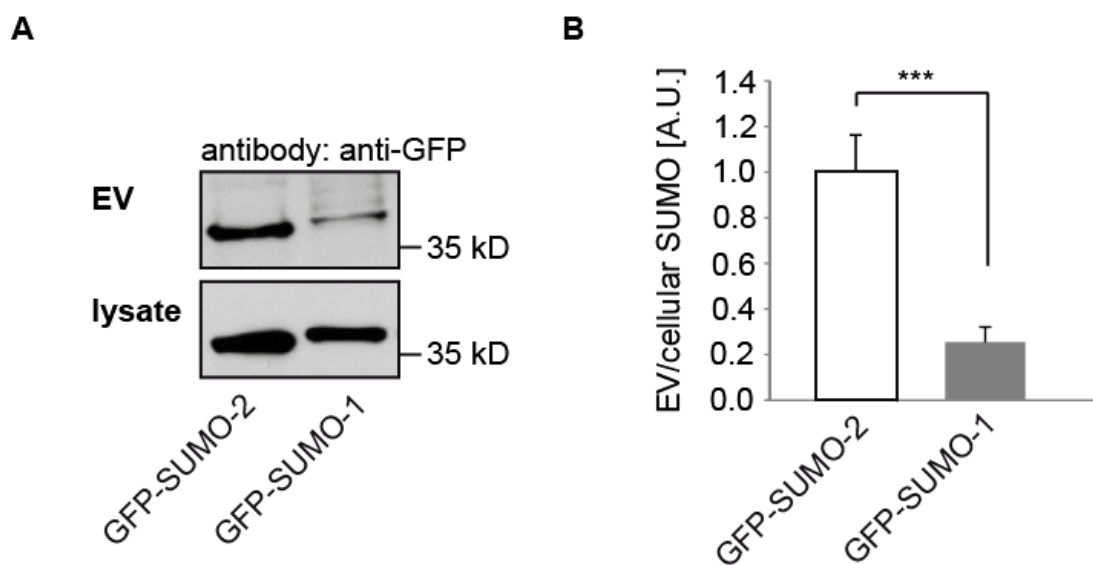


Fig. 24: Comparison of SUMO-1 and SUMO-2 release within extracellular vesicles

For the determination of EV release, **(A)** Western blot analysis of EV pellets and parental cell lysates of transfected mouse neuroblastoma cells, with the plasmids indicated above was conducted. **(B)** For the quantification of EV release, the ratio of GFP signal in the EV fraction versus the cell lysate was calculated. The histogram shows a decrease for GFP-SUMO-1- Δ GG (grey bar) release within EVs up to 5-fold, compare to the release of GFP-SUMO-2- Δ GG (white bar). All values are given as mean + SEM of $n = 12$ independent experiments; SUMO-2 was arbitrarily normalised to 1; student's 2-side t-test; *** indicates $p \leq 0.001$.

3.4.3. SUMOylation increases the extracellular vesicle release of the transmembrane protein amyloid precursor protein (APP)

The amyloid precursor protein (APP) is an integral type I membrane protein. After identifying SUMOylation as a potential sorting factor for the EV release of cytosolic proteins, we wanted to explore whether SUMOylation might also target transmembrane proteins into EVs. Therefore N2a cells were transfected with plasmids either encoding for YFP-APP_{sw} (bearing the Swedish mutation K670N M671L) or the corresponding C-terminal SUMO-2 fusion construct YFP-APP_{sw}-SUMO-2 ΔGG. We then prepared cell lysates and EVs from cultured medium, which were subsequently subjected to SDS-PAGE and further subjected to Western blot analysis (Fig. 25 A) and probed with an antibody against APP (6E10 see Table 2). To quantify APP secretion with EVs, the ratio of APP in EVs to cell lysates was determined. We found that the EV release of a SUMO fusion protein of YFP-APP_{sw}, is increased compared to YFP-APP_{sw}, (Fig. 25 B).

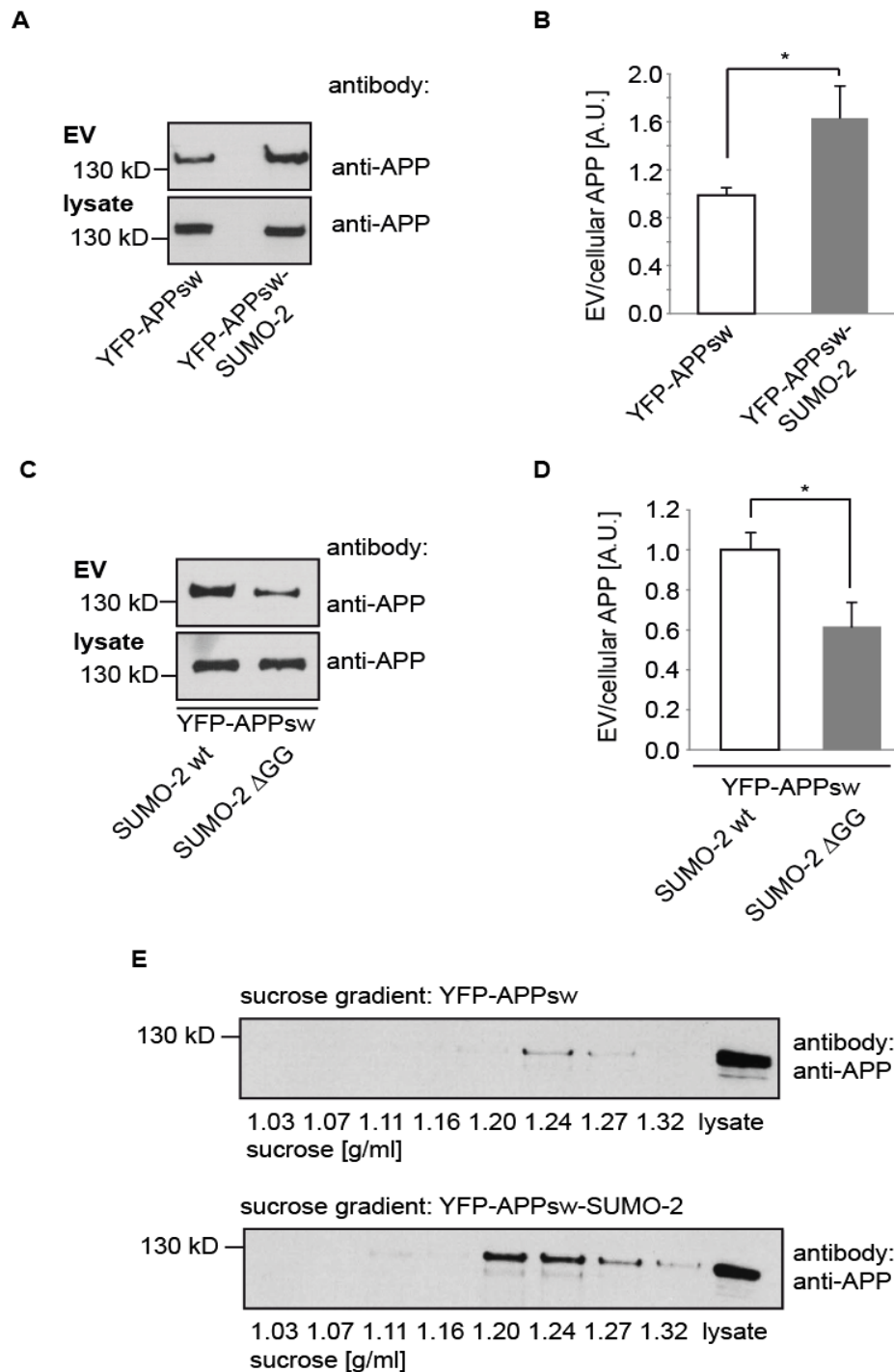


Fig. 25: SUMO-2 increases extracellular vesicle release of the transmembrane protein APP

(A) APP bearing the Swedish mutation (APP_{sw}) was N-terminally fused to SUMO-2 ΔGG. YFP-APP_{sw} or YFP-APP_{sw}-SUMO-2 ΔGG were transfected into N2a cells. EVs and the corresponding cell lysates were prepared, according, to the protocol described previously. Obtained EV pellets and the cell lysates were analysed via Western Blot. **(B)** Signal intensities of the blots were analysed using ImageJ and by calculating the ratio between EV signals versus total cellular APP signals, YFP-APP_{sw} was normalised to 1 (histogram upper right panel.). Values are given as mean + SEM from $n = 9$ independent experiments; student's 2-side t-test; * indicates $p \leq 0.05$. **(C)** YFP-APP_{sw} was either co-transfected with wildtype SUMO-2 or with the conjugation deficient mutant SUMO-2 ΔGG. EVs and parental cell lysates were subjected to Western blot analysis. Blots were scanned and analysed for signal intensities. **(D)** The histogram displays the calculated ratios for EVs versus the total cellular APP (lys), for SUMO-2 (normalised to 1, white bar) and for the conjugation deficient mutant SUMO-2 ΔGG (grey bar). Values are given as mean + SEM from $n = 9$ independent experiments; student's 2-side t-test; * indicates $p \leq 0.05$.

Likewise, co-transfection of YFP-APP_{sw} either with SUMO-2 wildtype or with the conjugation deficient mutant SUMO-2-ΔGG into N2a cells resulted in increased release of APP co-transfected with SUMO-2 wt (Fig. 25 D histogram, white bar) as compared to the conjugation deficient mutant SUMO-2-ΔGG (Fig. 25 D histogram, grey bar).

Additionally, we used sucrose density gradient to show that APP and APP-SUMO-2 fusion are truly released with EVs. As shown in Fig. 25 E both float at the same density as the EV marker protein Flotillin-2 at 1.20 to 1.27 g/mL sucrose. Supporting our quantitative results with ultracentrifugation, a higher proportion of the fusion construct YFP-APP_{sw}-SUMO-2 was found in the EV fraction compared to YFP-APP_{sw} (Fig. 25 E upper and lower panel).

Thus, our data show that SUMO modification not only increases EV release of cytosolic but also at least of one transmembrane protein.

3.5. Extracellular vesicle release of SUMO-2 is ESCRT-dependent

We next tried to elucidate the molecular mechanism of SUMO-dependent sorting into EVs. Protein delivery to EVs can be mediated by ESCRT dependent and independent pathways. Therefore, we first blocked components of the ESCRT machinery and assessed SUMO release with EVs under these conditions.

3.5.1. RNA Interference with the ESCRT components Alix and Tsg101 decrease extracellular vesicle release of a SUMO-2-GFP fusion protein

To answer the question whether SUMO-2 is targeted to EVs by the ESCRT pathway, we used RNA interference (RNAi) against the ESCRT proteins Tumor susceptibility gene 101 (Tsg 101) and Alix (see Table 4). To test the knockdown efficiency of the used siRNA constructs, cells were treated either with Tsg 101 siRNA, with Alix siRNA or mock treated. After 36 h incubation time, the cells were lysed with CHAPS buffer as described before. The obtained cell lysates were subjected to Western blot analysis (Fig. 26 A and Fig. 26 C) with antibodies directed against Tsg101, Alix and either Actin or Calnexin as a loading control. The signal intensities were determined with ImageJ software and the ratios for Tsg 101 to Calnexin and Alix to Actin were calculated. Protein levels of Tsg 101 were down-regulated by approx. 70 % and protein levels of Alix by approx. 90 % (Fig. 26 B and Fig. 26 D).

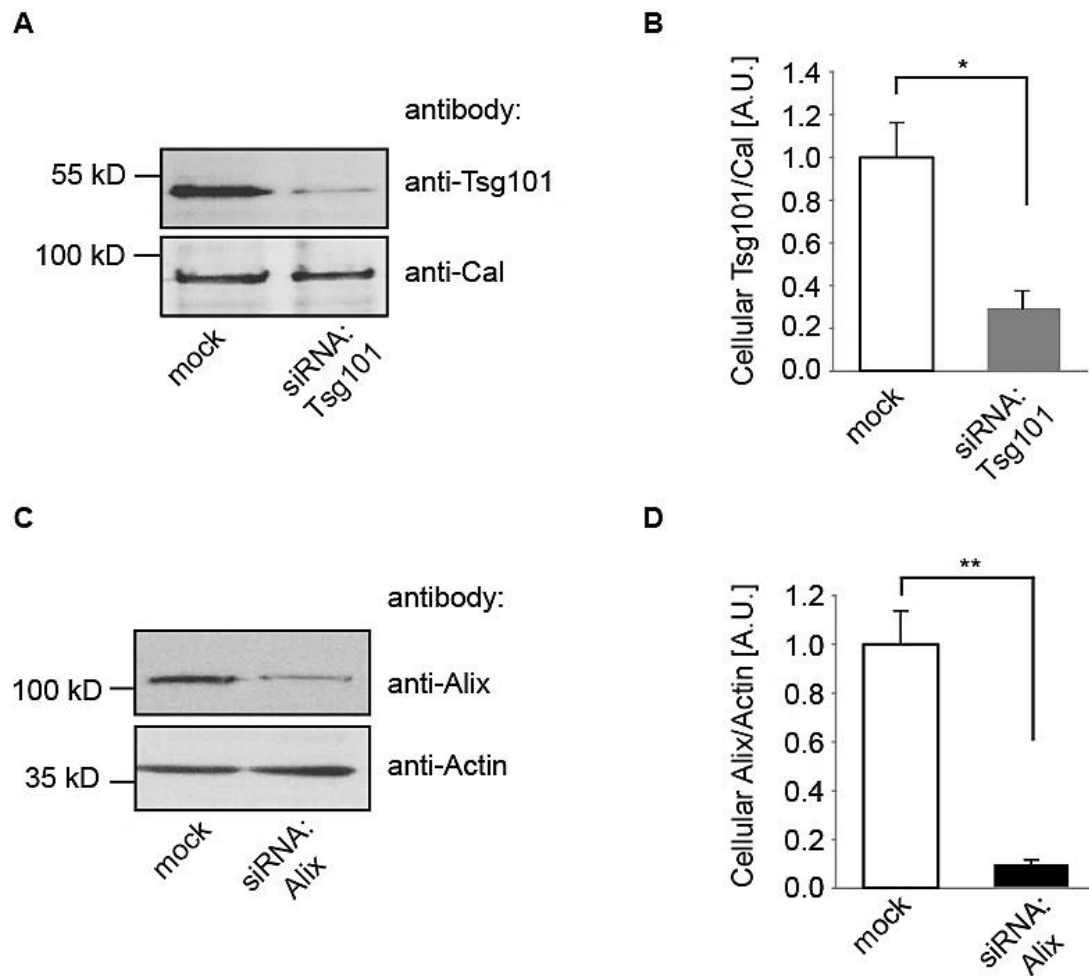


Fig. 26: Down-regulation of Tsg 101 and Alix with siRNA

Efficiency of siRNA-mediated down-regulation was determined by Western blot analysis. **(A)** Western blot of cell lysates was performed with antibodies against Tsg 101 and Calnexin as loading control. **(B)** The ratio of signal intensities for Tsg 101 versus Calnexin was calculated for mock (white bar) transfected and siRNA against Tsg 101 treated cells (grey bar). Efficiency of Tsg 101 down-regulation was around 70 %. **(C)** Western blot analysis of mock and Alix siRNA transfected cells with antibodies against Alix and Actin (loading control). **(D)** The ratio Alix/Actin was quantified for mock treated cells (white bar, normalized to 1) and for siRNA transfected cells (grey bar). Efficiency of Alix down-regulation was around 90 %. Results are given as mean + SEM from $n = 6$ independent experiments for Alix and $n = 3$ independent experiments for Tsg101; student's 2-side t-test; * indicates $p \leq 0.05$.

Next, we down-regulated the expression of both ESCRT complex proteins, Alix and Tsg101 and subsequently determined the EV release of a GFP-SUMO-2 fusion protein (see section 2.1.4.2). N2a cells were treated either with siRNA against Alix or with siRNA against Tsg101. As a control cells were also mock treated. After 36 h, the cells were transfected with a construct expressing a GFP-SUMO-2 fusion protein. After 16 h we harvested the parental cell lysates and prepared EVs from the culture medium. Western blot analysis of lysates and EV fractions revealed RNAi mediated down-regulation of Tsg101 (left panel) or Alix (right panel), resulted in a marked decrease of GFP-SUMO-2 release with EVs.

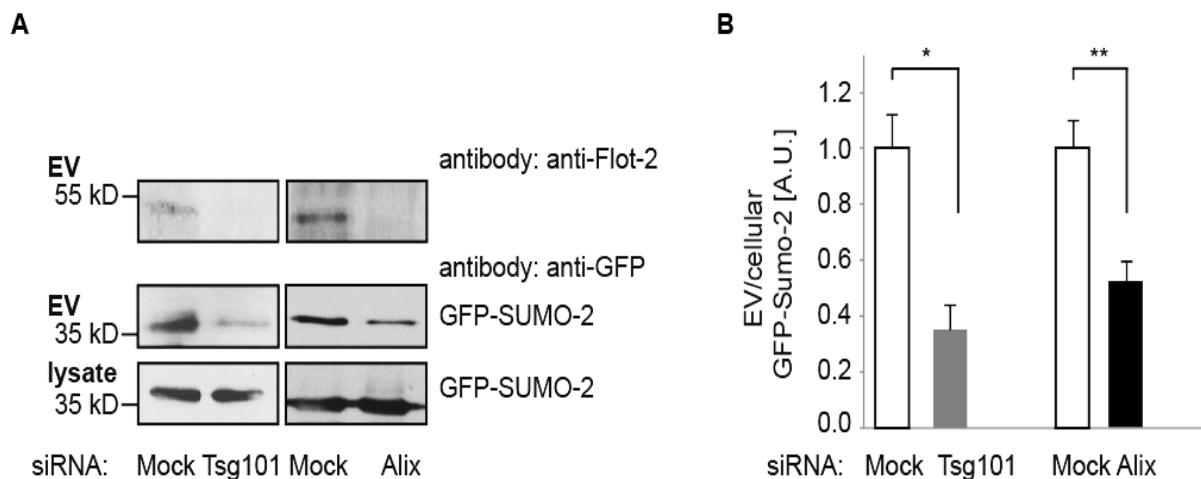


Fig. 27: Alix and TSG101 are required for the extracellular vesicle release of SUMO-2

N2a cells were transfected with siRNAs directed against Alix or Tsg101 and Mock transfected (only treated with oligofectamin). **(A)** EVs and corresponding cell lysates were prepared and analysed by Western blotting by staining with antibodies against GFP and Flotilin-2. **(B)** The histogram shows the calculated ratios for extracellular vesicle GFP signal versus cellular GFP signal in cells treated with siRNA against Tsg101 (grey bar) versus Mock treated cells and for cells treated with siRNA against Alix (black bar) versus Mock treated cells. All results are given as means + SEM for $n=12$ for Alix siRNA and $n = 6$ for Tsg101 siRNA experiments. * indicates $p<0.05$ and ** $p<0.005$; 2-side t-test.

The quantification revealed an approximately 2.8-fold reduction of the EV/cell lysate ratio of GFP-SUMO-2 for Tsg101 RNAi and an approximately 2-fold reduction for Alix siRNA treated N2a cells (black bar) compared to mock treated controls (Fig. 27 B). The responsible protein for the final fission of vesicles is the AAA (ATPase associated in various cellular activities) ATPase VPS4 (vacuolar protein sorting 4) (Roxrud *et al.* 2010). The dominant negative mutation E233Q abrogates the ATP hydrolysis of VPS4 (Bishop *et al.* 2000) and prevents the budding of vesicles (Roxrud *et al.* 2010). To elucidate the influence of the dominant negative mutation E233Q on the EV release of SUMO-2, we transiently co-transfected a myc-SUMO-2- Δ GG construct (Δ GG mutation prevents the conjugation to SUMO and other proteins) with a plasmid encoding for the dominant negative (dn) mutant of VPS4 E233Q. EVs and the corresponding parental lysates were prepared from conditioned cultured medium and conducted to SDS-PAGE and subsequently conducted to Western blot analysis (Fig. 28 A). We detected a significant decrease in the EV release of a myc-SUMO-2 protein (Fig. 28 B). As an internal control, the WB blot membranes were also probed with an antibody against the EV marker protein Alix (Fig. 28 A upper panel). Alix release with EVs was decreased upon Vps4dn expression which is consistent with the fact that Alix interacts with the ESCRT machinery. In line with the function of VPS4, expression of its dominant negative form also decreased the total amount of EV release. The number of total released EVs was analysed by nanoparticle tracking analysis in the collecting medium (see Appendix, Table 13).

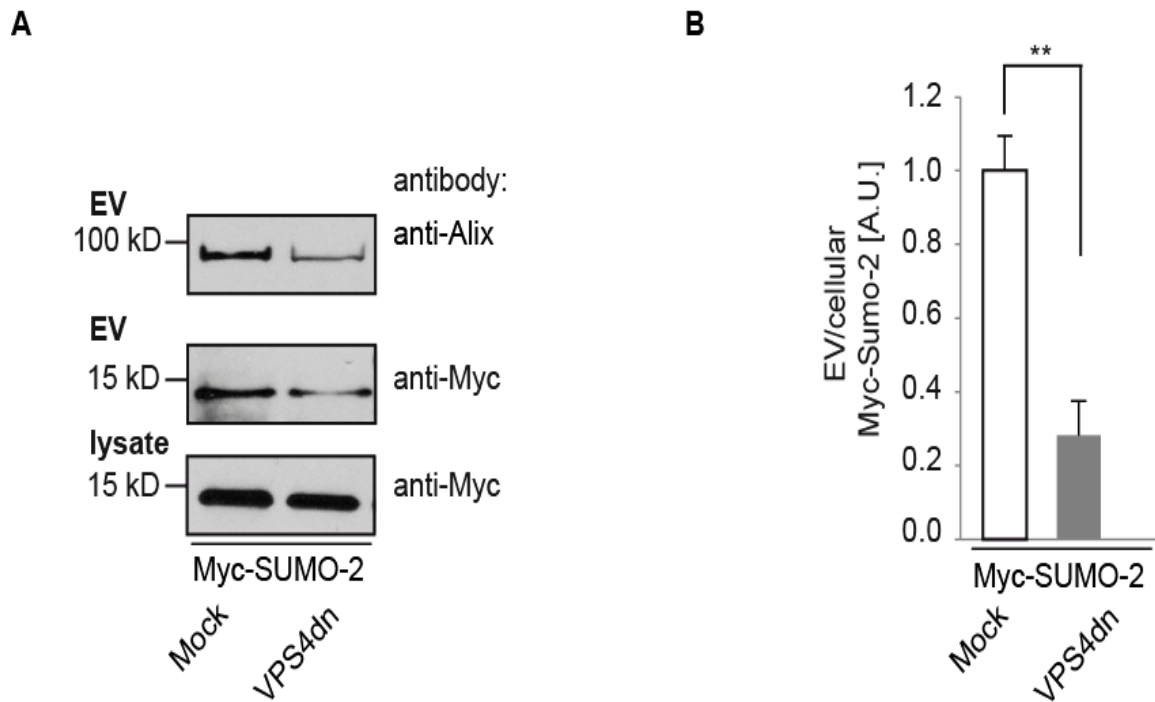


Fig. 28: Release of SUMO-2 with extracellular vesicles is dependent on ESCRT

(A) Myc-SUMO-2 and was transiently co-transfected with the dominant negative VPS4 E233Q mutant and the EV release was determined by Western blot analysis with an antibody against α -Syn. The blots of the extracellular vesicle fractions were accessorially probed with an antibody against the EV marker protein Alix. **(B)** The histogram displays the calculated ratio between signal intensity of the extracellular fraction versus the corresponding cell lysate. All values are given as mean + SEM from $n = 4$ independent experiments. ** indicates $p \leq 0.005$; student's 2-side t-test.

3.5.2. Co-expression of the dominant negative mutant of VPS4 decreases the extracellular vesicles release of a GFP-SUMO-2 fusion protein

As positive and negative controls for the effect of VPS4dn overexpression on the release of EVs, we studied the VPS4dn effect on a GFP-SUMO-2 fusion protein, for the Moloney murine leukemia virus Gag protein, fused to a GFP (MLV-Gag-GFP) and for PLP-myc (proteo-lipid protein 1). MLV-Gag is known to be released with EVs in an ESCRT dependent manner (Fang *et al.* 2007), whereas PLP release with EVs is ESCRT independent and requires ceramide (Trajkovic *et al.* 2008). As shown in Fig. 29 A-B, VPS4dn co-expression inhibited the EV release of GFP-SUMO-2 and MLV-Gag-GFP compared to mock co-transfection. As expected, there was no change in the EV secretion of PLP-myc, when N2a cells were co-transfected with VPS4dn (Fig. 29 C). Additionally, the membranes were probed with antibodies directed against Tsg101 or Alix as an internal control. As expected, the VPS4dn expression reduced the amount of Tsg101 and Alix in the EV fractions (Fig. 29 A and B). For quantification, the blots were scanned and quantified for their signal intensities to calculate the ratio of EV versus cellular protein. This quantification revealed a significant reduction of the EV release of MLV-Gag-GFP (grey bar) and GFP-SUMO-2 (black bar), due to the inference with VPS4dn E233Q (Fig. 29 D). Taken together, the EV release of SUMO-2 requires several components of the ESCRT machinery.

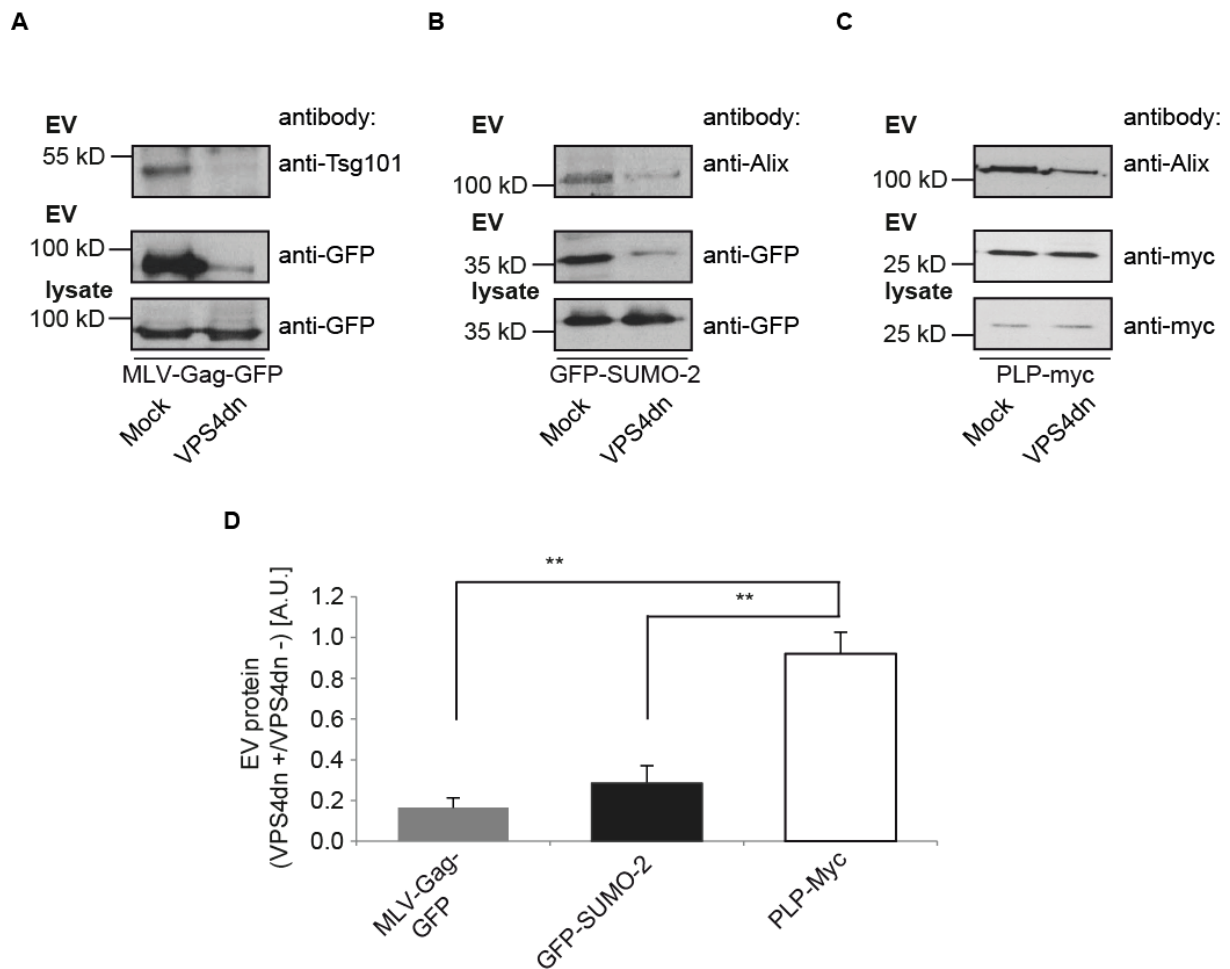


Fig. 29: Interference with VPS4 function inhibits release of SUMO-2 within extracellular vesicles

(A-C) N2a cells were co-transfected with VPS4dn and either MLV-Gag-GFP or GFP-SUMO-2 Δ GG or PLP-Myc. Cells transfected with MLV-Gag-GFP, GFP-SUMO-2 Δ GG or PLP-Myc alone were used as controls. EVs were prepared and cell lysates and vesicle pellets were subjected to Western blotting and probed with anti-GFP and anti-Myc antibodies. Blot membranes were also re-probed with antibodies against the EV marker proteins Tsg101 and Alix (AIP1). (D) The ratio of protein in the EV fraction from cells co-transfected with VPS4dn to mock-transfected cells was quantified by analysing signal intensities on the Western blots via ImageJ software. The negative control PLP-myc was normalised to 1. All values are given as mean + SEM for $n = 5$ independent experiments, ** indicates $p < 0.005$, 2-side t-test.

3.5.3. Extracellular vesicle release of SUMO-2 does not depend on the canonical SUMO protein interaction motif Q30 F31 I33

We next asked how SUMO-2 would interact with the ESCRT machinery. Tsg101 contains a SUMO-interaction motif for non-covalent interaction with SUMO proteins. We therefore assumed that SUMO interaction with the ESCRT could be mediated by protein-protein binding. Mutation of a canonical protein interaction motif Q30, F31, I33 in SUMO-2 had recently been shown to disrupt binding to SUMO interacting proteins (Hecker *et al.* 2006, Sun *et al.* 2007). We therefore compared EV release of SUMO-2 wt-GFP and the Q30A F31A I33A triple mutant of SUMO-2 GFP (SUMO-2- Δ SIM). For further analysis we subjected cell lysates and EV fractions to SDS-PAGE and subsequently to Western blot analysis. The membranes were probed with an antibody against GFP (Fig. 30 A). The ratio of EV/cellular SUMO-2GFP was increased for SUMO-2 bearing the Δ SIM mutant as compared to wt SUMO-2 GFP (Fig. 30 B).

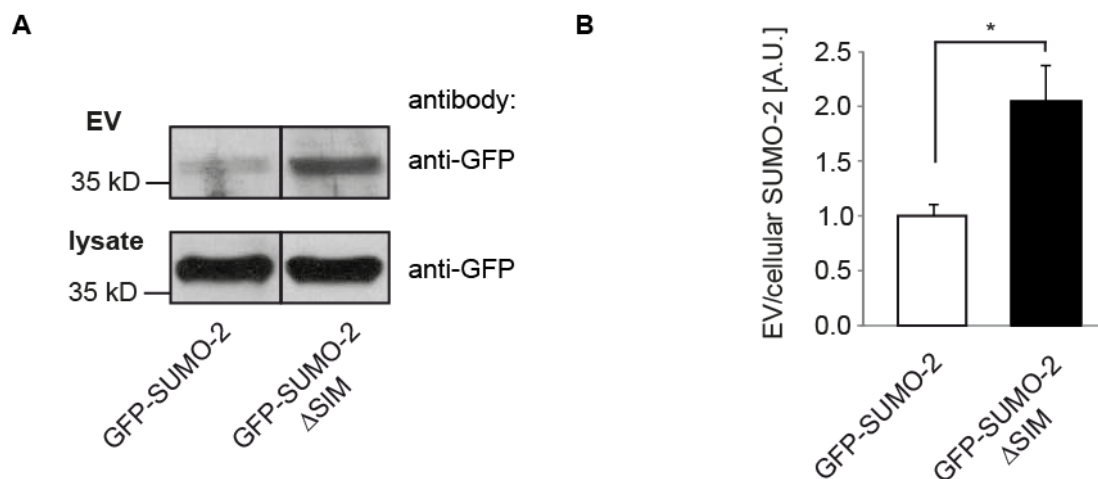


Fig. 30: Mutation of the SIM motif in SUMO-2 increases extracellular vesicle release of SUMO-2

(A) Western blotting of EV pellets and cell lysates from N2a cells transfected with either GFP-SUMO-2 or the triple A mutant (GFP-SUMO-2 Δ SIM). The blots were scanned and analysed for protein signal intensities. **(B)** The histogram depicted the ratio of GFP-SUMO-2 (white bar) versus the Δ SIM mutant (black bar) signal intensities of EV pellets versus the corresponding cell lysates. GFP-SUMO-2 was normalized to 1. All values are given as means +SEM for $n = 10$ independent experiments, * indicates $p < 0.05$, 2-side t-test.

Based on this observation, we assumed that the release of GFP-SUMO-2 within EVs is not mediated by a classical SIM protein-protein interaction. A possible explanation for this finding is that mutations of the SIM interaction motif might increase the amount of unbound cytosolic SUMO-2, which would then be available for EV release.

3.6. SUMO-lipid interaction

3.6.1. SUMO-2 interacts with phosphoinositols

The previous section 3.5.3 has shown, that EV sorting of SUMO-2 is not promoted via SIM-mediated protein interaction. We therefore investigated, whether the EV sorting and release of SUMO-2 was driven by an interaction with lipids at the ESCRT formation site. It has been shown that for a variety of SUMO-2 interacting proteins, like the EV protein polymyositis-scleoderma overlap syndrome (PMSCL1), the tumor suppressor protein promyelocytic leukaemia (PML) and the E3 SUMO ligase protein inhibitor of activated STAT 1 (PIAS1), phosphorylation of serine residues in the SUMO interaction domain is required for SUMO binding. This suggests an interaction of SUMO-2 with negatively charged domains (Stehmeier *et al.* 2009).

We therefore established an assay to test for SUMO-2 binding to different, negatively charged lipids. For this assay, recombinant SUMO-2 was labelled with the polarity-sensitive excited state intramolecular proton transfer (ESIPT) probe MFM (Shvadchak *et al.* 2011) and purified as described in section 2.2.4.5. Small unilamellar vesicles (SUV) were prepared from mixtures of 1-palmitoyl,2-oleoyl-sn-glycero-3-phosphocholine (POPC) in various combinations with different negatively charged lipids: phosphatidylserine (POPS, 10%) and a low fraction (5%) of the phosphoinositides PI(3)P, PI(5)P, PI(3,5)P₂, PI(4,5)P₂ or PI(3,4,5)P₃. Briefly, a stock solution of labelled SUMO-2-MFM was diluted to 100nM, 200nM and 300nM; the dilutions were mixed with different SUV concentrations of each lipid indicated above (up to 120µM) and transferred into a 96 well quartz glass microplate. To equilibrate the whole system an incubation time of at least 10 min was chosen. Subsequently the fluorescence of the MFM probe was recorded in a plate reader and the data were analysed with a tool implemented in the program Mathematica (Wolfram Research).

As shown in Fig. 31 the individual affinity of each lipid for SUMO-2 was calculated from a global analysis of the obtained and combined data of the fluorescence recording (all data analysis for this approach was kindly performed by Thomas M. Jovin, Laboratory of Cellular Dynamics, MPI for Biophysical Chemistry, Göttingen).

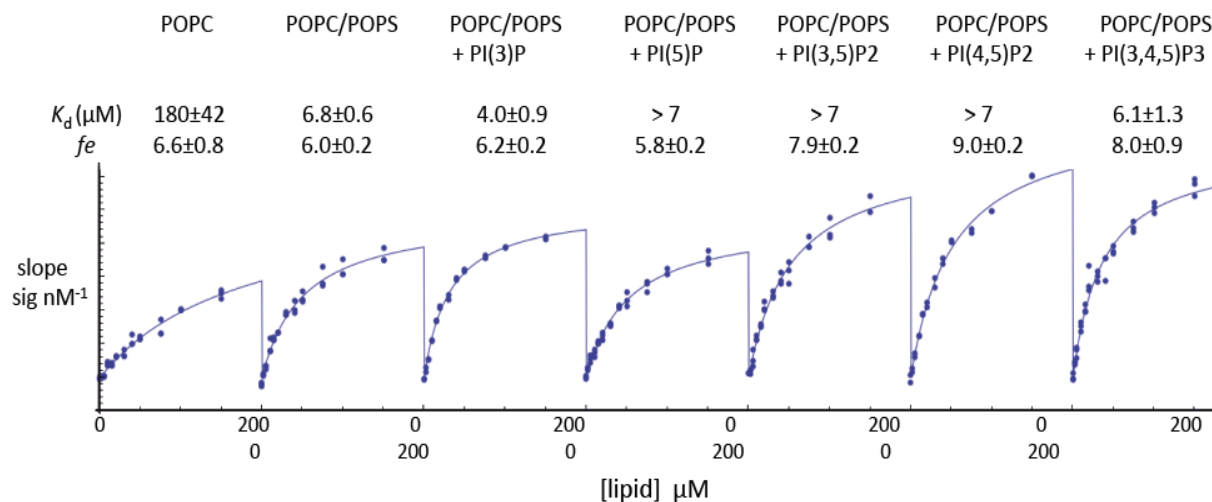


Fig. 31: Microplate titration assay of SUMO-2-MFM

The binding affinities of each lipid that contributes to the apparent affinity of the protein for the liposome was calculated as described in the Methods part. K_d s are given \pm standard measurement errors. The values corresponding to PI(5)P, PI(3,5)P₂ and PI(4,5)P₂ were too high to be determined (affinity less than that of the POPS co-lipid, i.e. > 7 μM). Statistically significant differences were obtained for POPC versus POPS ($p < 0.001$), and POPS versus PI(3)P ($p = 0.01$). No significant difference is found for PI(3,4,5)P₃ versus POPS; $n = 19$ titrations for each lipid mixture. The fluorescence enhancement factors (fe) are indicated with their respective standard measurement errors. See Methods for further details of this novel measurement approach.

As indicated in Fig. 31, SUMO-2 binds with weak affinity to uncharged membranes (K_d for DOPC binding: 180 μM) and with moderate affinity to a variety of PIPs. Highest affinities were observed for PI(3)P with a K_d of 4 μM and for P(3,4,5)P₃ with a K_d of 6.1 μM , indicating a preferential binding to PI3P and PI(3,4,5)P₃.

3.7. Identification of the membrane interaction motif of SUMO-2

3.7.1. The membrane interaction motif of SUMO-2 is localised to the hydrophobic cleft and nearby loops

To map the membrane interaction motif in SUMO-2 we collaborated with the group of Prof. M. Zweckstetter, DZNE Göttingen, Germany. For this purpose, recombinant SUMO-2 was expressed and purified as described in section 2.2.1.6 and the NMR analysis was performed according to the protocol presented in section 2.2.6. To identify the membrane interaction motif of SUMO-2 by NMR, 200 μM ^{15}N -labeled SUMO-2 in 20 mM $\text{NaH}_2\text{PO}_4/\text{Na}_2\text{HPO}_4$, pH 6.8, 100 mM KCl, 1 mM DTT was titrated with increasing concentrations of 8, 16 and 32 mM DHPC (1,2-dihexanoyl-sn-glycero-3-phosphocholine).

By NMR the major residues which might mediate interaction with lipid membranes were mapped to the hydrophobic cleft of SUMO-2 between the second β -strand and the α -helix (F31, K32, I33, L42 and Y46) Additional residues were located to the loops at the N-terminus of SUMO-2 (H16, H36 and D62) (Fig. 32). To sum up these results, we assume that the main membrane interaction motif of SUMO-2 is localised at the N-terminal end of the hydrophobic cleft and nearby loops.

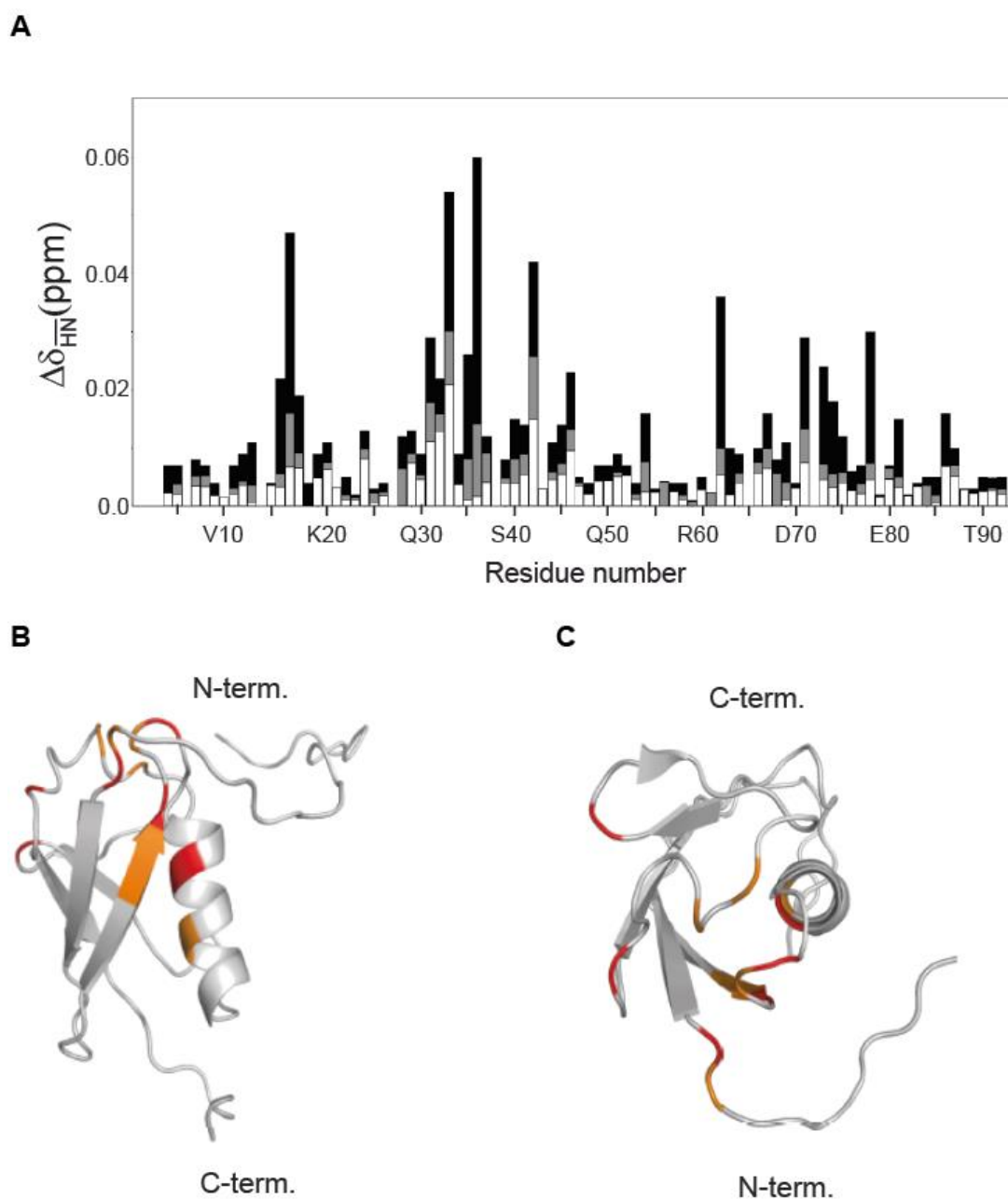


Fig. 32: Membrane binding of SUMO-2 analysed by NMR spectroscopy

(A) Mean weighted ^1H - ^{15}N chemical shifts of Sumo-2 at DHPC concentrations of 8 mM (white bars), 16 mM (grey bars) and 32 mM (black bars). Below the critical micellar concentration (CMC) of DHPC of 16 mM only few chemical shift changes in SUMO-2 were observed. (B+C) The chemical shift perturbation at 32 mM DHPC is plotted onto the SUMO-2 NMR structure (pdb-code: 2AWT). Residues in red display a perturbation greater than 0.03 ppm and residues in orange between 0.02-0.03 ppm. The structure in panel (C) is rotated by 90° relative to panel (B).

3.7.1.1. Mutations in the hydrophobic cleft and N-terminally loop domains of SUMO-2 decreases the membrane binding propensity of SUMO-2

To prove that the membrane interaction motif of SUMO-2 is located to the hydrophobic cleft and the N-terminally loop, additional experiments were performed to study how a mutation in the residues would affect the recruitment to membranes and the sorting of mutant SUMO into the EVs. Therefore, conjugation-deficient SUMO-2 Δ GG cDNA with *Bam*HI and *Xho*I restriction sites was synthesized containing the mutations Q30A, F31A, K32A, I33A, L42A, and Y46A (“cleft mutant”) and with the mutations H16A, Q30A, F31A, K32A, I33A, H36A, L42A, Y46A, and D62A (“cleft and loop mutant”). The cDNA was cloned into pcDNA 3 Myc vector via *Bam*HI and *Xho*I restriction sites. To determine membrane binding of these mutants, N2a cells were transiently transfected either with myc-SUMO-2- Δ GG cleft, myc-SUMO-2- Δ GG cleft+loop or myc-SUMO-2- Δ GG. To separate membranes and the cytosolic supernatant, cells were washed with PBS and collected in homogenization buffer. Subsequently, the cells were mechanically disrupted and centrifuged, to remove nuclei and cell debris. The obtained postnuclear supernatant was subjected to ultracentrifugation to separate the membrane and cytosol containing fractions. The membrane pellet and the corresponding cytosolic fractions were subjected to SDS-PAGE and Western blot analysis. As indicated in Fig. 33, we found that both, the myc-SUMO-2-cleft and the myc-SUMO-2 cleft+loop mutant, significantly decrease the membrane binding propensity of SUMO-2 compared to the myc-SUMO-2- Δ GG construct (Fig. 33 A+B).

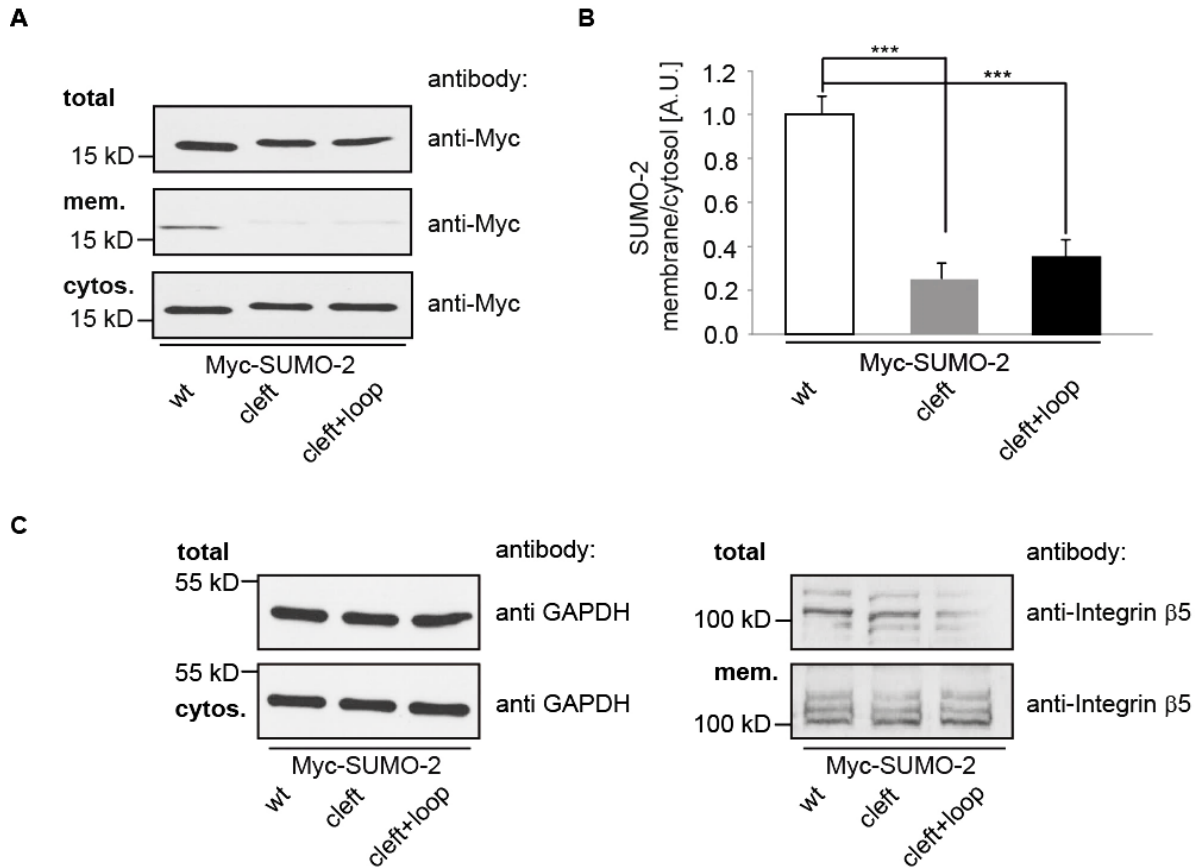


Fig. 33: Mutation of amino acids H16A, Q30A, F31A, K32A, I33A, H36, L42A, Y46A and D62 in the cleft and loop domains of SUMO-2 decreases membrane binding

(A) N2a cells were transfected with Myc-SUMO-2, Myc-SUMO-cleft mutant or Myc-SUMO-cleft+loop mutant. The postnuclear supernatant of the mechanically disrupted cells was centrifuged at $196,000 \times g$ for 30 min to separate the membrane containing pellet and the cytosolic supernatant. Membrane pellets and a proportion of the total cell lysate and the cytosol-containing supernatant were subjected to Western blot analysis and immunostained with an anti-myc antibody. **(B)** The Histogram displays the quantification of the Western blot analysis by calculating the ratio of signal intensities for membrane versus cytosolic fractions for wt (white bar, normalised to 1), for the cleft mutant (grey bar) and for the cleft+loop mutant (black bar). All values are given as means+SEM for $n = 8$ independent experiments, *** indicates $p < 0.0005$, 2-side t-test. **(C)** As fraction controls, blots were re-probed with an antibody against GAPDH as a cytosolic marker and with an antibody against $\beta 5$ -Integrin, as a membrane marker.

3.7.1.2. Mutations in the hydrophobic cleft and N-terminally loop domains of SUMO-2 decreases sorting into extracellular vesicles

If SUMO-2 interaction with the ESCRT pathway requires lipid binding, we would expect that mutations which interfere with SUMO-2 lipid binding would inhibit SUMO-2 release with EVs. N2a cells were transfected with SUMO-2- Δ GG cleft, SUMO-2- Δ GG cleft+loop mutants and SUMO-2- Δ GG and quantified EV release. After 8 h post-transfection we changed the medium and collected EVs for 16 hours. EVs and the corresponding cell lysates were subjected to Western blot analysis (Fig. 34 A). By determining the signal intensities of the Western blots and by calculating the ratio of SUMO-2 in EV versus cell lysates we found that both mutants were significantly decreased in the EV fractions (Fig. 34 B, white bar).

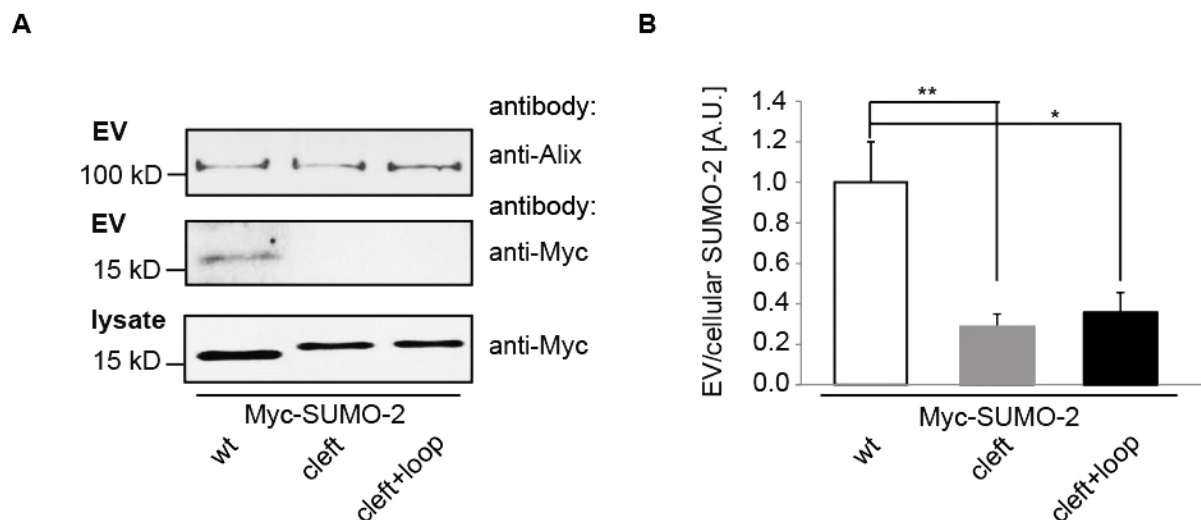


Fig. 34: Mutated amino acids H16A, Q30A, F31A, K32A, I33A, H36, L42A, Y46A and D62 in the cleft and loop domains of SUMO-2 decreases extracellular vesicle sorting

(A) Extracellular vesicles and corresponding lysates were prepared of cells, transfected either with Myc-SUMO-2-cleft mutant or Myc-SUMO-2-cleft+loop mutant and with Myc-SUMO-2 serving as a control. Lysates and EV fractions were processed to Western blotting and probed with an antibody against the myc-tag. Membranes were re-probed with an antibody against Alix as a marker for EVs in the different preparations. **(B)** Blots were scanned and analysed with Image J software to determine the signal intensities. Thereafter the ratio between extracellular protein versus cellular protein was calculated. All values are given as mean+SEM of $n = 9$ independent experiments, * indicates $p < 0.05$, ** indicates $p < 0.005$, 2-side t-test.

To conclude this, we can assume that the membrane interaction motif of SUMO-2 is located to the hydrophobic cleft and the N-terminally loop of SUMO-2, due to the decreased membrane binding and release within EVs of both SUMO mutant versions.

3.8. Co-expression of the dominant negative mutant of VPS4 decreases extracellular vesicle release of α -Synuclein

In line with the observations in section 3.5.1 (Fig. 28) we wanted to elucidate the influence of the dominant negative (dn) mutant of VPS4 E233Q on the EV release of myc- α -Syn-SUMO-2 fusion construct. To determine the EV release, a myc- α -Syn-SUMO-2 fusion construct (bearing the Δ GG mutation to prevent the conjugation to SUMO and other proteins) was co-transfected with a plasmid encoding for a dominant negative (dn) mutant of VPS4 E233Q. EVs and the corresponding parental lysates were prepared from conditioned cultured medium and conducted to SDS-PAGE and subsequently analysed by Western blotting (Fig. 35 A). We detected a significant decrease in the EV release of the myc- α -Syn-SUMO-2 fusion protein when co-expressed with the mutant Version of VPS4dn (Fig. 35 B).

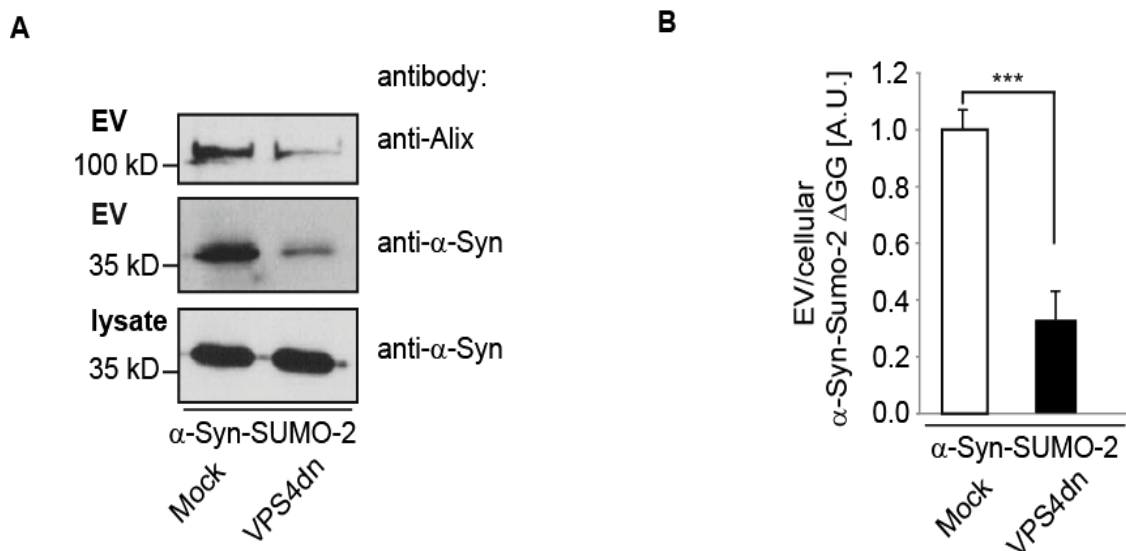


Fig. 35: Release of α -Syn-SUMO-2 fusion protein with extracellular vesicles is dependent on the ESCRT

(A) Myc- α -Syn-SUMO-2 were transiently co-transfected with the dominant negative VPS4 E233Q mutant and the EV release of both constructs was determined by Western blot analysis with antibodies against α -Syn and myc-tagged SUMO-2. The blots of the extracellular vesicle fractions were subsequently probed with an antibody against the EV marker protein Alix. **(B)** Quantification of protein signal intensity analysis was performed via ImageJ software. The histogram indicates the calculated ratio of sumoylated extracellular vesicle α -Syn versus the parental cell lysate of single transfected N2a cells (Mock, white bar), compare to cells which were co-transfected with the mutated version of VPS4. All values are given as mean + SEM of $n = 12$ independent experiments. *** indicates $p < 0.0005$; 2-side t-test.

By nanoparticle tracking analysis of the cultured medium (see section 2.2.3.3) we could observe a significant reduction of EV release in the case of VPS4dn co-transfection (see Appendix, Table 13). To conclude this, similar to SUMO-2, the release of α -Syn within EVs was inhibited by co-expression of a dominant negative VPS4 mutant, indicating that EV sorting by SUMO modification is ESCRT-dependent.

3.9. Inhibition of endosome maturation by overexpression of dominant negative Rab5 does not trap α -Syn or SUMO-2 in enlarged intraluminal vesicles

Next we wanted to differentiate between the release of vesicles promoted by plasma membrane shedding and release which is mediated by the MVB pathway. To address this issue we co-expressed constructs encoding for myc- α -Syn wt or myc-SUMO-2 wt, together with the dominant negative mutant of Rab5 (Rab5Q79L).

Rab5Q79L induces homotypic fusion of early endosomes and stops the endosomal maturation at the level of early endosomes by inhibiting the intraendosomal trafficking (Stenmark *et al.* 1994a, Stenmark *et al.* 1994b, Raiborg *et al.* 2001). This leads to the trapping of ILV like structures within enlarged endosomes and allows the visualisation of proteins sorted into ILVs by immune fluorescence (Trajkovic 2008, Baietti 2012).

Previously, it was shown by electron microscopy that the giant early endosomes induced by Rab5Q79L overexpression are filled with intraluminal vesicle (Trajkovic *et al.* 2008). Their morphology does not differ from the ILVs detected in MVBs (Trajkovic *et al.* 2008). The authors also showed by immunofluorescence analysis that EV marker proteins such as Flotillin-2 were trapped in the intraluminal vesicles of Rab5Q79L positive endosomes. We co-transfected N2a cells either with myc-SUMO-2- Δ GG or with myc- α -Syn-SUMO-2- Δ GG and rab5Q79L and performed an immunostaining after 24 hours with an antibody against the myc-epitope of SUMO-2, PLP and with an antibody against α -Syn.

As a positive control, we performed the same experiment with co-expression of rab5Q79L and PLP-myc which has recently been shown to accumulate in ILVs of rab5Q79L positive endosomes (Trajkovic 2008). As indicated in Fig. 36 A and B (left panel red arrows) we found PLP in rab5Q79L induced endosomal ILVs. In contrast, SUMO-2 (Fig. 36 A, right panel) and α -Syn (Fig. 36 B, right panel) were absent from enlarged rab5Q79L positive endosomes. This data indicates that SUMO-2 and α -Syn may not be sorted via the endosomal MVB pathway but rather bud from the plasma membrane within shedding microvesicles.

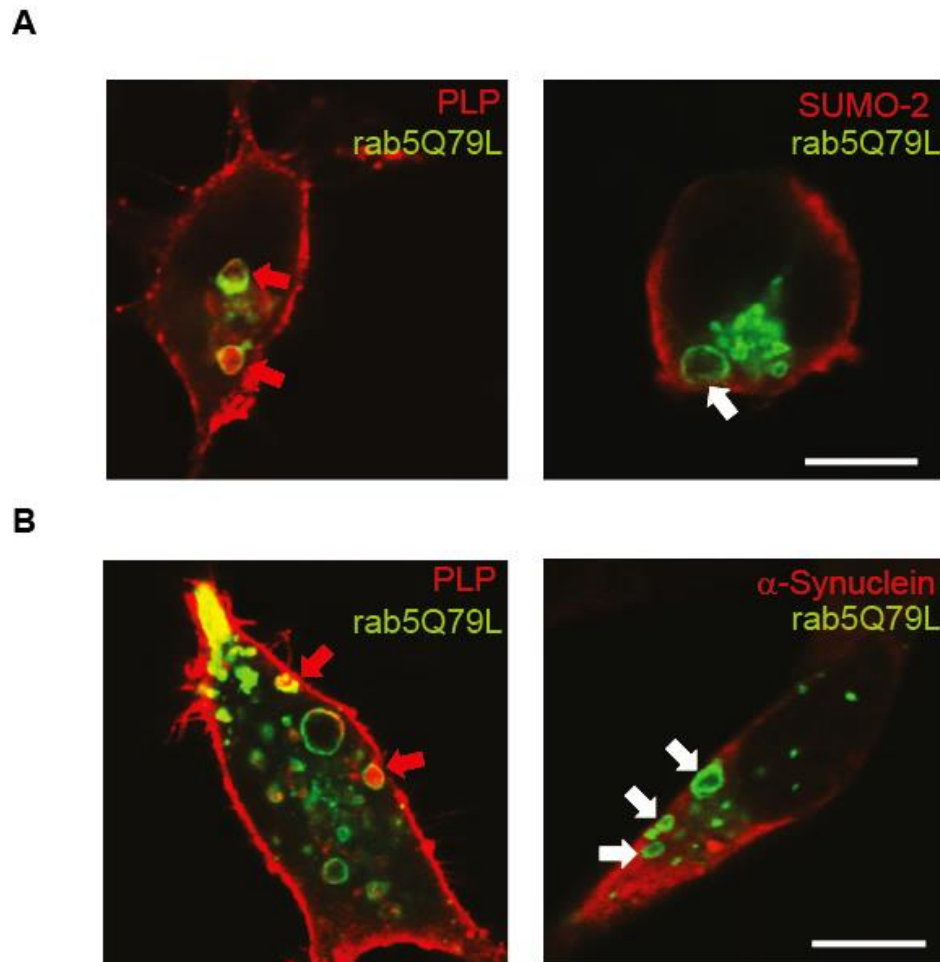


Fig. 36: Subcellular distribution of SUMO-2 and α -Synuclein

(A) N2a cells were co-transfected with Rab5Q79L-GFP (green) and PLP-myc (red) or with Rab5Q79L-GFP (green) and Myc-SUMO-2 (red). **(B)** Same controls were transfected as indicated in (A) and N2a cells were co-transfected with or with Rab5Q79L-GFP (green) and Myc- α -Syn (red). Images were taken with by laser scanning confocal microscopy. Localization of positive control PLP-myc within Rab5Q79L endosomes are highlighted by red arrows. No localization for SUMO-2 and α -Syn in Rab5Q79L endosomes was observed (white arrows right upper and lower panel). For each condition $n = 20$ endosomes were analysed, scale bar = 10 μ m.

4. Discussion

4.1. α -Synuclein is localised in EVs *in vitro*

Neuronal cells are able to release EVs to their environment (Fauré *et al.* 2006, Trajkovic *et al.* 2008). Consistent with previous studies (Danzer *et al.* 2012, Emmanouilidou *et al.* 2012), we could detect α -Syn in EVs derived from N2a cells.

To clarify whether α -Syn is truly encapsulated in EVs or rather attached to the outer membrane, different trypsination assays were performed. Thus, we found that the vast bulk of α -Syn recovered by ultracentrifugation resides within the EVs rather than being localised to the surface membrane of the vesicles. Our findings are contradictory to previous published results. Danzer *et al.* reported that only a small amount of α -Syn in the EV preparation was affected by trypsin digestion, which led to the assumption the α -Syn is primarily localised to the outer vesicle membrane. However, EVs in this study were frozen after preparation and prior to trypsin digestion (Danzer, personal communication). In our assay, all EV preparations were digested immediately after preparation since freezing likely interferes with membrane integrity, making intravesicular protein accessible to trypsin. Under these experimental conditions, α -Syn was not degraded by trypsin and hence most likely localized within the vesicles.

Overexpression of exogenous α -Syn might artificially lead to its EV dependent release. To address this issue, we showed that cells also release endogenous α -Syn with EVs. The detection of endogenous α -Syn is difficult due to the low expression levels, even in cell lysates (Lee *et al.* 2011). We have therefore isolated EVs from HEK cells and quantified intracellular and extracellular vesicle α -Syn levels by the electrochemiluminescence assay described in section 2.2.4.4. For this approach we used HEK cells because this assay is only established for the detection of human α -Syn and does not detect mouse α -Syn (Kruse *et al.* 2012). (data not shown in the thesis).

4.2. Microvesicles or exosomes?

For the purification of EVs a protocol with subsequent centrifugation steps including a final ultracentrifugation step was applied. By using this purification method, potential contaminations of the ultracentrifugation pellet (P-100) with protein aggregates (e.g. α -Syn which possibly aggregates in the cultured medium and could co-sediment during the ultracentrifugation process) and other vesicles (Mathivanan *et al.* 2012, Tauro *et al.* 2013) cannot be excluded.

Therefore, we additionally used sucrose gradient ultracentrifugation to eliminate contaminating proteins which might be non-specifically associated with EVs. However, for an accurate quantification of EV protein content we used ultracentrifugation rather than density gradient centrifugation, once we had established by sucrose gradient centrifugation that α -Syn floats with EVs (Fig. 6 B).

Up to date it is not possible to discriminate between exosomes and (shedding) microvesicles in the size range of exosomes (~100 nm) (Booth *et al.* 2006). It has been stated in several articles that “differences in properties such as size, morphology, buoyant density, and protein composition seem insufficient for a clear distinction” (Raposo *et al.* 2013) between both types of vesicles (Bobrie *et al.* 2011) (Simons *et al.* 2009) (Shen *et al.* 2011a). Therefore, exosomes and shedding microvesicles “remain mostly associated in the subcellular fractions isolated by differential centrifugation and by various types of gradient centrifugation”(Cocucci *et al.* 2009). Shen *et al.* state that “differentiating between microvesicles and exosomes is problematic because (i) there is no known physical property or molecular marker that can unambiguously differentiate exosomes from microvesicles (Simons *et al.* 2009), and (ii) it is conceptually impossible to know where any particular secreted vesicle was made once it has left the cell (Shen *et al.* 2011a). The authors in this study therefore coined the umbrella term EMV for exosomes/microvesicles. Recently, due to the overlapping size range, the biochemical and physical properties of exosomes and microvesicles, it was recommended to use the term extracellular vesicle (EV) as “a generic term for all secreted vesicles” (Gould *et al.* 2013). Thus, we do not claim to distinguish between exosomes and microvesicles since clearly the methods we used do not allow to differentiate between both vesicle types. For this reason we use the term extracellular vesicles and not exosomes or microvesicles. Based on our ultracentrifugation/gradient density experiments, we cannot differentiate whether α -Syn and SUMO-2 are released via bona fide exosomes or shedding microvesicles.

Although the lack of α -Syn and SUMO-2 in intraluminal vesicles after overexpression of rab5dn suggests that both proteins may be shedded from the plasma membrane, this experiment does not exclude that α -Syn and SUMO-2 are released by the exosomal/multivesicular body pathway (Fig. 36).

4.3. SUMO-2 interacts with phosphoinositols

We show that SUMO-2 binds to PI3P with a K_d of 4 μ M and to PI(3,4,5)P₃ with a K_d of 6.1 μ M (Fig. 31). The similar lipid binding affinity of SUMO-2 for PI(3)P and PI(3,4,5)P₃ would be compatible with both pathways, plasma membrane shedding and the MVB dependent SUMO-2 EV release. Phosphorylated inositols can act as mediators of sorting cargo proteins to the ESCRT complex. The ESCRT-0 complex can be recruited to sites of intraluminal vesicle formation by PI(3)P binding of the Hrs FYVE domains (Hurley 2008).

In addition, further studies have revealed that PI(3,5)P₂ recruits cargo proteins to the ESCRT machinery localized at multivesicular endosomes (Friant *et al.* 2003, Whitley *et al.* 2003, Huotari *et al.* 2011). The cytosolic protein TyA can fuse with the PI(3,4,5)P₃-binding domain of AKT protein kinase and efficiently targets the protein to budding sites at the plasma membrane for extracellular vesicle release (Shen *et al.* 2011b). Both lipids, PI(3)P and PI(3,4,5)P₃ are known to recruit the ESCRT complex and interaction of SUMO-2 and SUMO-2 modified proteins with these lipids might explain the ESCRT dependent sorting of SUMO-2 into EVs. Of note, PI(3)P is known to be localized to endosomal membranes, while PI(3,4,5)P₃ is predominantly enriched in plasma membranes (Henne *et al.* 2011).

4.3.1. SUMO binding to plasma membranes is mediated by PI(3,4,5)P₃

Based on our experiments with rab5Q79L overexpression (Fig. 36), it is likely that SUMO rather binds to the plasma membrane mediated by interaction with PI(3,4,5)P₃ than to endosomal membranes mediated by PI(3)P. The specificity of SUMO-2 binding to the plasma membrane (as opposed to endosomal PI(3)P binding) may be caused by differences in the overall lipid composition of the inner plasma membrane leaflet compared to the endosomal membrane. One important difference regarding the lipid composition is the ratio of cholesterol to phospholipids which is significantly higher in the plasma membrane compared to endosomal membranes (van Meer *et al.* 2008). Interestingly, it has been shown that cholesterol can act as a spacer to segregate phosphoinositide lipids thereby reducing their electrostatic repulsion followed by a stabilization of membrane micro domains (Jiang *et al.* 2014). E.g., in the case of the tumor suppressor protein PTEN the presence of cholesterol enhances its binding to a variety of different phosphoinositides (Jiang *et al.* 2014). Thus, a preferential binding of SUMO to the plasma membrane may be mediated by a combination of high local cholesterol and the presence of PI(3,4,5)P₃. Clearly, further lipid binding experiments with different PIPs and a variety of PIP/cholesterol ratios would be required to unequivocally prove this assumption.

4.4. α -Synuclein is localised in EVs *in vivo*

At the beginning of this study it was not known whether α -Syn is present in EVs *in vivo*. EVs are abundant in different body fluids such as blood, plasma and urine (Keller *et al.* 2011) but have never been isolated from human CSF. We show for the first time, that EVs can be prepared from human CSF. From the presence of the CNS expressed proteins GluR1, 2, and 3 we conclude that these vesicles are at least partially derived from the CNS. We also deliver the first evidence of α -Syn in extracellular vesicles in the human central nervous system *in vivo* (Fig. 7).

Interestingly, Danzer *et al.* could show that EVs contain α -Syn oligomers, that EV associated α -Syn is more likely to be taken up by target cells and is more neurotoxic than free, non-vesicular α -Syn oligomers (Emmanouilidou *et al.* 2010, Danzer *et al.* 2012, Luk *et al.* 2012a, Luk *et al.* 2012b, Mougnot *et al.* 2012).

Free α -Syn may aggregate into oligomers and fibrils. Therefore, it could be difficult to avoid contaminations of free α -Syn or its aggregated form when examining α -Syn in Evs. To prove that α -Syn is indeed localised in EVs *in vivo* in human CSF, we provided evidence that α -Syn can be detected in the “correct” sucrose gradient fractions. Due to the fact the sensitivity of Western blot analysis was not sufficient for this approach we decided to use an electrochemiluminescence based assay (2.2.4.4). We found that sucrose gradient ultracentrifugation of CSF derived EVs followed by electrochemiluminescence assay detection of α -Syn (see section 3.1.2, Fig. 7 F) displayed a flotation behavior similar to the EV marker protein Flotilin-2 3.1.2, Fig. 7 D).

Thus, our findings that α -Syn is present in EVs *in vivo*, strongly supports the hypothesis that EVs could contribute to disease propagation in PD and other synucleinopathies.

4.5. Extracellular vesicles as carrier for pathogenic proteins

EV transfer of pathogenic proteins has for example been shown for prion protein. The misfolded PrP^{Sc} co-purifies with the cellular PrP^C within EVs isolated from cell culture (Fevrier *et al.* 2004b, Vella *et al.* 2007), CSF (Vella *et al.* 2008) and blood (Robertson *et al.* 2006). PrP containing EVs can transmit infection to other cells, thus indicating a potential role for EVs mediated cell to cell spread of prion infection. A variety of neurodegenerative disorders are characterized by the misfolding and aggregation of proteins and peptides, including tau and A β in Alzheimer’s disease (Takahashi *et al.* 2015), Cu/Zn superoxide dismutase (SOD1) and TAR-DNA binding protein 43 (TDP43) in Amyotrophic lateral sclerosis (ALS) (Pokrishevsky *et al.* 2012).

Interestingly, these proteins have also been detected in EVs (Rajendran *et al.* 2006, Vingdeux *et al.* 2012, Feneberg *et al.* 2014, Grad *et al.* 2014).

It is tempting to speculate that these proteins are packed into EVs in their aggregated misfolded form which would enable their pathological function as a nucleus to induce the aggregation of soluble proteins in recipient cells. *In vitro*, this has already been shown for EV associated α -Syn (Danzer *et al.* 2012). It is interesting to note, that oligomerization of proteins alone is sufficient for their sorting and release with EVs (Booth *et al.* 2006). Therefore, it is feasible that especially pathological aggregates of proteins are enriched in EVs.

4.5.1. Interneuronal spreading of α -Syn pathology

Intracellular aggregates of α -Syn, so called Lewy bodies (LB) are the neuropathological hallmark of Parkinson's disease (PD) and Lewy Body dementia (LBD) (Spillantini *et al.* 1998b). The progression of α -Syn pathology in PD seems to follow a stereotypical anatomical path through the brain (Braak *et al.* 2003). This, together with the emergence of LBs in transplanted embryonic nigral cells in PD patients lead to the assumption of interneuronal spreading of disease pathology (Kordower *et al.* 2008a, Li *et al.* 2008). Supporting this notion, cell to cell transfer of α -Syn followed by aggregation of soluble α -Syn in recipient cells was demonstrated in mouse brain and cell culture (Desplats *et al.* 2009, Hansen *et al.* 2011, Luk *et al.* 2012a, Luk *et al.* 2012b), however the transfer mode of pathogenic α -Syn between neuronal cells is not known. Extracellular α -Syn has been proposed as a crucial mechanism for induction of pathological aggregate formation in previously healthy cells. Although α -Syn does not contain a sorting signal for extracellular release, soluble and aggregated α -Syn was detected in tissue culture medium and body fluids, such as brain interstitial fluid, plasma and CSF (El-Agnaf *et al.* 2003, Lee *et al.* 2005, El-Agnaf *et al.* 2006, Tokuda *et al.* 2010, Emmanouilidou *et al.* 2011, Hansson *et al.* 2014, Lee *et al.* 2014).

4.6. SUMO modification in neurodegenerative diseases

We have identified SUMO modification as an important factor for EV release of cytosolic proteins. A growing body of evidence has linked SUMO modification to neurodegenerative diseases. E.g., Steffan and co-workers report an increased sumoylation of huntingtin in a *Drosophila* model which exacerbates neurodegeneration (Steffan *et al.* 2004). SUMOylation was also shown to induce the pathological hyper-phosphorylation of tau observed in Alzheimer's disease and also inhibits tau degradation (Luo *et al.* 2014) and sumoylated tau was also detected in AD brains (Luo *et al.* 2014). Importantly, an upregulation of tau SUMOylation was observed *in vitro* after exposure of neurons to toxic $\text{a}\beta$ (Luo *et al.* 2014).

5. Summary

We hypothesized that cells release and transfer α -Syn associated with EVs, followed by highly efficient internalization and induction of α -Syn aggregation in previously healthy neurons. EVs of 40-100 nm diameter can either be derived from the multivesicular endosome (MVE) (exosomes) or shedded from the plasma membrane (microvesicles). Both types of vesicles are involved in the release of toxic cellular content and intercellular transfer of proteins, lipids and RNA and vesicular α -Syn may be internalized more efficiently by recipient cells than the free protein and induce greater toxicity (Danzer *et al.* 2012).

We could show that α -Syn is released with EVs and targeted to EVs by a completely novel mechanism based on SUMO modification. So far, ubiquitination had been regarded as an exclusive, necessary and sufficient signal for EV release of proteins. We could decipher the molecular mechanism of this novel sorting pathway, demonstrating that SUMO-dependent targeting to EVs depends on the endosomal sorting complex required for transport (ESCRT). Interestingly, the interaction of SUMO with ESCRT formation sites is mediated by SUMO binding to phosphoinositol containing membrane microdomains, most likely at the inner leaflet of the plasma membrane. By NMR spectrometry, we mapped the lipid interaction domain of SUMO to its hydrophobic cleft. Moreover, we could demonstrate that inhibition of SUMOylation by different genetic approaches strongly decreases the release of α -Syn with EVs. In contrast, enhancing SUMOylation by co-expression of SUMO or fusion of SUMO to α -Syn increased α -Syn sorting to EVs. Similar to SUMO, the release of α -Syn within EVs was inhibited by co-expression of a dominant-negative VPS4 mutant, indicating that EV sorting by SUMO modification is ESCRT-dependent.

Our findings are thus of highest relevance for the understanding of Parkinson's disease pathogenesis and progression at the molecular level. Moreover, we propose that SUMO-dependent sorting constitutes a mechanism with more general implications for cell biology.

6. References

1. **M. Aalberts, F. M. van Dissel-Emiliani, N. P. van Adrichem, M. van Wijnen, M. H. Wauben, T. A. Stout, W. Stoorvogel**, Identification of distinct populations of prostasomes that differentially express prostate stem cell antigen, annexin A1, and GLIPR2 in humans. *Biology of reproduction* **86**(3):82, 81-88, (2012).
2. **A. Abeliovich, Y. Schmitz, I. Farinas, D. Choi-Lundberg, W. H. Ho, P. E. Castillo, N. Shinsky, J. M. Verdugo, M. Armanini, A. Ryan, M. Hynes, H. Phillips, D. Sulzer, A. Rosenthal**, Mice lacking alpha-synuclein display functional deficits in the nigrostriatal dopamine system. *Neuron* **25**(1):239-252, (2000).
3. **A. Aguzzi, L. Rajendran**, The transcellular spread of cytosolic amyloids, prions, and prionoids. *Neuron* **64**(6):783-790, (2009).
4. **J. P. Anderson, D. E. Walker, J. M. Goldstein, R. de Laat, K. Banducci, R. J. Caccavello, R. Barbour, J. Huang, K. Kling, M. Lee, L. Diep, P. S. Keim, X. Shen, T. Chataway, M. G. Schlossmacher, P. Seubert, D. Schenk, S. Sinha, W. P. Gai, T. J. Chilcote**, Phosphorylation of Ser-129 is the dominant pathological modification of alpha-synuclein in familial and sporadic Lewy body disease. *The Journal of biological chemistry* **281**(40):29739-29752, (2006).
5. **E. Angot, J. A. Steiner, C. Hansen, J. Y. Li, P. Brundin**, Are synucleinopathies prion-like disorders? *Lancet neurology* **9**(11):1128-1138, (2010).
6. **M. Babst**, A protein's final ESCRT. *Traffic* **6**(1):2-9, (2005).
7. **M. Babst**, MVB vesicle formation: ESCRT-dependent, ESCRT-independent and everything in between. *Current opinion in cell biology* **23**(4):452-457, (2011).
8. **M. Babst, B. Wendland, E. J. Estepa, S. D. Emr**, The Vps4p AAA ATPase regulates membrane association of a Vps protein complex required for normal endosome function. *The EMBO journal* **17**(11):2982-2993, (1998).
9. **M. F. Baietti, Z. Zhang, E. Mortier, A. Melchior, G. Degeest, A. Geeraerts, Y. Ivarsson, F. Depoortere, C. Coomans, E. Vermeiren, P. Zimmermann, G. David**, Syndecan-syntenin-ALIX regulates the biogenesis of exosomes. *Nature cell biology* **14**(7):677-685, (2012).
10. **K. G. Baker, Y. Huang, H. McCann, W. P. Gai, P. H. Jensen, G. M. Halliday**, P25alpha immunoreactive but alpha-synuclein immunonegative neuronal inclusions in multiple system atrophy. *Acta neuropathologica* **111**(2):193-195, (2006).
11. **T. Bartels, L. S. Ahlstrom, A. Leftin, F. Kamp, C. Haass, M. F. Brown, K. Beyer**, The N-terminus of the intrinsically disordered protein alpha-synuclein triggers membrane binding and helix folding. *Biophysical journal* **99**(7):2116-2124, (2010).
12. **K. Beckett, S. Monier, L. Palmer, C. Alexandre, H. Green, E. Bonneil, G. Raposo, P. Thibault, R. Le Borgne, J. P. Vincent**, Drosophila S2 cells secrete wingless on exosome-like vesicles but the wingless gradient forms independently of exosomes. *Traffic* **14**(1):82-96, (2013).
13. **S. A. Bellingham, B. B. Guo, B. M. Coleman, A. F. Hill**, Exosomes: vehicles for the transfer of toxic proteins associated with neurodegenerative diseases? *Frontiers in physiology* **3**(124), (2012).
14. **J. T. Bendor, T. P. Logan, R. H. Edwards**, The function of alpha-synuclein. *Neuron* **79**(6):1044-1066, (2013).
15. **V. Bernier-Villamor, D. A. Sampson, M. J. Matunis, C. D. Lima**, Structural basis for E2-mediated SUMO conjugation revealed by a complex between ubiquitin-conjugating enzyme Ubc9 and RanGAP1. *Cell* **108**(3):345-356, (2002).
16. **U. Bertsch, K. F. Winklhofer, T. Hirschberger, J. Bieschke, P. Weber, F. U. Hartl, P. Tavan, J. Tatzelt, H. A. Kretzschmar, A. Giese**, Systematic identification of anti-prion drugs by high-throughput screening based on scanning for intensely fluorescent targets. *Journal of virology* **79**(12):7785-7791, (2005).

17. **J. Bieschke, A. Giese, W. Schulz-Schaeffer, I. Zerr, S. Poser, M. Eigen, H. Kretzschmar**, Ultrasensitive detection of pathological prion protein aggregates by dual-color scanning for intensely fluorescent targets. *Proceedings of the National Academy of Sciences of the United States of America* **97**(10):5468-5473, (2000).
18. **N. Bishop, P. Woodman**, ATPase-defective mammalian VPS4 localizes to aberrant endosomes and impairs cholesterol trafficking. *Molecular biology of the cell* **11**(1):227-239, (2000).
19. **A. Bjorklund, S. B. Dunnett, P. Brundin, A. J. Stoessl, C. R. Freed, R. E. Breeze, M. Levivier, M. Peschanski, L. Studer, R. Barker**, Neural transplantation for the treatment of Parkinson's disease. *Lancet neurology* **2**(7):437-445, (2003).
20. **A. Bobrie, M. Colombo, G. Raposo, C. Thery**, Exosome secretion: molecular mechanisms and roles in immune responses. *Traffic* **12**(12):1659-1668, (2011).
21. **A. M. Bodles, D. J. Guthrie, B. Greer, G. B. Irvine**, Identification of the region of non-Abeta component (NAC) of Alzheimer's disease amyloid responsible for its aggregation and toxicity. *Journal of neurochemistry* **78**(2):384-395, (2001).
22. **C. R. Bodner, A. S. Maltsev, C. M. Dobson, A. Bax**, Differential phospholipid binding of alpha-synuclein variants implicated in Parkinson's disease revealed by solution NMR spectroscopy. *Biochemistry* **49**(5):862-871, (2010).
23. **V. Bonifati, P. Rizzu, F. Squitieri, E. Krieger, N. Vanacore, J. C. van Swieten, A. Brice, C. M. van Duijn, B. Oostra, G. Meco, P. Heutink**, DJ-1(PARK7), a novel gene for autosomal recessive, early onset parkinsonism. *Neurological sciences : official journal of the Italian Neurological Society and of the Italian Society of Clinical Neurophysiology* **24**(3):159-160, (2003).
24. **A. M. Booth, Y. Fang, J. K. Fallon, J. M. Yang, J. E. Hildreth, S. J. Gould**, Exosomes and HIV Gag bud from endosome-like domains of the T cell plasma membrane. *The Journal of cell biology* **172**(6):923-935, (2006).
25. **H. Braak, K. Del Tredici, U. Rub, R. A. de Vos, E. N. Jansen Steur, E. Braak**, Staging of brain pathology related to sporadic Parkinson's disease. *Neurobiology of aging* **24**(2):197-211, (2003).
26. **C. Braicu, C. Tomuleasa, P. Monroig, A. Cucuianu, I. Berindan-Neagoe, G. A. Calin**, Exosomes as divine messengers: are they the Hermes of modern molecular oncology? *Cell death and differentiation* **22**(1):34-45, (2015).
27. **J. Braman, C. Papworth, A. Greener**, Site-directed mutagenesis using double-stranded plasmid DNA templates. *Methods Mol Biol* **57**(31-44), (1996).
28. **J. F. Brouwers, M. Aalberts, J. W. Jansen, G. van Niel, M. H. Wauben, T. A. Stout, J. B. Helms, W. Stoorvogel**, Distinct lipid compositions of two types of human prostasomes. *Proteomics* **13**(10-11):1660-1666, (2013).
29. **P. Brundin, J. Y. Li, J. L. Holton, O. Lindvall, T. Revesz**, Research in motion: the enigma of Parkinson's disease pathology spread. *Nature reviews. Neuroscience* **9**(10):741-745, (2008).
30. **V. L. Buchman, H. J. Hunter, L. G. Pinon, J. Thompson, E. M. Privalova, N. N. Ninkina, A. M. Davies**, Persyn, a member of the synuclein family, has a distinct pattern of expression in the developing nervous system. *The Journal of neuroscience : the official journal of the Society for Neuroscience* **18**(22):9335-9341, (1998).
31. **M. P. Caby, D. Lankar, C. Vincendeau-Scherrer, G. Raposo, C. Bonnerot**, Exosomal-like vesicles are present in human blood plasma. *International immunology* **17**(7):879-887, (2005).
32. **M. Chaineau, L. Danglot, T. Galli**, Multiple roles of the vesicular-SNARE TI-VAMP in post-Golgi and endosomal trafficking. *FEBS letters* **583**(23):3817-3826, (2009).
33. **E. Cocucci, G. Racchetti, J. Meldolesi**, Shedding microvesicles: artefacts no more. *Trends in cell biology* **19**(2):43-51, (2009).
34. **M. Colombo, G. Raposo, C. Thery**, Biogenesis, secretion, and intercellular interactions of exosomes and other extracellular vesicles. *Annual review of cell and developmental biology* **30**(255-289), (2014).

35. **J. Conde-Vancells, E. Rodriguez-Suarez, N. Embade, D. Gil, R. Matthiesen, M. Valle, F. Elortza, S. C. Lu, J. M. Mato, J. M. Falcon-Perez,** Characterization and comprehensive proteome profiling of exosomes secreted by hepatocytes. *Journal of proteome research* **7**(12):5157-5166, (2008).
36. **M. R. Cookson,** The biochemistry of Parkinson's disease. *Annual review of biochemistry* **74**(29-52), (2005).
37. **A. A. Cooper, A. D. Gitler, A. Cashikar, C. M. Haynes, K. J. Hill, B. Bhullar, K. Liu, K. Xu, K. E. Strathearn, F. Liu, S. Cao, K. A. Caldwell, G. A. Caldwell, G. Marsischky, R. D. Kolodner, J. Labaer, J. C. Rochet, N. M. Bonini, S. Lindquist,** Alpha-synuclein blocks ER-Golgi traffic and Rab1 rescues neuron loss in Parkinson's models. *Science* **313**(5785):324-328, (2006).
38. **O. Corti, S. Lesage, A. Brice,** What genetics tells us about the causes and mechanisms of Parkinson's disease. *Physiological reviews* **91**(4):1161-1218, (2011).
39. **M. Costanzo, S. Abounit, L. Marzo, A. Danckaert, Z. Chamoun, P. Roux, C. Zurzolo,** Transfer of polyglutamine aggregates in neuronal cells occurs in tunneling nanotubes. *Journal of cell science* **126**(Pt 16):3678-3685, (2013).
40. **S. R. Danielson, J. M. Held, B. Schilling, M. Oo, B. W. Gibson, J. K. Andersen,** Preferentially increased nitration of alpha-synuclein at tyrosine-39 in a cellular oxidative model of Parkinson's disease. *Analytical chemistry* **81**(18):7823-7828, (2009).
41. **K. M. Danzer, L. R. Kranich, W. P. Ruf, O. Cagsal-Getkin, A. R. Winslow, L. Zhu, C. R. Vandenburg, P. J. McLean,** Exosomal cell-to-cell transmission of alpha synuclein oligomers. *Molecular neurodegeneration* **7**(42), (2012).
42. **A. de Gassart, C. Geminard, B. Fevrier, G. Raposo, M. Vidal,** Lipid raft-associated protein sorting in exosomes. *Blood* **102**(13):4336-4344, (2003).
43. **L. M. de Lau, M. M. Breteler,** Epidemiology of Parkinson's disease. *Lancet neurology* **5**(6):525-535, (2006).
44. **P. Desplats, H. J. Lee, E. J. Bae, C. Patrick, E. Rockenstein, L. Crews, B. Spencer, E. Masliah, S. J. Lee,** Inclusion formation and neuronal cell death through neuron-to-neuron transmission of alpha-synuclein. *Proceedings of the National Academy of Sciences of the United States of America* **106**(31):13010-13015, (2009).
45. **J. M. Desterro, M. S. Rodriguez, G. D. Kemp, R. T. Hay,** Identification of the enzyme required for activation of the small ubiquitin-like protein SUMO-1. *The Journal of biological chemistry* **274**(15):10618-10624, (1999).
46. **J. M. Desterro, J. Thomson, R. T. Hay,** Ubch9 conjugates SUMO but not ubiquitin. *FEBS letters* **417**(3):297-300, (1997).
47. **P. C. Donaghy, I. G. McKeith,** The clinical characteristics of dementia with Lewy bodies and a consideration of prodromal diagnosis. *Alzheimer's research & therapy* **6**(4):46, (2014).
48. **V. Dorval, P. E. Fraser,** Small ubiquitin-like modifier (SUMO) modification of natively unfolded proteins tau and alpha-synuclein. *The Journal of biological chemistry* **281**(15):9919-9924, (2006).
49. **V. Dorval, P. E. Fraser,** SUMO on the road to neurodegeneration. *Biochimica et biophysica acta* **1773**(6):694-706, (2007a).
50. **V. Dorval, M. J. Mazzella, P. M. Mathews, R. T. Hay, P. E. Fraser,** Modulation of Abeta generation by small ubiquitin-like modifiers does not require conjugation to target proteins. *The Biochemical journal* **404**(2):309-316, (2007b).
51. **L. M. Duncan, S. Piper, R. B. Dodd, M. K. Saville, C. M. Sanderson, J. P. Luzio, P. J. Lehner,** Lysine-63-linked ubiquitination is required for endolysosomal degradation of class I molecules. *The EMBO journal* **25**(8):1635-1645, (2006).
52. **O. M. El-Agnaf, A. M. Bodles, D. J. Guthrie, P. Harriott, G. B. Irvine,** The N-terminal region of non-A beta component of Alzheimer's disease amyloid is responsible for its tendency to assume beta-sheet and aggregate to form fibrils. *European journal of biochemistry / FEBS* **258**(1):157-163, (1998).

53. **O. M. El-Agnaf, S. A. Salem, K. E. Paleologou, L. J. Cooper, N. J. Fullwood, M. J. Gibson, M. D. Curran, J. A. Court, D. M. Mann, S. Ikeda, M. R. Cookson, J. Hardy, D. Allsop**, Alpha-synuclein implicated in Parkinson's disease is present in extracellular biological fluids, including human plasma. *FASEB J* **17**(13):1945-1947, (2003).
54. **O. M. El-Agnaf, S. A. Salem, K. E. Paleologou, M. D. Curran, M. J. Gibson, J. A. Court, M. G. Schlossmacher, D. Allsop**, Detection of oligomeric forms of alpha-synuclein protein in human plasma as a potential biomarker for Parkinson's disease. *FASEB J* **20**(3):419-425, (2006).
55. **E. Emmanouilidou, D. Elenis, T. Papisilekas, G. Stranjalis, K. Gerozissis, P. C. Ioannou, K. Vekrellis**, Assessment of alpha-synuclein secretion in mouse and human brain parenchyma. *PLoS One* **6**(7):e22225, (2011).
56. **E. Emmanouilidou, K. Melachroinou, T. Roumeliotis, S. D. Garbis, M. Ntzouni, L. H. Margaritis, L. Stefanis, K. Vekrellis**, Cell-produced alpha-synuclein is secreted in a calcium-dependent manner by exosomes and impacts neuronal survival. *The Journal of neuroscience : the official journal of the Society for Neuroscience* **30**(20):6838-6851, (2010).
57. **E. Emmanouilidou, T. Papisilekas, K. Gerozissis, P. C. Ioannou, K. Vekrellis**, Investigation of the mechanisms of alpha-synuclein secretion in vivo. *Movement Disord* **27**(S479-S479), (2012).
58. **C. M. Fader, D. G. Sanchez, M. B. Mestre, M. I. Colombo**, TI-VAMP/VAMP7 and VAMP3/cellubrevin: two v-SNARE proteins involved in specific steps of the autophagy/multivesicular body pathways. *Biochimica et biophysica acta* **1793**(12):1901-1916, (2009).
59. **L. J. Falomir-Lockhart, G. R. Franchini, M. X. Guerbi, J. Storch, B. Corsico**, Interaction of enterocyte FABPs with phospholipid membranes: clues for specific physiological roles. *Biochimica et biophysica acta* **1811**(7-8):452-459, (2011).
60. **Y. Fang, N. Wu, X. Gan, W. Yan, J. C. Morrell, S. J. Gould**, Higher-order oligomerization targets plasma membrane proteins and HIV gag to exosomes. *PLoS biology* **5**(6):e158, (2007).
61. **J. Fauré, G. Lachenal, M. Court, J. Hirrlinger, C. Chatellard-Causse, B. Blot, J. Grange, G. Schoehn, Y. Goldberg, V. Boyer, F. Kirchhoff, G. Raposo, J. Garin, R. Sadoul**, Exosomes are released by cultured cortical neurones. *Molecular and cellular neurosciences* **31**(4):642-648, (2006).
62. **E. Feneberg, P. Steinacker, S. Lehnert, A. Schneider, P. Walther, D. R. Thal, M. Linsenmeier, A. C. Ludolph, M. Otto**, Limited role of free TDP-43 as a diagnostic tool in neurodegenerative diseases. *Amyotrophic lateral sclerosis & frontotemporal degeneration* **15**(5-6):351-356, (2014).
63. **B. Fevrier, G. Raposo**, Exosomes: endosomal-derived vesicles shipping extracellular messages. *Current opinion in cell biology* **16**(4):415-421, (2004a).
64. **B. Fevrier, D. Vilette, F. Archer, D. Loew, W. Faigle, M. Vidal, H. Laude, G. Raposo**, Cells release prions in association with exosomes. *Proceedings of the National Academy of Sciences of the United States of America* **101**(26):9683-9688, (2004b).
65. **S. Friant, E. I. Pecheur, A. Eugster, F. Michel, Y. Lefkir, D. Nourrisson, F. Letourneur**, Ent3p Is a PtdIns(3,5)P2 effector required for protein sorting to the multivesicular body. *Developmental cell* **5**(3):499-511, (2003).
66. **H. Fujiwara, M. Hasegawa, N. Dohmae, A. Kawashima, E. Masliah, M. S. Goldberg, J. Shen, K. Takio, T. Iwatsubo**, alpha-Synuclein is phosphorylated in synucleinopathy lesions. *Nature cell biology* **4**(2):160-164, (2002).
67. **J. R. Gareau, C. D. Lima**, The SUMO pathway: emerging mechanisms that shape specificity, conjugation and recognition. **11**(12):861-871, (2010).
68. **R. Gastpar, M. Gehrman, M. A. Bausero, A. Asea, C. Gross, J. A. Schroeder, G. Multhoff**, Heat shock protein 70 surface-positive tumor exosomes stimulate migratory and cytolytic activity of natural killer cells. *Cancer research* **65**(12):5238-5247, (2005).
69. **R. Geiss-Friedlander, F. Melchior**, Concepts in sumoylation: a decade on. *Nature reviews. Molecular cell biology* **8**(12):947-956, (2007).

70. **B. I. Giasson, J. E. Duda, I. V. Murray, Q. Chen, J. M. Souza, H. I. Hurtig, H. Ischiropoulos, J. Q. Trojanowski, V. M. Lee**, Oxidative damage linked to neurodegeneration by selective alpha-synuclein nitration in synucleinopathy lesions. *Science* **290**(5493):985-989, (2000).
71. **B. I. Giasson, I. V. Murray, J. Q. Trojanowski, V. M. Lee**, A hydrophobic stretch of 12 amino acid residues in the middle of alpha-synuclein is essential for filament assembly. *The Journal of biological chemistry* **276**(4):2380-2386, (2001).
72. **A. Giese, B. Bader, J. Bieschke, G. Schaffar, S. Odoj, P. J. Kahle, C. Haass, H. Kretzschmar**, Single particle detection and characterization of synuclein co-aggregation. *Biochemical and biophysical research communications* **333**(4):1202-1210, (2005).
73. **A. Giese, J. Bieschke, M. Eigen, H. A. Kretzschmar**, Putting prions into focus: application of single molecule detection to the diagnosis of prion diseases. *Archives of virology. Supplementum* **16**:161-171, (2000).
74. **A. Giese, J. Levin, U. Bertsch, H. Kretzschmar**, Effect of metal ions on de novo aggregation of full-length prion protein. *Biochemical and biophysical research communications* **320**(4):1240-1246, (2004).
75. **J. M. Gil, A. C. Rego**, Mechanisms of neurodegeneration in Huntington's disease. *The European journal of neuroscience* **27**(11):2803-2820, (2008).
76. **P. K. Giri, J. S. Schorey**, Exosomes derived from M. Bovis BCG infected macrophages activate antigen-specific CD4+ and CD8+ T cells in vitro and in vivo. *PloS one* **3**(6):e2461, (2008).
77. **A. D. Gitler, B. J. Bevis, J. Shorter, K. E. Strathearn, S. Hamamichi, L. J. Su, K. A. Caldwell, G. A. Caldwell, J. C. Rochet, J. M. McCaffery, C. Barlowe, S. Lindquist**, The Parkinson's disease protein alpha-synuclein disrupts cellular Rab homeostasis. *Proceedings of the National Academy of Sciences of the United States of America* **105**(1):145-150, (2008).
78. **C. B. Gocke, H. Yu, J. Kang**, Systematic identification and analysis of mammalian small ubiquitin-like modifier substrates. *The Journal of biological chemistry* **280**(6):5004-5012, (2005).
79. **M. Goedert, B. Falcon, F. Clavaguera, M. Tolnay**, Prion-like mechanisms in the pathogenesis of tauopathies and synucleinopathies. *Current neurology and neuroscience reports* **14**(11):495, (2014).
80. **G. Gomori**, A modification of the colorimetric phosphorus determination for use with the photoelectric colorimeter. *J. Lab. Clin. Med* **27**(955):1941-1942, (1942).
81. **S. Goncalves, T. F. Outeiro**, Assessing the subcellular dynamics of alpha-synuclein using photoactivation microscopy. *Molecular neurobiology* **47**(3):1081-1092, (2013).
82. **L. Gong, B. Li, S. Millas, E. T. Yeh**, Molecular cloning and characterization of human AOS1 and UBA2, components of the sentrin-activating enzyme complex. *FEBS letters* **448**(1):185-189, (1999).
83. **S. J. Gould, G. Raposo**, As we wait: coping with an imperfect nomenclature for extracellular vesicles. *Journal of extracellular vesicles* **2**(2013).
84. **L. I. Grad, E. Pokrishevsky, J. M. Silverman, N. R. Cashman**, Exosome-dependent and independent mechanisms are involved in prion-like transmission of propagated Cu/Zn superoxide dismutase misfolding. *Prion* **8**(5):331-335, (2014).
85. **F. L. Graham, A. J. van der Eb**, A new technique for the assay of infectivity of human adenovirus 5 DNA. *Virology* **52**(2):456-467, (1973a).
86. **F. L. Graham, A. J. van der Eb**, Transformation of rat cells by DNA of human adenovirus 5. *Virology* **54**(2):536-539, (1973b).
87. **J. C. Gross, V. Chaudhary, K. Bartscherer, M. Boutros**, Active Wnt proteins are secreted on exosomes. *Nature cell biology* **14**(10):1036-1045, (2012).
88. **D. Guo, M. Li, Y. Zhang, P. Yang, S. Eckenrode, D. Hopkins, W. Zheng, S. Purohit, R. H. Podolsky, A. Muir, J. Wang, Z. Dong, T. Brusko, M. Atkinson, P. Pozzilli, A. Zeidler, L. J. Raffel, C. O. Jacob, Y. Park, M. Serrano-Rios, M. T. Larrad, Z. Zhang, H. J. Garchon, J. F. Bach, J. I. Rotter, J. X. She, C. Y. Wang**, A functional variant of SUMO4, a new I kappa B alpha modifier, is associated with type 1 diabetes. *Nature genetics* **36**(8):837-841, (2004).

89. **P. Gutwein, A. Stoeck, S. Riedle, D. Gast, S. Runz, T. P. Condon, A. Marme, M. C. Phong, O. Linderkamp, A. Skorokhod, P. Altevogt**, Cleavage of L1 in exosomes and apoptotic membrane vesicles released from ovarian carcinoma cells. *Clinical cancer research : an official journal of the American Association for Cancer Research* **11**(7):2492-2501, (2005).
90. **B. György, T. G. Szabo, M. Pasztoi, Z. Pal, P. Misjak, B. Aradi, V. Laszlo, E. Pallinger, E. Pap, A. Kittel, G. Nagy, A. Falus, E. I. Buzas**, Membrane vesicles, current state-of-the-art: emerging role of extracellular vesicles. *Cellular and molecular life sciences : CMLS* **68**(16):2667-2688, (2011).
91. **C. Haan, I. Behrmann**, A cost effective non-commercial ECL-solution for Western blot detections yielding strong signals and low background. *Journal of immunological methods* **318**(1-2):11-19, (2007).
92. **K. Haglund, I. Dikic**, Ubiquitylation and cell signaling. *The EMBO journal* **24**(19):3353-3359, (2005).
93. **J. T. Hannich, A. Lewis, M. B. Kroetz, S. J. Li, H. Heide, A. Emili, M. Hochstrasser**, Defining the SUMO-modified proteome by multiple approaches in *Saccharomyces cerevisiae*. *The Journal of biological chemistry* **280**(6):4102-4110, (2005).
94. **C. Hansen, E. Angot, A. L. Bergstrom, J. A. Steiner, L. Pieri, G. Paul, T. F. Outeiro, R. Melki, P. Kallunki, K. Fog, J. Y. Li, P. Brundin**, alpha-Synuclein propagates from mouse brain to grafted dopaminergic neurons and seeds aggregation in cultured human cells. *The Journal of clinical investigation* **121**(2):715-725, (2011).
95. **O. Hansson, S. Hall, A. Ohrfelt, H. Zetterberg, K. Blennow, L. Minthon, K. Nagga, E. Londos, S. Varghese, N. K. Majbour, A. Al-Hayani, O. M. El-Agnaf**, Levels of cerebrospinal fluid alpha-synuclein oligomers are increased in Parkinson's disease with dementia and dementia with Lewy bodies compared to Alzheimer's disease. *Alzheimer's research & therapy* **6**(3):25, (2014).
96. **C. Harding, J. Heuser, P. Stahl**, Receptor-mediated endocytosis of transferrin and recycling of the transferrin receptor in rat reticulocytes. *The Journal of cell biology* **97**(2):329-339, (1983).
97. **C. Harding, J. Heuser, P. Stahl**, Endocytosis and intracellular processing of transferrin and colloidal gold-transferrin in rat reticulocytes: demonstration of a pathway for receptor shedding. *European journal of cell biology* **35**(2):256-263, (1984).
98. **J. Hardy**, Expression of normal sequence pathogenic proteins for neurodegenerative disease contributes to disease risk: 'permissive templating' as a general mechanism underlying neurodegeneration. *Biochemical Society transactions* **33**(Pt 4):578-581, (2005).
99. **R. T. Hay**, SUMO: a history of modification. *Molecular cell* **18**(1):1-12, (2005).
100. **R. T. Hay**, SUMO-specific proteases: a twist in the tail. *Trends in cell biology* **17**(8):370-376, (2007).
101. **C. M. Hecker, M. Rabiller, K. Haglund, P. Bayer, I. Dikic**, Specification of SUMO1- and SUMO2-interacting motifs. *The Journal of biological chemistry* **281**(23):16117-16127, (2006).
102. **W. M. Henne, N. J. Buchkovich, S. D. Emr**, The ESCRT pathway. *Developmental cell* **21**(1):77-91, (2011).
103. **C. Hess, S. Sadallah, A. Hefti, R. Landmann, J. A. Schifferli**, Ectosomes released by human neutrophils are specialized functional units. *J Immunol* **163**(8):4564-4573, (1999).
104. **L. Hicke, R. Dunn**, Regulation of membrane protein transport by ubiquitin and ubiquitin-binding proteins. *Annual review of cell and developmental biology* **19**:141-172, (2003).
105. **M. Hochstrasser**, SP-RING for SUMO: new functions bloom for a ubiquitin-like protein. *Cell* **107**(1):5-8, (2001).
106. **M. Hochstrasser**, Origin and function of ubiquitin-like proteins. **458**(7237):422-429, (2009).
107. **T. Högen, J. Levin, F. Schmidt, M. Caruana, N. Vassallo, H. Kretzschmar, K. Botzel, F. Kamp, A. Giese**, Two different binding modes of alpha-synuclein to lipid vesicles depending on its aggregation state. *Biophysical journal* **102**(7):1646-1655, (2012).
108. **P. A. Holme, N. O. Solum, F. Brosstad, M. Roger, M. Abdelnoor**, Demonstration of platelet-derived microvesicles in blood from patients with activated coagulation and fibrinolysis using a filtration technique and western blotting. *Thrombosis and haemostasis* **72**(5):666-671, (1994).

109. **C. Huang, T. E. Thompson**, Preparation of homogeneous, single-walled phosphatidylcholine vesicles. *Methods in enzymology* **32**(485-489), (1974).
110. **F. Huang, D. Kirkpatrick, X. Jiang, S. Gygi, A. Sorkin**, Differential regulation of EGF receptor internalization and degradation by multiubiquitination within the kinase domain. *Molecular cell* **21**(6):737-748, (2006).
111. **Y. Huang, Y. J. Song, K. Murphy, J. L. Holton, T. Lashley, T. Revesz, W. P. Gai, G. M. Halliday**, LRRK2 and parkin immunoreactivity in multiple system atrophy inclusions. *Acta neuropathologica* **116**(6):639-646, (2008).
112. **M. P. Hunter, N. Ismail, X. Zhang, B. D. Aguda, E. J. Lee, L. Yu, T. Xiao, J. Schafer, M. L. Lee, T. D. Schmittgen, S. P. Nana-Sinkam, D. Jarjoura, C. B. Marsh**, Detection of microRNA expression in human peripheral blood microvesicles. *PLoS one* **3**(11):e3694, (2008).
113. **J. Huotari, A. Helenius**, Endosome maturation. *The EMBO journal* **30**(17):3481-3500, (2011).
114. **J. H. Hurley**, ESCRT complexes and the biogenesis of multivesicular bodies. *Current opinion in cell biology* **20**(1):4-11, (2008).
115. **J. H. Hurley**, The ESCRT complexes. *Critical reviews in biochemistry and molecular biology* **45**(6):463-487, (2010).
116. **K. W. Hwang, T. J. Won, H. Kim, H. J. Chun, T. Chun, Y. Park**, Erratum to "Characterization of the regulatory roles of the SUMO. *Diabetes/metabolism research and reviews* **28**(2):196-202, (2012).
117. **M. C. Irizarry, T. W. Kim, M. McNamara, R. E. Tanzi, J. M. George, D. F. Clayton, B. T. Hyman**, Characterization of the precursor protein of the non-A beta component of senile plaques (NACP) in the human central nervous system. *Journal of neuropathology and experimental neurology* **55**(8):889-895, (1996).
118. **A. Iwai, E. Masliah, M. Yoshimoto, N. Ge, L. Flanagan, H. R. de Silva, A. Kittel, T. Saitoh**, The precursor protein of non-A β component of Alzheimer's disease amyloid is a presynaptic protein of the central nervous system. *Neuron* **14**(2):467-475, (1995).
119. **R. Jakes, M. G. Spillantini, M. Goedert**, Identification of two distinct synucleins from human brain. *FEBS letters* **345**(1):27-32, (1994).
120. **P. Jenner**, Oxidative stress in Parkinson's disease. *Annals of neurology* **53** Suppl 3(S26-36; discussion S36-28), (2003).
121. **T. Jia, Y. E. Liu, J. Liu, Y. E. Shi**, Stimulation of breast cancer invasion and metastasis by synuclein gamma. *Cancer research* **59**(3):742-747, (1999).
122. **Z. Jiang, R. E. Redfern, Y. Isler, A. H. Ross, A. Gericke**, Cholesterol stabilizes fluid phosphoinositide domains. *Chemistry and physics of lipids* **182**(52-61), (2014).
123. **H. Jin, K. Ishikawa, T. Tsunemi, T. Ishiguro, T. Amino, H. Mizusawa**, Analyses of copy number and mRNA expression level of the alpha-synuclein gene in multiple system atrophy. *Journal of medical and dental sciences* **55**(1):145-153, (2008).
124. **E. S. Johnson**, Protein modification by SUMO. *Annual review of biochemistry* **73**(355-382), (2004).
125. **E. S. Johnson, G. Blobel**, Ubc9p is the conjugating enzyme for the ubiquitin-like protein Smt3p. *Journal of Biological Chemistry* **272**(43):26799-26802, (1997).
126. **E. S. Johnson, A. A. Gupta**, An E3-like factor that promotes SUMO conjugation to the yeast septins. *Cell* **106**(6):735-744, (2001).
127. **R. M. Johnstone, M. Adam, J. R. Hammond, L. Orr, C. Turbide**, Vesicle formation during reticulocyte maturation. Association of plasma membrane activities with released vesicles (exosomes). *The Journal of biological chemistry* **262**(19):9412-9420, (1987).
128. **H. Karube, M. Sakamoto, S. Arawaka, S. Hara, H. Sato, C. H. Ren, S. Goto, S. Koyama, M. Wada, T. Kawanami, K. Kurita, T. Kato**, N-terminal region of alpha-synuclein is essential for the fatty acid-induced oligomerization of the molecules. *FEBS letters* **582**(25-26):3693-3700, (2008).
129. **S. Keller, J. Ridinger, A. K. Rupp, J. W. Janssen, P. Altevogt**, Body fluid derived exosomes as a novel template for clinical diagnostics. *Journal of translational medicine* **9**(86), (2011).

130. **S. Keller, M. P. Sanderson, A. Stoeck, P. Altevogt**, Exosomes: from biogenesis and secretion to biological function. *Immunology letters* **107**(2):102-108, (2006).
131. **W. S. Kim, K. Kagedal, G. M. Halliday**, Alpha-synuclein biology in Lewy body diseases. *Alzheimer's research & therapy* **6**(5):73, (2014).
132. **C. Klein, K. Lohmann-Hedrich, E. Rogaeva, M. G. Schlossmacher, A. E. Lang**, Deciphering the role of heterozygous mutations in genes associated with parkinsonism. *Lancet neurology* **6**(7):652-662, (2007).
133. **V. S. Kokhan, M. A. Afanasyeva, G. I. Van'kin**, alpha-Synuclein knockout mice have cognitive impairments. *Behavioural brain research* **231**(1):226-230, (2012).
134. **J. H. Kordower, Y. Chu, R. A. Hauser, T. B. Freeman, C. W. Olanow**, Lewy body-like pathology in long-term embryonic nigral transplants in Parkinson's disease. *Nature medicine* **14**(5):504-506, (2008a).
135. **J. H. Kordower, Y. Chu, R. A. Hauser, C. W. Olanow, T. B. Freeman**, Transplanted dopaminergic neurons develop PD pathologic changes: a second case report. *Movement disorders : official journal of the Movement Disorder Society* **23**(16):2303-2306, (2008b).
136. **J. H. Kordower, T. B. Freeman, B. J. Snow, F. J. Vingerhoets, E. J. Mufson, P. R. Sanberg, R. A. Hauser, D. A. Smith, G. M. Nauert, D. P. Perl, et al.**, Neuropathological evidence of graft survival and striatal reinnervation after the transplantation of fetal mesencephalic tissue in a patient with Parkinson's disease. *The New England journal of medicine* **332**(17):1118-1124, (1995).
137. **R. Krüger, W. Kuhn, T. Muller, D. Voitalla, M. Graeber, S. Kosel, H. Przuntek, J. T. Epplen, L. Schols, O. Riess**, Ala30Pro mutation in the gene encoding alpha-synuclein in Parkinson's disease. *Nature genetics* **18**(2):106-108, (1998).
138. **P. Krumova, E. Meulmeester, M. Garrido, M. Tirard, H. H. Hsiao, G. Bossis, H. Urlaub, M. Zweckstetter, S. Kügler, F. Melchior, M. Bähr, J. H. Weishaupt**, Sumoylation inhibits alpha-synuclein aggregation and toxicity. *The Journal of cell biology* **194**(1):49-60, (2011).
139. **N. Kruse, W. J. Schulz-Schaeffer, M. G. Schlossmacher, B. Mollenhauer**, Development of electrochemiluminescence-based singleplex and multiplex assays for the quantification of alpha-synuclein and other proteins in cerebrospinal fluid. *Methods* **56**(4):514-518, (2012).
140. **T. Kuwahara, A. Koyama, S. Koyama, S. Yoshina, C. H. Ren, T. Kato, S. Mitani, T. Iwatsubo**, A systematic RNAi screen reveals involvement of endocytic pathway in neuronal dysfunction in alpha-synuclein transgenic *C. elegans*. *Human molecular genetics* **17**(19):2997-3009, (2008).
141. **U. K. Laemmli**, Cleavage of structural proteins during the assembly of the head of bacteriophage T4. *Nature* **227**(5259):680-685, (1970).
142. **K. Laulagnier, C. Motta, S. Hamdi, S. Roy, F. Fauvelle, J. F. Pageaux, T. Kobayashi, J. P. Salles, B. Perret, C. Bonnerot, M. Record**, Mast cell- and dendritic cell-derived exosomes display a specific lipid composition and an unusual membrane organization. *The Biochemical journal* **380**(Pt 1):161-171, (2004).
143. **C. Lavedan**, The synuclein family. *Genome research* **8**(9):871-880, (1998).
144. **C. Lavedan, E. Leroy, A. Dehejia, S. Buchholtz, A. Dutra, R. L. Nussbaum, M. H. Polymeropoulos**, Identification, localization and characterization of the human gamma-synuclein gene. *Human genetics* **103**(1):106-112, (1998).
145. **B. R. Lee, T. Kamitani**, Improved immunodetection of endogenous alpha-synuclein. *PLoS one* **6**(8):e23939, (2011).
146. **G. W. Lee, F. Melchior, M. J. Matunis, R. Mahajan, Q. Tian, P. Anderson**, Modification of Ran GTPase-activating protein by the small ubiquitin-related modifier SUMO-1 requires Ubc9, an E2-type ubiquitin-conjugating enzyme homologue. *The Journal of biological chemistry* **273**(11):6503-6507, (1998).
147. **H. J. Lee, E. J. Bae, S. J. Lee**, Extracellular alpha-synuclein-a novel and crucial factor in Lewy body diseases. *Nat Rev Neurol* **10**(2):92-98, (2014).
148. **H. J. Lee, S. Patel, S. J. Lee**, Intravesicular localization and exocytosis of alpha-synuclein and its aggregates. *The Journal of neuroscience : the official journal of the Society for Neuroscience* **25**(25):6016-6024, (2005).

149. **V. M. Lee, J. Q. Trojanowski**, Mechanisms of Parkinson's disease linked to pathological alpha-synuclein: new targets for drug discovery. *Neuron* **52**(1):33-38, (2006).
150. **E. Leroy, R. Boyer, G. Auburger, B. Leube, G. Ulm, E. Mezey, G. Harta, M. J. Brownstein, S. Jonnalagada, T. Chernova, A. Dehejia, C. Lavedan, T. Gasser, P. J. Steinbach, K. D. Wilkinson, M. H. Polymeropoulos**, The ubiquitin pathway in Parkinson's disease. *Nature* **395**(6701):451-452, (1998).
151. **J. Y. Li, E. Englund, J. L. Holton, D. Soulet, P. Hagell, A. J. Lees, T. Lashley, N. P. Quinn, S. Rehnrota, A. Bjorklund, H. Widner, T. Revesz, O. Lindvall, P. Brundin**, Lewy bodies in grafted neurons in subjects with Parkinson's disease suggest host-to-graft disease propagation. *Nature medicine* **14**(5):501-503, (2008).
152. **Y. Li, H. Wang, S. Wang, D. Quon, Y. W. Liu, B. Cordell**, Positive and negative regulation of APP amyloidogenesis by sumoylation. *Proceedings of the National Academy of Sciences of the United States of America* **100**(1):259-264, (2003).
153. **Y. Liu, M. Qiang, Y. Wei, R. He**, A novel molecular mechanism for nitrated {alpha}-synuclein-induced cell death. *Journal of molecular cell biology* **3**(4):239-249, (2011).
154. **L. M. Lois, C. D. Lima**, Structures of the SUMO E1 provide mechanistic insights into SUMO activation and E2 recruitment to E1. **24**(3):439-451, (2005).
155. **V. Luga, L. Zhang, A. M. Vitoria-Petit, A. A. Ogunjimi, M. R. Inanlou, E. Chiu, M. Buchanan, A. N. Hosein, M. Basik, J. L. Wrana**, Exosomes mediate stromal mobilization of autocrine Wnt-PCP signaling in breast cancer cell migration. *Cell* **151**(7):1542-1556, (2012).
156. **K. C. Luk, V. Kehm, J. Carroll, B. Zhang, P. O'Brien, J. Q. Trojanowski, V. M. Lee**, Pathological alpha-synuclein transmission initiates Parkinson-like neurodegeneration in nontransgenic mice. *Science* **338**(6109):949-953, (2012a).
157. **K. C. Luk, V. M. Kehm, B. Zhang, P. O'Brien, J. Q. Trojanowski, V. M. Lee**, Intracerebral inoculation of pathological alpha-synuclein initiates a rapidly progressive neurodegenerative alpha-synucleinopathy in mice. *The Journal of experimental medicine* **209**(5):975-986, (2012b).
158. **K. C. Luk, V. M. Lee**, Modeling Lewy pathology propagation in Parkinson's disease. *Parkinsonism & related disorders* **20 Suppl 1**(S85-87, (2014).
159. **H. B. Luo, Y. Y. Xia, X. J. Shu, Z. C. Liu, Y. Feng, X. H. Liu, G. Yu, G. Yin, Y. S. Xiong, K. Zeng, J. Jiang, K. Q. Ye, X. C. Wang, J. Z. Wang**, SUMOylation at K340 inhibits tau degradation through deregulating its phosphorylation and ubiquitination. *Proceedings of the National Academy of Sciences of the United States of America* **111**(46):16586-16591, (2014).
160. **J. P. Luzio, S. R. Gray, N. A. Bright**, Endosome-lysosome fusion. *Biochemical Society transactions* **38**(6):1413-1416, (2010).
161. **L. Maroteaux, J. T. Campanelli, R. H. Scheller**, Synuclein: a neuron-specific protein localized to the nucleus and presynaptic nerve terminal. *The Journal of neuroscience : the official journal of the Society for Neuroscience* **8**(8):2804-2815, (1988).
162. **L. Maroteaux, R. H. Scheller**, The rat brain synucleins; family of proteins transiently associated with neuronal membrane. *Brain research. Molecular brain research* **11**(3-4):335-343, (1991).
163. **S. Martin, K. A. Wilkinson, A. Nishimune, J. M. Henley**, Emerging extranuclear roles of protein SUMOylation in neuronal function and dysfunction. *Nature reviews. Neuroscience* **8**(12):948-959, (2007).
164. **I. F. Mata, W. J. Wedemeyer, M. J. Farrer, J. P. Taylor, K. A. Gallo**, LRRK2 in Parkinson's disease: protein domains and functional insights. *Trends in neurosciences* **29**(5):286-293, (2006).
165. **S. Mathivanan, H. Ji, B. J. Tauro, Y. S. Chen, R. J. Simpson**, Identifying mutated proteins secreted by colon cancer cell lines using mass spectrometry. *Journal of proteomics* **76 Spec No.**(141-149, (2012).

166. I. G. McKeith, D. W. Dickson, J. Lowe, M. Emre, J. T. O'Brien, H. Feldman, J. Cummings, J. E. Duda, C. Lippa, E. K. Perry, D. Aarsland, H. Arai, C. G. Ballard, B. Boeve, D. J. Burn, D. Costa, T. Del Ser, B. Dubois, D. Galasko, S. Gauthier, C. G. Goetz, E. Gomez-Tortosa, G. Halliday, L. A. Hansen, J. Hardy, T. Iwatsubo, R. N. Kalara, D. Kaufer, R. A. Kenny, A. Korczyn, K. Kosaka, V. M. Lee, A. Lees, I. Litvan, E. Londos, O. L. Lopez, S. Minoshima, Y. Mizuno, J. A. Molina, E. B. Mukaetova-Ladinska, F. Pasquier, R. H. Perry, J. B. Schulz, J. Q. Trojanowski, M. Yamada, Diagnosis and management of dementia with Lewy bodies: third report of the DLB Consortium. *Neurology* **65**(12):1863-1872, (2005).
167. I. G. McKeith, E. Rowan, K. Askew, A. Naidu, L. Allan, N. Barnett, D. Lett, U. P. Mosimann, D. Burn, J. T. O'Brien, More severe functional impairment in dementia with lewy bodies than Alzheimer disease is related to extrapyramidal motor dysfunction. *The American journal of geriatric psychiatry : official journal of the American Association for Geriatric Psychiatry* **14**(7):582-588, (2006).
168. P. J. McLean, S. Ribich, B. T. Hyman, Subcellular localization of alpha-synuclein in primary neuronal cultures: effect of missense mutations. *Journal of neural transmission. Supplementum* **58**:53-63, (2000).
169. F. Melchior, SUMO--nonclassical ubiquitin. *Annual review of cell and developmental biology* **16**(591-626, (2000).
170. I. Mellman, Endocytosis and molecular sorting. *Annual review of cell and developmental biology* **12**(575-625, (1996).
171. I. Mendez, A. Vinuela, A. Astradsson, K. Mukhida, P. Hallett, H. Robertson, T. Tierney, R. Holness, A. Dagher, J. Q. Trojanowski, O. Isacson, Dopamine neurons implanted into people with Parkinson's disease survive without pathology for 14 years. *Nature medicine* **14**(5):507-509, (2008).
172. E. Meulmeester, M. Kunze, H. H. Hsiao, H. Urlaub, F. Melchior, Mechanism and consequences for paralog-specific sumoylation of ubiquitin-specific protease 25. *Molecular cell* **30**(5):610-619, (2008).
173. A. Michael, S. D. Bajracharya, P. S. Yuen, H. Zhou, R. A. Star, G. G. Illei, I. Alevizos, Exosomes from human saliva as a source of microRNA biomarkers. *Oral diseases* **16**(1):34-38, (2010).
174. A. Minty, X. Dumont, M. Kaghad, D. Caput, Covalent modification of p73alpha by SUMO-1. Two-hybrid screening with p73 identifies novel SUMO-1-interacting proteins and a SUMO-1 interaction motif. *The Journal of biological chemistry* **275**(46):36316-36323, (2000).
175. S. Misra, J. H. Hurley, Crystal structure of a phosphatidylinositol 3-phosphate-specific membrane-targeting motif, the FYVE domain of Vps27p. *Cell* **97**(5):657-666, (1999).
176. F. Mori, K. Tanji, M. Yoshimoto, H. Takahashi, K. Wakabayashi, Immunohistochemical comparison of alpha- and beta-synuclein in adult rat central nervous system. *Brain research* **941**(1-2):118-126, (2002).
177. H. R. Morris, J. R. Vaughan, S. R. Datta, R. Bandopadhyay, H. A. Rohan De Silva, A. Schrag, N. J. Cairns, D. Burn, U. Nath, P. L. Lantos, S. Daniel, A. J. Lees, N. P. Quinn, N. W. Wood, Multiple system atrophy/progressive supranuclear palsy: alpha-Synuclein, synphilin, tau, and APOE. *Neurology* **55**(12):1918-1920, (2000).
178. A. L. Mougnot, S. Nicot, A. Bencsik, E. Morignat, J. Verchere, L. Lakhdar, S. Legastelois, T. Baron, Prion-like acceleration of a synucleinopathy in a transgenic mouse model. *Neurobiology of aging* **33**(9):2225-2228, (2012).
179. D. Mukhopadhyay, M. Dasso, Modification in reverse: the SUMO proteases. *Trends in biochemical sciences* **32**(6):286-295, (2007).
180. I. V. Murray, B. I. Giasson, S. M. Quinn, V. Koppaka, P. H. Axelsen, H. Ischiropoulos, J. Q. Trojanowski, V. M. Lee, Role of alpha-synuclein carboxy-terminus on fibril formation in vitro. *Biochemistry* **42**(28):8530-8540, (2003).
181. S. Nakajo, S. Shioda, Y. Nakai, K. Nakaya, Localization of phosphoneuroprotein 14 (PNP 14) and its mRNA expression in rat brain determined by immunocytochemistry and in situ hybridization. *Brain research. Molecular brain research* **27**(1):81-86, (1994).

182. **T. Nakamura, H. Yamashita, T. Takahashi, S. Nakamura**, Activated Fyn phosphorylates alpha-synuclein at tyrosine residue 125. *Biochemical and biophysical research communications* **280**(4):1085-1092, (2001).
183. **V. M. Nemani, W. Lu, V. Berge, K. Nakamura, B. Onoa, M. K. Lee, F. A. Chaudhry, R. A. Nicoll, R. H. Edwards**, Increased expression of alpha-synuclein reduces neurotransmitter release by inhibiting synaptic vesicle reclustering after endocytosis. *Neuron* **65**(1):66-79, (2010).
184. **M. Okochi, J. Walter, A. Koyama, S. Nakajo, M. Baba, T. Iwatsubo, L. Meijer, P. J. Kahle, C. Haass**, Constitutive phosphorylation of the Parkinson's disease associated alpha-synuclein. *The Journal of biological chemistry* **275**(1):390-397, (2000).
185. **C. W. Olanow, C. G. Goetz, J. H. Kordower, A. J. Stoessl, V. Sossi, M. F. Brin, K. M. Shannon, G. M. Nauert, D. P. Perl, J. Godbold, T. B. Freeman**, A double-blind controlled trial of bilateral fetal nigral transplantation in Parkinson's disease. *Annals of neurology* **54**(3):403-414, (2003).
186. **M. Ostrowski, N. B. Carmo, S. Krumeich, I. Fanget, G. Raposo, A. Savina, C. F. Moita, K. Schauer, A. N. Hume, R. P. Freitas, B. Goud, P. Benaroch, N. Hacohen, M. Fukuda, C. Desnos, M. C. Seabra, F. Darchen, S. Amigorena, L. F. Moita, C. Thery**, Rab27a and Rab27b control different steps of the exosome secretion pathway. *Nature cell biology* **12**(1):19-30; sup pp 11-13, (2010).
187. **T. F. Outeiro, S. Lindquist**, Yeast cells provide insight into alpha-synuclein biology and pathobiology. *Science* **302**(5651):1772-1775, (2003).
188. **T. F. Outeiro, P. Putcha, J. E. Tetzlaff, R. Spoelgen, M. Koker, F. Carvalho, B. T. Hyman, P. J. McLean**, Formation of toxic oligomeric alpha-synuclein species in living cells. *PLoS one* **3**(4):e1867, (2008).
189. **D. Owerbach, E. M. McKay, E. T. Yeh, K. H. Gabbay, K. M. Bohren**, A proline-90 residue unique to SUMO-4 prevents maturation and sumoylation. *Biochemical and biophysical research communications* **337**(2):517-520, (2005).
190. **T. Ozawa, H. Takano, O. Onodera, H. Kobayashi, T. Ikeuchi, R. Koide, K. Okuizumi, T. Shimohata, K. Wakabayashi, H. Takahashi, S. Tsuji**, No mutation in the entire coding region of the alpha-synuclein gene in pathologically confirmed cases of multiple system atrophy. *Neuroscience letters* **270**(2):110-112, (1999).
191. **J. J. Palvimo**, PIAS proteins as regulators of small ubiquitin-related modifier (SUMO) modifications and transcription. *Biochemical Society transactions* **35**(Pt 6):1405-1408, (2007).
192. **B. T. Pan, R. M. Johnstone**, Fate of the transferrin receptor during maturation of sheep reticulocytes in vitro: selective externalization of the receptor. *Cell* **33**(3):967-978, (1983).
193. **B. T. Pan, K. Teng, C. Wu, M. Adam, R. M. Johnstone**, Electron microscopic evidence for externalization of the transferrin receptor in vesicular form in sheep reticulocytes. *The Journal of cell biology* **101**(3):942-948, (1985).
194. **K. H. Park, B. J. Kim, J. Kang, T. S. Nam, J. M. Lim, H. T. Kim, J. K. Park, Y. G. Kim, S. W. Chae, U. H. Kim**, Ca²⁺ signaling tools acquired from prostasomes are required for progesterone-induced sperm motility. *Science signaling* **4**(173):ra31, (2011).
195. **I. Parolini, C. Federici, C. Raggi, L. Lugini, S. Palleschi, A. De Milito, C. Coscia, E. Iessi, M. Logozzi, A. Molinari, M. Colone, M. Tatti, M. Sargiacomo, S. Fais**, Microenvironmental pH is a key factor for exosome traffic in tumor cells. *The Journal of biological chemistry* **284**(49):34211-34222, (2009).
196. **D. M. Pegtel, K. Cosmopoulos, D. A. Thorley-Lawson, M. A. van Eijndhoven, E. S. Hopmans, J. L. Lindenberg, T. D. de Gruijl, T. Wurdinger, J. M. Middeldorp**, Functional delivery of viral miRNAs via exosomes. *Proceedings of the National Academy of Sciences of the United States of America* **107**(14):6328-6333, (2010).
197. **H. R. B. Pelham**, SNAREs and the specificity of membrane fusion. *Trends in cell biology* **11**(3):99-101, (2001).
198. **R. J. Perrin, W. S. Woods, D. F. Clayton, J. M. George**, Interaction of human alpha-Synuclein and Parkinson's disease variants with phospholipids. Structural analysis using site-directed mutagenesis. *The Journal of biological chemistry* **275**(44):34393-34398, (2000).

199. **A. Pichler, A. Gast, J. S. Seeler, A. Dejean, F. Melchior**, The nucleoporin RanBP2 has SUMO1 E3 ligase activity. *Cell* **108**(1):109-120, (2002).
200. **R. C. Piper, P. J. Lehner**, Endosomal transport via ubiquitination. *Trends in cell biology* **21**(11):647-655, (2011).
201. **T. Pisitkun, R. F. Shen, M. A. Knepper**, Identification and proteomic profiling of exosomes in human urine. *Proceedings of the National Academy of Sciences of the United States of America* **101**(36):13368-13373, (2004).
202. **M. Pitschke, R. Prior, M. Haupt, D. Riesner**, Detection of single amyloid beta-protein aggregates in the cerebrospinal fluid of Alzheimer's patients by fluorescence correlation spectroscopy. *Nature medicine* **4**(7):832-834, (1998).
203. **E. Pokrishevsky, L. I. Grad, M. Yousefi, J. Wang, I. R. Mackenzie, N. R. Cashman**, Aberrant localization of FUS and TDP43 is associated with misfolding of SOD1 in amyotrophic lateral sclerosis. *PLoS one* **7**(4):e35050, (2012).
204. **M. H. Polymeropoulos, C. Lavedan, E. Leroy, S. E. Ide, A. Dehejia, A. Dutra, B. Pike, H. Root, J. Rubenstein, R. Boyer, E. S. Stenroos, S. Chandrasekharappa, A. Athanassiadou, T. Papapetropoulos, W. G. Johnson, A. M. Lazzarini, R. C. Duvoisin, G. Di Iorio, L. I. Golbe, R. L. Nussbaum**, Mutation in the alpha-synuclein gene identified in families with Parkinson's disease. *Science* **276**(5321):2045-2047, (1997).
205. **K. Post, M. Pitschke, O. Schafer, H. Wille, T. R. Appel, D. Kirsch, I. Mehlhorn, H. Serban, S. B. Prusiner, D. Riesner**, Rapid acquisition of beta-sheet structure in the prion protein prior to multimer formation. *Biological chemistry* **379**(11):1307-1317, (1998).
206. **D. L. Pountney, F. Chegini, X. Shen, P. C. Blumbergs, W. P. Gai**, SUMO-1 marks subdomains within glial cytoplasmic inclusions of multiple system atrophy. *Neuroscience letters* **381**(1-2):74-79, (2005).
207. **P. Putcha, K. M. Danzer, L. R. Kranich, A. Scott, M. Silinski, S. Mabbett, C. D. Hicks, J. M. Veal, P. M. Steed, B. T. Hyman, P. J. McLean**, Brain-permeable small-molecule inhibitors of Hsp90 prevent alpha-synuclein oligomer formation and rescue alpha-synuclein-induced toxicity. *The Journal of pharmacology and experimental therapeutics* **332**(3):849-857, (2010).
208. **G. Rabinowits, C. Gercel-Taylor, J. M. Day, D. D. Taylor, G. H. Kloecker**, Exosomal microRNA: a diagnostic marker for lung cancer. *Clinical lung cancer* **10**(1):42-46, (2009).
209. **C. Raiborg, K. G. Bache, A. Mehlum, E. Stang, H. Stenmark**, Hrs recruits clathrin to early endosomes. *EMBO J* **20**(17):5008-5021, (2001).
210. **C. Raiborg, T. E. Rusten, H. Stenmark**, Protein sorting into multivesicular endosomes. *Current opinion in cell biology* **15**(4):446-455, (2003).
211. **L. Rajendran, M. Honsho, T. R. Zahn, P. Keller, K. D. Geiger, P. Verkade, K. Simons**, Alzheimer's disease beta-amyloid peptides are released in association with exosomes. *Proceedings of the National Academy of Sciences of the United States of America* **103**(30):11172-11177, (2006).
212. **S. Rana, S. Yue, D. Stadel, M. Zoller**, Toward tailored exosomes: the exosomal tetraspanin web contributes to target cell selection. *The international journal of biochemistry & cell biology* **44**(9):1574-1584, (2012).
213. **S. Rana, M. Zoller**, Exosome target cell selection and the importance of exosomal tetraspanins: a hypothesis. *Biochemical Society transactions* **39**(2):559-562, (2011).
214. **G. Raposo, H. W. Nijman, W. Stoorvogel, R. Liejendekker, C. V. Harding, C. J. Melief, H. J. Geuze**, B lymphocytes secrete antigen-presenting vesicles. *The Journal of experimental medicine* **183**(3):1161-1172, (1996).
215. **G. Raposo, W. Stoorvogel**, Extracellular vesicles: exosomes, microvesicles, and friends. *The Journal of cell biology* **200**(4):373-383, (2013).
216. **J. Ratajczak, M. Wysoczynski, F. Hayek, A. Janowska-Wieczorek, M. Z. Ratajczak**, Membrane-derived microvesicles: important and underappreciated mediators of cell-to-cell communication. *Leukemia* **20**(9):1487-1495, (2006).

217. **A. Recasens, B. Dehay, J. Bove, I. Carballo-Carbajal, S. Dovero, A. Perez-Villalba, P. O. Fernagut, J. Blesa, A. Parent, C. Perier, I. Farinas, J. A. Obeso, E. Bezard, M. Vila,** Lewy body extracts from Parkinson disease brains trigger alpha-synuclein pathology and neurodegeneration in mice and monkeys. *Annals of neurology* **75**(3):351-362, (2014).
218. **I. Remy, S. W. Michnick,** A highly sensitive protein-protein interaction assay based on Gaussia luciferase. *Nature methods* **3**(12):977-979, (2006).
219. **D. Reverter, C. D. Lima,** Insights into E3 ligase activity revealed by a SUMO-RanGAP1-Ubc9-Nup358 complex. *Nature* **435**(7042):687-692, (2005).
220. **N. L. Rey, G. H. Petit, L. Bousset, R. Melki, P. Brundin,** Transfer of human alpha-synuclein from the olfactory bulb to interconnected brain regions in mice. *Acta neuropathologica* **126**(4):555-573, (2013).
221. **C. Robertson, S. A. Booth, D. R. Beniac, M. B. Coulthart, T. F. Booth, A. McNicol,** Cellular prion protein is released on exosomes from activated platelets. *Blood* **107**(10):3907-3911, (2006).
222. **M. S. Rodriguez, C. Dargemont, R. T. Hay,** SUMO-1 conjugation in vivo requires both a consensus modification motif and nuclear targeting. *The Journal of biological chemistry* **276**(16):12654-12659, (2001).
223. **G. Rosas-Acosta, W. K. Russell, A. Deyrieux, D. H. Russell, V. G. Wilson,** A universal strategy for proteomic studies of SUMO and other ubiquitin-like modifiers. *Molecular & cellular proteomics : MCP* **4**(1):56-72, (2005).
224. **I. Roxrud, H. Stenmark, L. Malerod,** ESCRT & Co. *Biology of the cell / under the auspices of the European Cell Biology Organization* **102**(5):293-318, (2010).
225. **H. Saitoh, J. Hinchev,** Functional heterogeneity of small ubiquitin-related protein modifiers SUMO-1 versus SUMO-2/3. *The Journal of biological chemistry* **275**(9):6252-6258, (2000).
226. **J. Sambrook, D. W. Russell,** *Molecular cloning: a laboratory manual (3-volume set)*. (Cold spring harbor laboratory press Cold Spring Harbor, New York., 2001), vol. 999.
227. **D. A. Sampson, M. Wang, M. J. Matunis,** The small ubiquitin-like modifier-1 (SUMO-1) consensus sequence mediates Ubc9 binding and is essential for SUMO-1 modification. *The Journal of biological chemistry* **276**(24):21664-21669, (2001).
228. **A. Sapetschnig, G. Rischitor, H. Braun, A. Doll, M. Schergaut, F. Melchior, G. Suske,** Transcription factor Sp3 is silenced through SUMO modification by PIAS1. *The EMBO journal* **21**(19):5206-5215, (2002).
229. **J. S. Schorey, S. Bhatnagar,** Exosome function: from tumor immunology to pathogen biology. *Traffic* **9**(6):871-881, (2008).
230. **D. Schubert, S. Humphreys, C. Baroni, M. Cohn,** In vitro differentiation of a mouse neuroblastoma. *Proceedings of the National Academy of Sciences of the United States of America* **64**(1):316-323, (1969).
231. **S. Schulz, G. Chachami, L. Kozackiewicz, U. Winter, N. Stankovic-Valentin, P. Haas, K. Hofmann, H. Urlaub, H. Ovaa, J. Wittbrodt, E. Meulmeester, F. Melchior,** Ubiquitin-specific protease-like 1 (USPL1) is a SUMO isopeptidase with essential, non-catalytic functions. *EMBO reports* **13**(10):930-938, (2012).
232. **P. Schwille, J. Bieschke, F. Oehlenschlaeger,** Kinetic investigations by fluorescence correlation spectroscopy: the analytical and diagnostic potential of diffusion studies. *Biophysical chemistry* **66**(2-3):211-228, (1997).
233. **D. Scott, S. Roy,** alpha-Synuclein inhibits intersynaptic vesicle mobility and maintains recycling-pool homeostasis. *The Journal of neuroscience : the official journal of the Society for Neuroscience* **32**(30):10129-10135, (2012).
234. **H. Sheldon, E. Heikamp, H. Turley, R. Dragovic, P. Thomas, C. E. Oon, R. Leek, M. Edelmann, B. Kessler, R. C. Sainson, I. Sargent, J. L. Li, A. L. Harris,** New mechanism for Notch signaling to endothelium at a distance by Delta-like 4 incorporation into exosomes. *Blood* **116**(13):2385-2394, (2010).
235. **B. Shen, Y. Fang, N. Wu, S. J. Gould,** Biogenesis of the Posterior Pole Is Mediated by the Exosome/Microvesicle Protein-sorting Pathway. *J Biol Chem* **286**(51):44162-44176, (2011a).

236. **B. Shen, N. Wu, J. M. Yang, S. J. Gould**, Protein targeting to exosomes/microvesicles by plasma membrane anchors. *The Journal of biological chemistry* **286**(16):14383-14395, (2011b).
237. **S. B. Shields, R. C. Piper**, How ubiquitin functions with ESCRTs. *Traffic* **12**(10):1306-1317, (2011).
238. **E. J. Shin, H. M. Shin, E. Nam, W. S. Kim, J. H. Kim, B. H. Oh, Y. Yun**, DeSUMOylating isopeptidase: a second class of SUMO protease. *EMBO reports* **13**(4):339-346, (2012).
239. **Y. Shinbo, T. Niki, T. Taira, H. Ooe, K. Takahashi-Niki, C. Maita, C. Seino, S. M. Iguchi-Ariga, H. Ariga**, Proper SUMO-1 conjugation is essential to DJ-1 to exert its full activities. *Cell death and differentiation* **13**(1):96-108, (2006).
240. **V. V. Shvadchak, L. J. Falomir-Lockhart, D. A. Yushchenko, T. M. Jovin**, Specificity and kinetics of alpha-synuclein binding to model membranes determined with fluorescent excited state intramolecular proton transfer (ESIPT) probe. *The Journal of biological chemistry* **286**(15):13023-13032, (2011).
241. **M. Simons, G. Raposo**, Exosomes--vesicular carriers for intercellular communication. *Current opinion in cell biology* **21**(4):575-581, (2009).
242. **J. Song, L. K. Durrin, T. A. Wilkinson, T. G. Krontiris, Y. Chen**, Identification of a SUMO-binding motif that recognizes SUMO-modified proteins. *Proceedings of the National Academy of Sciences of the United States of America* **101**(40):14373-14378, (2004).
243. **Y. J. Song, D. M. Lundvig, Y. Huang, W. P. Gai, P. C. Blumbergs, P. Hojrup, D. Otzen, G. M. Halliday, P. H. Jensen**, p25alpha relocalizes in oligodendroglia from myelin to cytoplasmic inclusions in multiple system atrophy. *The American journal of pathology* **171**(4):1291-1303, (2007).
244. **M. G. Spillantini, R. A. Crowther, R. Jakes, N. J. Cairns, P. L. Lantos, M. Goedert**, Filamentous alpha-synuclein inclusions link multiple system atrophy with Parkinson's disease and dementia with Lewy bodies. *Neuroscience letters* **251**(3):205-208, (1998a).
245. **M. G. Spillantini, R. A. Crowther, R. Jakes, M. Hasegawa, M. Goedert**, alpha-Synuclein in filamentous inclusions of Lewy bodies from Parkinson's disease and dementia with lewy bodies. *Proceedings of the National Academy of Sciences of the United States of America* **95**(11):6469-6473, (1998b).
246. **M. G. Spillantini, M. L. Schmidt, V. M. Lee, J. Q. Trojanowski, R. Jakes, M. Goedert**, Alpha-synuclein in Lewy bodies. *Nature* **388**(6645):839-840, (1997).
247. **J. S. Steffan, N. Agrawal, J. Pallos, E. Rockabrand, L. C. Trotman, N. Slepko, K. Illes, T. Lukacsovich, Y. Z. Zhu, E. Cattaneo, P. P. Pandolfi, L. M. Thompson, J. L. Marsh**, SUMO modification of Huntingtin and Huntington's disease pathology. *Science* **304**(5667):100-104, (2004).
248. **P. Stehmeier, S. Müller**, Phospho-regulated SUMO interaction modules connect the SUMO system to CK2 signaling. *Molecular cell* **33**(3):400-409, (2009).
249. **H. Stenmark, R. G. Parton, O. Steele-Mortimer, A. Lutcke, J. Gruenberg, M. Zerial**, Inhibition of rab5 GTPase activity stimulates membrane fusion in endocytosis. *EMBO J* **13**(6):1287-1296, (1994a).
250. **H. Stenmark, A. Valencia, O. Martinez, O. Ullrich, B. Goud, M. Zerial**, Distinct structural elements of rab5 define its functional specificity. *EMBO J* **13**(3):575-583, (1994b).
251. **J. Storch, A. M. Kleinfeld**, Transfer of long-chain fluorescent free fatty acids between unilamellar vesicles. *Biochemistry* **25**(7):1717-1726, (1986).
252. **K. Strauss, C. Goebel, H. Runz, W. Möbius, S. Weiss, I. Feussner, M. Simons, A. Schneider**, Exosome secretion ameliorates lysosomal storage of cholesterol in Niemann-Pick type C disease. *The Journal of biological chemistry* **285**(34):26279-26288, (2010).
253. **C. Subra, K. Laulagnier, B. Perret, M. Record**, Exosome lipidomics unravels lipid sorting at the level of multivesicular bodies. *Biochimie* **89**(2):205-212, (2007).
254. **H. Sun, J. D. Leverson, T. Hunter**, Conserved function of RNF4 family proteins in eukaryotes: targeting a ubiquitin ligase to SUMOylated proteins. *The EMBO journal* **26**(18):4102-4112, (2007).

255. T. Taira, Y. Saito, T. Niki, S. M. Iguchi-Ariga, K. Takahashi, H. Ariga, DJ-1 has a role in antioxidative stress to prevent cell death. *EMBO reports* **5**(2):213-218, (2004).
256. M. Takahashi, H. Miyata, F. Kametani, T. Nonaka, H. Akiyama, S. I. Hisanaga, M. Hasegawa, Extracellular association of APP and tau fibrils induces intracellular aggregate formation of tau. *Acta neuropathologica* (2015).
257. Y. Takahashi, T. Kahyo, E. A. Toh, H. Yasuda, Y. Kikuchi, Yeast Ull1/Siz1 is a novel SUMO1/Smt3 ligase for septin components and functions as an adaptor between conjugating enzyme and substrates. *The Journal of biological chemistry* **276**(52):48973-48977, (2001).
258. M. H. Tatham, E. Jaffray, O. A. Vaughan, J. M. Desterro, C. H. Botting, J. H. Naismith, R. T. Hay, Polymeric chains of SUMO-2 and SUMO-3 are conjugated to protein substrates by SAE1/SAE2 and Ubc9. *The Journal of biological chemistry* **276**(38):35368-35374, (2001).
259. B. J. Tauro, D. W. Greening, R. A. Mathias, S. Mathivanan, H. Ji, R. J. Simpson, Two distinct populations of exosomes are released from LIM1863 colon carcinoma cell-derived organoids. *Molecular & cellular proteomics : MCP* **12**(3):587-598, (2013).
260. S. Tenreiro, K. Eckermann, T. F. Outeiro, Protein phosphorylation in neurodegeneration: friend or foe? *Frontiers in molecular neuroscience* **7**(42), (2014).
261. J. E. Tetzlaff, P. Putcha, T. F. Outeiro, A. Ivanov, O. Berezovska, B. T. Hyman, P. J. McLean, CHIP targets toxic alpha-Synuclein oligomers for degradation. *The Journal of biological chemistry* **283**(26):17962-17968, (2008).
262. N. Thayanidhi, J. R. Helm, D. C. Nycz, M. Bentley, Y. Liang, J. C. Hay, Alpha-synuclein delays endoplasmic reticulum (ER)-to-Golgi transport in mammalian cells by antagonizing ER/Golgi SNAREs. *Molecular biology of the cell* **21**(11):1850-1863, (2010).
263. A. C. Theos, S. T. Truschel, D. Tenza, I. Hurbain, D. C. Harper, J. F. Berson, P. C. Thomas, G. Raposo, M. S. Marks, A luminal domain-dependent pathway for sorting to intraluminal vesicles of multivesicular endosomes involved in organelle morphogenesis. *Developmental cell* **10**(3):343-354, (2006).
264. C. Thery, S. Amigorena, The cell biology of antigen presentation in dendritic cells. *Current opinion in immunology* **13**(1):45-51, (2001a).
265. C. Théry, S. Amigorena, G. Raposo, A. Clayton, Isolation and characterization of exosomes from cell culture supernatants and biological fluids. *Current protocols in cell biology / editorial board, Juan S. Bonifacino ... [et al.] Chapter 3*(Unit 3 22, (2006).
266. C. Thery, M. Boussac, P. Veron, P. Ricciardi-Castagnoli, G. Raposo, J. Garin, S. Amigorena, Proteomic analysis of dendritic cell-derived exosomes: a secreted subcellular compartment distinct from apoptotic vesicles. *J Immunol* **166**(12):7309-7318, (2001b).
267. C. Théry, M. Ostrowski, E. Segura, Membrane vesicles as conveyors of immune responses. *Nature reviews. Immunology* **9**(8):581-593, (2009).
268. T. Tokuda, M. M. Qureshi, M. T. Ardah, S. Varghese, S. A. Shehab, T. Kasai, N. Ishigami, A. Tamaoka, M. Nakagawa, O. M. El-Agnaf, Detection of elevated levels of alpha-synuclein oligomers in CSF from patients with Parkinson disease. *Neurology* **75**(20):1766-1772, (2010).
269. H. Towbin, T. Staehelin, J. Gordon, Electrophoretic transfer of proteins from polyacrylamide gels to nitrocellulose sheets: procedure and some applications. *Proceedings of the National Academy of Sciences of the United States of America* **76**(9):4350-4354, (1979).
270. K. Trajkovic, C. Hsu, S. Chiantia, L. Rajendran, D. Wenzel, F. Wieland, P. Schwille, B. Brugger, M. Simons, Ceramide triggers budding of exosome vesicles into multivesicular endosomes. *Science* **319**(5867):1244-1247, (2008).
271. P. H. Tu, J. E. Galvin, M. Baba, B. Giasson, T. Tomita, S. Leight, S. Nakajo, T. Iwatsubo, J. Q. Trojanowski, V. M. Lee, Glial cytoplasmic inclusions in white matter oligodendrocytes of multiple system atrophy brains contain insoluble alpha-synuclein. *Annals of neurology* **44**(3):415-422, (1998).
272. Y. Uchimura, M. Nakamura, K. Sugawara, M. Nakao, H. Saitoh, Overproduction of eukaryotic SUMO-1- and SUMO-2-conjugated proteins in Escherichia coli. *Analytical biochemistry* **331**(1):204-206, (2004).

273. **K. Ueda, H. Fukushima, E. Masliah, Y. Xia, A. Iwai, M. Yoshimoto, D. A. Otero, J. Kondo, Y. Ihara, T. Saitoh**, Molecular cloning of cDNA encoding an unrecognized component of amyloid in Alzheimer disease. *Proceedings of the National Academy of Sciences of the United States of America* **90**(23):11282-11286, (1993).
274. **H. D. Ulrich**, SUMO modification: wrestling with protein conformation. *Current biology : CB* **15**(7):R257-259, (2005).
275. **A. Ulusoy, R. E. Musgrove, R. Rusconi, M. Klinkenberg, M. Helwig, A. Schneider, D. A. Di Monte**, Neuron-to-neuron alpha-synuclein propagation in vivo is independent of neuronal injury. *Acta neuropathologica communications* **3**(1):13, (2015).
276. **A. Ulusoy, R. Rusconi, B. I. Perez-Revelta, R. E. Musgrove, M. Helwig, B. Winzen-Reichert, D. A. Di Monte**, Caudo-rostral brain spreading of alpha-synuclein through vagal connections. *EMBO molecular medicine* **5**(7):1051-1059, (2013).
277. **J. W. Um, K. C. Chung**, Functional modulation of parkin through physical interaction with SUMO-1. *Journal of neuroscience research* **84**(7):1543-1554, (2006).
278. **V. N. Uversky**, Neuropathology, biochemistry, and biophysics of alpha-synuclein aggregation. *Journal of neurochemistry* **103**(1):17-37, (2007).
279. **V. N. Uversky, J. Li, P. Souillac, I. S. Millett, S. Doniach, R. Jakes, M. Goedert, A. L. Fink**, Biophysical properties of the synucleins and their propensities to fibrillate: inhibition of alpha-synuclein assembly by beta- and gamma-synucleins. *The Journal of biological chemistry* **277**(14):11970-11978, (2002).
280. **H. Valadi, K. Ekstrom, A. Bossios, M. Sjostrand, J. J. Lee, J. O. Lotvall**, Exosome-mediated transfer of mRNAs and microRNAs is a novel mechanism of genetic exchange between cells. *Nature cell biology* **9**(6):654-659, (2007).
281. **E. M. Valente, F. Brancati, V. Caputo, E. A. Graham, M. B. Davis, A. Ferraris, M. M. Breteler, T. Gasser, V. Bonifati, A. R. Bentivoglio, G. De Michele, A. Durr, P. Cortelli, A. Filla, G. Meco, B. A. Oostra, A. Brice, A. Albanese, B. Dallapiccola, N. W. Wood**, PARK6 is a common cause of familial parkinsonism. *Neurological sciences : official journal of the Italian Neurological Society and of the Italian Society of Clinical Neurophysiology* **23 Suppl 2**(S117-118), (2002a).
282. **E. M. Valente, F. Brancati, A. Ferraris, E. A. Graham, M. B. Davis, M. M. Breteler, T. Gasser, V. Bonifati, A. R. Bentivoglio, G. De Michele, A. Durr, P. Cortelli, D. Wassilowsky, B. S. Harhangi, N. Rawal, V. Caputo, A. Filla, G. Meco, B. A. Oostra, A. Brice, A. Albanese, B. Dallapiccola, N. W. Wood**, PARK6-linked parkinsonism occurs in several European families. *Annals of neurology* **51**(1):14-18, (2002b).
283. **A. J. van der Eb**, Intermediates in type 5 adenovirus DNA replication. *Virology* **51**(1):11-23, (1973).
284. **T. J. van Ham, K. L. Thijssen, R. Breitling, R. M. Hofstra, R. H. Plasterk, E. A. Nollen, C. elegans model identifies genetic modifiers of alpha-synuclein inclusion formation during aging.** *PLoS genetics* **4**(3):e1000027, (2008).
285. **G. van Meer, D. R. Voelker, G. W. Feigenson**, Membrane lipids: where they are and how they behave. *Nature reviews. Molecular cell biology* **9**(2):112-124, (2008).
286. **G. van Niel, S. Charrin, S. Simoes, M. Romao, L. Rochin, P. Saftig, M. S. Marks, E. Rubinstein, G. Raposo**, The tetraspanin CD63 regulates ESCRT-independent and -dependent endosomal sorting during melanogenesis. *Developmental cell* **21**(4):708-721, (2011).
287. **G. van Niel, I. Porto-Carreiro, S. Simoes, G. Raposo**, Exosomes: a common pathway for a specialized function. *Journal of biochemistry* **140**(1):13-21, (2006).
288. **L. J. Vella, D. L. Greenwood, R. Cappai, J. P. Scheerlinck, A. F. Hill**, Enrichment of prion protein in exosomes derived from ovine cerebral spinal fluid. *Veterinary immunology and immunopathology* **124**(3-4):385-393, (2008).
289. **L. J. Vella, R. A. Sharples, V. A. Lawson, C. L. Masters, R. Cappai, A. F. Hill**, Packaging of prions into exosomes is associated with a novel pathway of PrP processing. *The Journal of pathology* **211**(5):582-590, (2007).

290. **A. C. Vertegaal, J. S. Andersen, S. C. Ogg, R. T. Hay, M. Mann, A. I. Lamond**, Distinct and overlapping sets of SUMO-1 and SUMO-2 target proteins revealed by quantitative proteomics. *Molecular & cellular proteomics : MCP* **5**(12):2298-2310, (2006).
291. **C. Villarroya-Beltri, C. Gutierrez-Vazquez, F. Sanchez-Cabo, D. Perez-Hernandez, J. Vazquez, N. Martin-Cofreces, D. J. Martinez-Herrera, A. Pascual-Montano, M. Mittelbrunn, F. Sanchez-Madrid**, Sumoylated hnRNPA2B1 controls the sorting of miRNAs into exosomes through binding to specific motifs. *Nature communications* **4**(2980), (2013).
292. **V. Vingtdeux, N. Sergeant, L. Buée**, Potential contribution of exosomes to the prion-like propagation of lesions in Alzheimer's disease. *Frontiers in physiology* **3**(229), (2012).
293. **K. Wakabayashi, M. Yoshimoto, S. Tsuji, H. Takahashi**, Alpha-synuclein immunoreactivity in glial cytoplasmic inclusions in multiple system atrophy. *Neuroscience letters* **249**(2-3):180-182, (1998).
294. **F. O. Walker**, Huntington's Disease. *Seminars in neurology* **27**(2):143-150, (2007).
295. **J. D. Walker, C. L. Maier, J. S. Pober**, Cytomegalovirus-infected human endothelial cells can stimulate allogeneic CD4+ memory T cells by releasing antigenic exosomes. *J Immunol* **182**(3):1548-1559, (2009).
296. **P. Whitley, B. J. Reaves, M. Hashimoto, A. M. Riley, B. V. Potter, G. D. Holman**, Identification of mammalian Vps24p as an effector of phosphatidylinositol 3,5-bisphosphate-dependent endosome compartmentalization. *The Journal of biological chemistry* **278**(40):38786-38795, (2003).
297. **K. A. Wilkinson, Y. Nakamura, J. M. Henley**, Targets and consequences of protein SUMOylation in neurons. *Brain research reviews* **64**(1):195-212, (2010).
298. **J. Wolfers, A. Lozier, G. Raposo, A. Regnault, C. Thery, C. Masurier, C. Flament, S. Pouzieux, F. Faure, T. Tursz, E. Angevin, S. Amigorena, L. Zitvogel**, Tumor-derived exosomes are a source of shared tumor rejection antigens for CTL cross-priming. *Nature medicine* **7**(3):297-303, (2001).
299. **S. J. Wood, J. Wypych, S. Steavenson, J. C. Louis, M. Citron, A. L. Biere**, alpha-synuclein fibrillogenesis is nucleation-dependent. Implications for the pathogenesis of Parkinson's disease. *The Journal of biological chemistry* **274**(28):19509-19512, (1999).
300. **R. Wubbolts, R. S. Leckie, P. T. Veenhuizen, G. Schwarzmann, W. Möbius, J. Hoernschemeyer, J. W. Slot, H. J. Geuze, W. Stoorvogel**, Proteomic and biochemical analyses of human B cell-derived exosomes. Potential implications for their function and multivesicular body formation. *The Journal of biological chemistry* **278**(13):10963-10972, (2003).
301. **Y. Xia, T. Saitoh, K. Ueda, S. Tanaka, X. Chen, M. Hashimoto, L. Hsu, C. Conrad, M. Sundsmo, M. Yoshimoto, L. Thal, R. Katzman, E. Masliah**, Characterization of the human alpha-synuclein gene: Genomic structure, transcription start site, promoter region and polymorphisms. *Journal of Alzheimer's disease : JAD* **3**(5):485-494, (2001).
302. **E. T. Yeh**, SUMOylation and De-SUMOylation: wrestling with life's processes. *The Journal of biological chemistry* **284**(13):8223-8227, (2009).
303. **S. C. L. Yeo, L. H. Xu, J. H. Ren, V. J. Boulton, M. D. Wagle, C. Liu, G. Ren, P. Wong, R. Zahn, P. Sasajala, H. Y. Yang, R. C. Piper, A. L. Munn**, Vps20p and Vta1p interact with Vps4p and function in multivesicular body sorting and endosomal transport in *Saccharomyces cerevisiae*. *Journal of cell science* **116**(19):3957-3970, (2003).
304. **M. Yonetani, T. Nonaka, M. Masuda, Y. Inukai, T. Oikawa, S. Hisanaga, M. Hasegawa**, Conversion of wild-type alpha-synuclein into mutant-type fibrils and its propagation in the presence of A30P mutant. *The Journal of biological chemistry* **284**(12):7940-7950, (2009).
305. **J. J. Zarranz, J. Alegre, J. C. Gomez-Esteban, E. Lezcano, R. Ros, I. Ampuero, L. Vidal, J. Hoenicka, O. Rodriguez, B. Atares, V. Llorens, E. Gomez Tortosa, T. del Ser, D. G. Munoz, J. G. de Yébenes**, The new mutation, E46K, of alpha-synuclein causes Parkinson and Lewy body dementia. *Annals of neurology* **55**(2):164-173, (2004).
306. **Y. Q. Zhang, K. D. Sarge**, Sumoylation of amyloid precursor protein negatively regulates Abeta aggregate levels. *Biochemical and biophysical research communications* **374**(4):673-678, (2008).

307. **J. Zhu, S. Zhu, C. M. Guzzo, N. A. Ellis, K. S. Sung, C. Y. Choi, M. J. Matunis**, Small ubiquitin-related modifier (SUMO) binding determines substrate recognition and paralog-selective SUMO modification. *The Journal of biological chemistry* **283**(43):29405-29415, (2008).
308. **L. Zitvogel, A. Regnault, A. Lozier, J. Wolfers, C. Flament, D. Tenza, P. Ricciardi-Castagnoli, G. Raposo, S. Amigorena**, Eradication of established murine tumors using a novel cell-free vaccine: dendritic cell-derived exosomes. *Nature medicine* **4**(5):594-600, (1998).
309. **A. Zomer, T. Vendrig, E. S. Hopmans, M. van Eijndhoven, J. M. Middeldorp, D. M. Pegtel**, Exosomes: Fit to deliver small RNA. *Communicative & integrative biology* **3**(5):447-450, (2010).

7. Appendix

Table 13: Summary of NTA measurements

transfected constructs	mean particle concentration adjusted to cell number	SEM
Myc-SUMO-2 wt/α-Syn wt	2.52E+07	1.67E+06
Myc-SUMO 2ΔGG/α-Syn wt	2.22E+07	2.31E+06
n	8	
t-test	0.16738	
α-Syn wt	2.24E+07	2.98E+06
α-Syn-SUMO-2	2.71E+07	4.15E+06
n	7	
t-test	0.06368	
α-Syn wt	2.16E+07	1.94E+06
α-Syn 2KR	2.07E+07	1.76E+06
α-Syn AA	2.36E+07	4.95E+06
n	6	
t-test (wt/2KR)	0.55184	
t-test (wt/2AA)	0.17285	
α-Syn wt	3.33E+07	3.78E+06
α-Syn wt/VPS4dn co-transfection	2.50E+07	5.12E+06
n	7	
t-test	0.000054	
α-Syn-SUMO-2	5.10E+07	1.40E+05
α-Syn-SUMO-2 /VPS4dn	4.07E+07	5.35E+06
n	8	
t-test	0.00281561	
YFP-APPsw	3.30E+07	3.50E+05
YFP-APPsw-SUMO-2	3.85E+07	2.96E+05
n	8	
t-test	0.104734285	
YFP-APPsw/SUMO-2-wt	4.60E+07	3.47E+06
YFP-APPsw/SUMO-2-ΔGG	4.02E+07	1.82E+06
n	8	
t-test	0.092198482	

Curriculum Vitae

Marcel Kunadt
born on March 4th 1984 in Eisenhüttenstadt, Germany

Sültebecksbreite 1
37075 Göttingen, Germany
Phone: +49 176 23 42 0179
E-Mail: mkunadt@gwdg.de

Education

- | | |
|-------------------|-----------------------------------------------------------------------------------------------------------------------------------------------------------------------------------------------------------------------------------------------------------------------|
| 07/2011 – present | Georg-August Universität Göttingen, Germany
PhD Thesis “Extracellular vesicle release of α -Synuclein is mediated by SUMOylation” in the Department of Psychiatry, University Medical Center Göttingen under supervision of Prof. Dr. Anja Schneider |
| 07/2011 – present | Georg-August Universität Göttingen, Germany
GGNB PhD Program “Molecular Physiology of the Brain” |
| 10/2004 – 10/2010 | Georg-August Universität Göttingen, Germany
Institute of Microbiology and Genetics
Dept. Genetics of Eukaryotic, diploma degree in biology |
| 07/2000 – 07/2003 | OSZ Gottfried-Wilhelm Leibniz Eisenhüttenstadt, Germany
Abitur degree (general qualification for university entrance) |

Publications

M. Kunadt, K. Eckermann, A. Stuendl, J. Gong, B. Russo, K. Strauss, S. Rai, S. Kügler, L. Falomir Lockhart, M. Schwalbe, P. Krumova, L. M. Oliveira, M. Bähr, W. Möbius, J. Levin, A. Giese, N. Kruse, B. Mollenhauer, R. Geiss-Friedländer, A. C. Ludolph, A. Freischmidt, M. S. Feiler, K. M. Danzer, M. Zweckstetter, T. M. Jovin, M. Simons, J. H. Weishaupt, A. Schneider, **Extracellular vesicle sorting of α -Synuclein is regulated by sumoylation.** *Acta neuropathologica*, DOI 10.1007/s00401-015-1408-1, (2015).